UNITED STATES
DEPARTMENT OF THE INTERIOR
GEOLOGICAL SURVEY

THE HYDROTHERMAL SYSTEM IN SOUTHERN GRASS VALLEY,

PERSHING COUNTY, NEVADA

By Alan H. Welch, M. L. Sorey, and F. H. Olmsted

OPEN-FILE REPORT 81-915

II

CONTENTS

CONTENTS (continued) | Page

ILLUSTRATIONS | Page

V

HYDROTHERMAL SYSTEM IN SOUTHERN GRASS VALLEY,
PERSHING COUNTY, NEVADA

Alan H. Welch, M. L. Sorey, and F. H. Olmsted

ABSTRACT

Southern Grass Valley is a fairly typical extensional basin in the Basin and Range province. Leach Hot Springs, in the southern part of the valley, represents the discharge end of an active hydrothermal flow system with an estimated deep aquifer temperature of 163-176°C. This report discusses results of geologic, hydrologic, geophysical and geochemical investigations in an attempt to construct an internally consistent model of the system.

Basin and Range extensional tectonics, responsible for the formation of Grass Valley and probably the existing hydrothermal system, began about 15 million years ago. Pre-Tertiary mountain-forming bedrock, which was already extensively folded and faulted, was affected by widespread east-west extension producing north-trending mountains and intervening basins. The basin was filled with predominantly poorly sorted clastic rocks derived from the adjacent rising consolidated bedrock. Southern Grass Valley evolved into a partly filled alluvial basin with sediments reaching a thickness of more than 1 kilometer (km). The basin is asymmetric with a much steeper bedrock surface near the eastern edge of the basin, which is apparently due to greater movement along the eastern basin-bounding fault(s). Leach Hot Springs is at the

base of a recent scarp which seems to be associated with the faulting that is responsible for the steep eastern bedrock surface.

The study area is in the Battle Mountain heat-flow high, a region typified by heat flow greater than normal for the Basin and Range province. Heat flow measurements over a 125 km^2 area including Leach Hot Springs indicate that the mean heat flow is 3-4 HFU, in agreement with the other measurements in the Battle Mountain high. Appproximately three-fourths of the heat is lost from the study area through conduction; the remainder is due to approximately equal proportions of advective and convective loss. The thermal data from shallower wells reveal areas of anomalously high heat flow associated with rising thermal water and areas of low heat flow caused by the recharge of cold water. The data also indicate the presence of a temperature distribution at the base of the sedimentary fill (top of the bedrock) that results from circulation within the underlying consolidated rocks.

Chemical and isotopic data indicate that the thermal water was recharged under cooler and possibly wetter conditions, which would imply a residence time for the water of at least 8,000 years. The chemical data have confirmed that thermal water is moving upward through the sedimentary fill in an area about 5 km southwest of Leach Hot Springs, in addition to the upward flow directly beneath Leach Hot Springs.

Numerical modeling has proved useful in delineating important aspects of the hydrothermal system. Analysis of a fault-plane flow model consisting of movement of ground water entirely within the fault zone from which the hot springs discharge indicates that the modeled residence time is much shorter than that implied by the isotope data and that circulation depths near 5 km are required for reservoir temperatures near 180°C to be attained. A more plausible model, consisting of lateral movement in the bedrock under the sedimentary

2

fill, implies a minimum depth of circulation of 3 km and a fluid residence time consistent with the isotope data. The results of this lateral-flow model indicate that the hydraulic conductivity of the deep aquifer and the upflow area are critical parameters needed to evaluate the exploitation potential of the system. If the present flow of thermal water is restricted mainly by the low hydraulic conductivity in the sediments in the vicinity of Leach Hot Springs, then a deep aquifer could be sufficiently permeable to allow exploitation for electric-power generation at rates exceeding 10 Mwe. However, if the flow of thermal water is restricted mainly by low hydraulic conductivity in the deep part of the system, then the potential for electrical-power generation is much less.

INTRODUCTION

Purpose of the Study

The present effort is an outgrowth of a reconnaissance of the hydrology of selected hydrothermal systems in Nevada. The purpose was to use a detailed multi-discipline approach to the examination of a high-temperature system in the Basin and Range province as well as to evaluate different exploration and evaluation techniques. Geophysical investigations by personnel of the Lawrence Berkeley Laboratory have been discussed in detail in various reports cited in the section "Previous Studies". This report therefore deals primarily with the results of the hydrologic, geochemical, and heat-flow work by the U.S. Geological Survey, although the geophysical data have been used extensively. It is hoped that the results of this effort will make any future studies more efficient by allowing them to concentrate on the more critical elements of the problem of understanding the hydrology of high-temperature systems.

Acknowledgements

Previous Studies

Prior to the 1970's, little information on Leach Hot Springs was published. The earliest mention of the hot springs was by Clarence King in his report on the 40th parallel survey (King, 1878). Russell (1896) and Jones (1915) later examined the fault scarp at Leach Hot Springs. Dreyer (1940) presented a brief description of the springs, along with a chemical analysis of the spring water and temperature data. Waring (1965) included limited data on the springs in a geographic listing of thermal waters.

Extensive and intensive geologic, hydrologic, geochemical, and geophysical studies are available for the area under consideration. Recent work in Grass Valley has combined effort by members of the U.S. Geological Survey and Environment Division of the Lawrence Berkeley Laboratory. A source list of data for evaluation of the geothermal potential of the Leach Hot Springs area has been assembled by Olmsted, Glancy, Harrill, Rush, and VanDenburgh (1973). Subseguent to this compilation, a variety of more recent studies has been published. Regional coverage of the geology (Johnson, 1977), gravity (Erwin, 1974), seismic refraction (Majer, 1978), aeromagnetics (Zietz and others, 1978 and U.S. Geological Survey, 1973), and heat flow (Sass and others, 1971) are also available.

Geologic reports concerned with the geothermal aspects of southern Grass Valley have been presented by Olmsted, Glancy, Harrill, Rush, and VanDenburgh (1975), Noble (written communication, 1975), Noble, Wollenberg, Silberman, and Archibald (1975), and Beyer and others (1975). Although there has not previously been a complete geochemical study of this area, there are several sources of published data. A single analysis is available in Dreyer (1940) on one of the springs. Chemical, isotopic and gas analyses have been published by Mariner, Rapp, Willey, and Presser (1974),and Mariner, Presser, Rapp, and Willey (1975) for samples from the thermal springs. Major, minor, and trace

6

elements analyses of the thermal and some nonthermal waters are presented in Bowman, Hebert, Wollenberg, and Asaro (1976) and Wollenberg, Bowman, and Asaro (1977). O'Connell and Kaufmann (1976), Wollenberg (1974) and Wollenberg, Bowman, and Asara (1977) have studied the radioactivity at Leach Hot Springs and several other northern Nevada geothermal areas. The sulfate-water geothermometry has been presented in comparative studies by Nehring and others (1979) and Nehring and Mariner (1979). Heat-flow studies by Sass, Lachenbruch, Munroe, Greene, and Moses (1976), Sass, and others (1977), and Olmsted, Glancy, Harrill, Rush, and VanDenburgh (1975) show the local heat-flow picture in the southern Grass Valley area.

A variety of geophysical techniques has been used in examining the southern Grass Valley to evaluate the techniques themselves in a Basin and Range setting and to examine the southern Grass Valley area in particular. The present interpretation has relied on the results of these investigations. For example, seismic-reflections profiling has been useful in delineating major faults, some of which extend into bedrock (Majer, 1978). These major faults, which may provide the primary avenues for deep fluid circulation, appear to be primarily on the eastern side of the basin. Interpretation of gravity data reveals a much steeper gradient on the eastern side of the basin (Goldstein and Paulson, 1977), with a northwest-trending trough immediately west of the springs. Meidav and Tonani (1975) noted that thermal-spring activity is most often associated with the eastern side of basins in the Basin and Range province; the eastern sides generally have the steeper gravity gradients, which is true in Grass Valley.

Geophysical studies in the vicinity of Leach Hot Springs indicate the presence of significant silica deposits beneath the spring area. Interpretation of the gravity data indicates excess mass, which is consistent with densification due to silicification (Goldstein and Paulson, 1977). Advanced

7

seismic P-wave arrival times and variations of frequency content in the seismic signal indicate that the silicified zone has a relatively small lateral extent but extends to an appreciable depth (Beyer and others, 1976; Majer 1978). Although microearthquakes of tectonic origin were not detected in the immediate vicinity of Leach Hot Springs, a very shallow source of seismic noise was detected which may be related to near-surface boiling (Liaw, 1977).

Several earlier papers discuss temperature and heat flow in southern Grass Valley or in the surrounding region. Sass, Lachenbruch, Munroe, Greene, and Moses (1971, p. 6407-6411) described regional heat flow in the Basin and Range province and first described the Battle Mountain (heat-flow) high, which includes southern Grass Valley. Their interpretations were necessarily generalized and tentative because of scanty data, but the general heat-flow pattern has been corroborated by more recent measurements. Among the data that helped to define the Battle Mountain high were corrected heat-flow values of 3.5 and 4.0 heat-flow units (hfu) determined in two wells in Panther Canyon in the southeastern part of the present study area (Sass and others, 1971, p. 6393, table 8). Coincidentally, the mean heat flow in these two holes, 3.8 hfu, is the same as the value estimated in the present study for the entire budget area in southern Grass Valley.

Olmsted, Glancy, Harrill, Rush, and VanDenburgh (1975, p. 193-204) defined the pattern of the shallow (0-50 m) subsurface temperature and heat flow in the Leach Hot Springs area and estimated the discharge of heat and water from the hydrothermal-discharge system. They concluded (p. 205-206) that the conductive heat flow in valley fill outside the Leach Hot Springs thermal anomaly is perhaps no more than 2 hfu, that the spring discharge represents thermal water which has risen along a steeply inclined conduit system or systems associated with the Leach Hot Springs fault, and that most of the

8

thermal water emerges at the springs rather than leaking from the conduit system laterally into shallow aquifers.

Sass and others (1977) defined the distribution of heat flow in southern Grass Valley on the basis data from of 82 test wells, most of which were drilled in cooperation with Lawrence Berkeley Laboratory and were outside the Leach Hot Springs thermal anomaly. They calculated a heat budget for southern Grass Valley which supported earlier inferences of high heat flow and the occurrence of the Battle Mountain high.

Numbering System for Wells and Springs

In this investigation, wells and springs are assigned numbers according to the rectangular system of subdividing public lands, referred to the Mount Diablo baseline and meridian. The first two elements of the number, separated by a slash, are, respectively, the township (north) and range (east); the third element, separated from the second by a hyphen, indicates the section number; and the lowercase letters following the section number indicate the successive quadrant subdivisions of the section. The letters, a, b, c, and d designate, respectively, the northeast, northwest, southwest, and southeast quadrants as shown in figure 1. Where more than one well or spring is catalogued within the smallest designated quadrant, the last lowercase letter is followed by a numeral that designates the order in which the feature was catalogued during the investigation. For example, well number 32/23-25bdb1 designates the first well recorded in the NW 1/4 SE 1/4 NW 1/4 section 25, T. 32 N., R. 23 E., Mount Diablo baseline and meridian.

In addition to the location numbers, test wells in the study area have been assigned a combination of letter(s) and number(s) as in table 1. Several sets of wells have been drilled for the U.S. Geological Survey and Lawrence Berkeley Laboratory with different letter designations being used to distinguish the various sets. The wells assigned the capital letters GVDH were drilled for the Geological Survey indicating that the wells are located in the Grass Valley area and are drilled wells (hydraulic rotary was used). The construction of the first 11 wells is discussed by Olmsted, Glancy, Harrill, Rush, and Van Denburgh (1975). Six additional wells were drilled by the U.S. Bureau of Reclamation in the spring of 1975 for the Geological Survey. Three of the holes were constructed for the collection of heat-flow data by capping the bottom of the casing and filling it with water and the other three wells
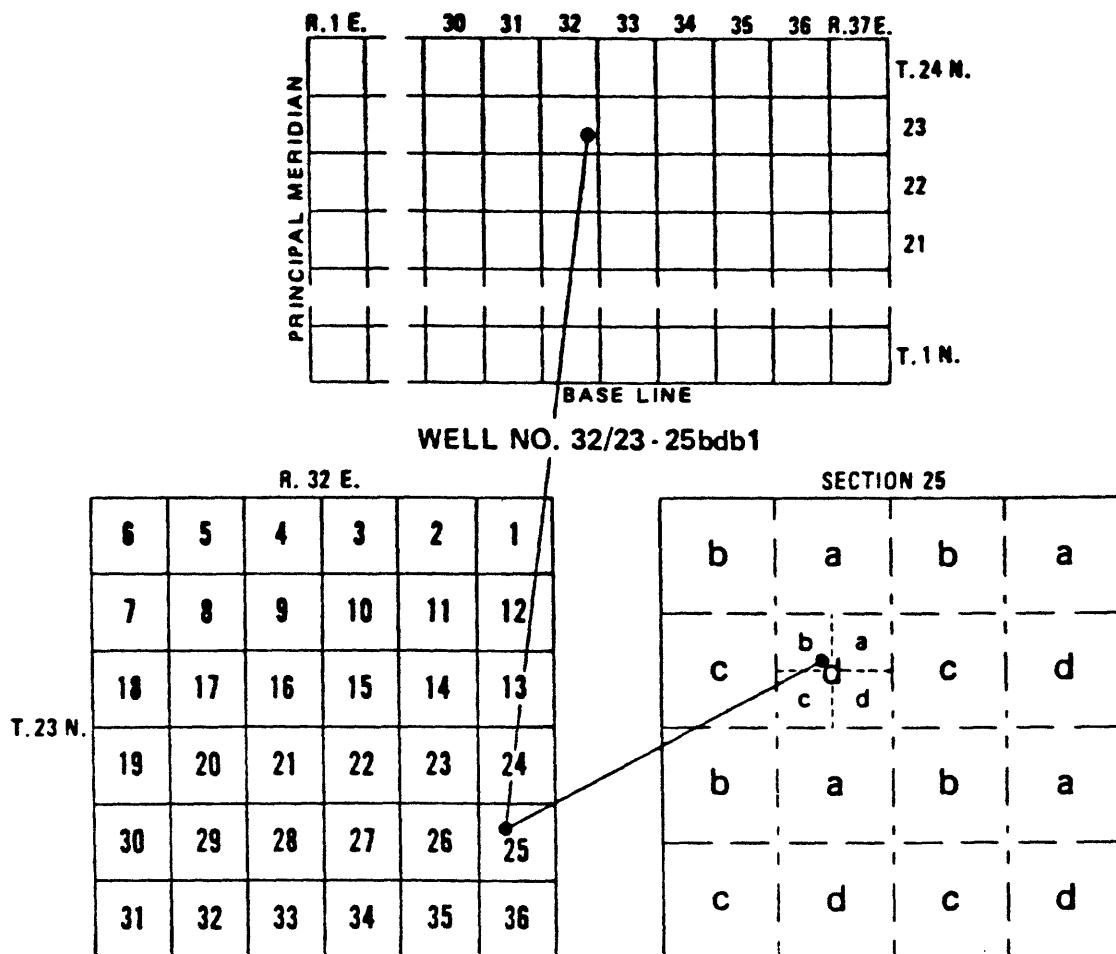
FIGURE 1. -- Diagram showing numbering system for wells, springs, and samples.

TABLE 1 -- Data for wells and test wells in southern Grass Valley

Name of test well	Location number	Latitude north	Longitude west	Altitude of land surface m	Height of measuring point above land surface		Depth of screen or cap at bottom		Nominal inside diameter of casing		Type of completion 1/	Geophysical logs available 2/	Other data available 3/
					m	ft	m	ft	mm	in			
DH1	33/38- 1dbc	40 35 15	117 39 10	1,406.835	0.152	0.52	44.42-44.88	145.7-147.2	51	2.00	P,Sc	G,G²,N,T	L,W
DH2	32/39-30acc	40 37 11	117 38 02	1,469	0.457	1.50	50.05	164.2	51	2.00	P,C	G,G²,N,T	L
DH3	-31cbb	40 36 13	117 38 29	1,455.252	0.610	2.00	49.98	164.0	51	2.00	P,C	G,G²(2),N(2),T	L
DH4	32/38-25ddc	40 36 43	117 38 45	1,429.4	0.610	2.00	49.83	163.83	51	2.00	P,C	G,G²,N,T	L
DH5	32/39-31cad	40 36 08	117 38 03	1,482	0.914	3.00	27.13	89.0	51	2.00	P,C	G,G²,N,T	L
DH6	31/39- 1aac	40 35 41	117 38 53	1,425.956	0.914	3.00	44.38-44.84	165.5-147.1	38	1.50	St,Sc	G,G²,N,T	L,W
DH7	32/38-25ccd	40 36 43	117 39 35	1,395.932	0.524	1.72	50.44	165.44	51	2.00	P,Sc	G,G²,N,T	L,W
DH8	-35dba	40 35 59	117 39 04	1,394.2	0.914	3.00	44.56-	146.2	38	1.50	St,Sc	G,G²,N,T	L,W
DH9	-36dcb	40 35 39	117 39 40	1,417.146	0.914	3.00	44.56-45.2	146.2-147.7	38	1.50	St,Sc	G,G²,N,T	L,W
DH10	-36ada	40 36 24	117 38 44	1,429.573	0.610	2.00	16.38-16.79	53.6-55.1	38	1.50	St,Sc	G,T	L,W
DH11	-36bdb	40 36 22	117 39 20	1,400.608	0.853	2.80	44.35-44.81	145.5-147.0	38	1.50	St,Sc	G,G²,N,R,T	L,W
DH12	31/38- 1bdd	40 35 40	117 39 29	1,401.172	0.518	1.70	44.18-44.64	145.0-146.5	51	2.00	P,Sc	G,G²,N,T	L,W
DH13A	32/38-36daa1	40 36 13	117 38 44	1,440.244	0.610	2.00	51.37-52.28	168.5-171.5	51	2.00	P,Sc	T	W
DH13B	-36daa2	40 36 13	117 38 44	1,440.244	0.607	1.99	41.43	135.9	32	1.25	St,C,c	T	
DH14A	-36abb1	40 36 34	117 39 02	1,415.186	0.305	1.00	45.00-	147.6-	51	2.00	P,Sc	G,G²,N,T	L,W

TABLE 1 -- Data for wells and test wells in southern Grass Valley (Continued)

Name of test well	Location number	Latitude north	Longitude west	Altitude of land surface m	Height of measuring point above land surface m	Height of measuring point above land surface ft	Depth of screen or cap at bottom m	Depth of screen or cap at bottom ft	Nominal inside diameter of casing mm	Nominal inside diameter of casing in	Type of completion 1/	Geophysical logs available 2/	Other data available 3/
DH14B	-36abb2 40 36 34		117 39 02	1,415.186	0.302	0.99	32.07	105.2	51	2.00	P,C	T	
DH15	32//39-31ccd 40 35 53		117 38 26	1,455	0.594	1.95	44.39	145.6	51	2.00	P,C	G,G²,N,T	L
QH1A	32/39-31bbb1 40 36 38		117 38 26	1,446.023	0.101	0.33	137.15	449.67	32	1.25	St,C,c	R,T,G,G²,N,T	L,Cs
QH1B	-31bbb2 40 36 3		117 38 26	1,446.023	0.152	0.50	152.4-(32.9)4/	500 (108)4/	38	1.50	St,Sc,c		M
QH1C	-31bbb3 40 36 38		117 38 26	1,446.023	0.128	0.42	25.20-25.66	82.68-84.19	35	1.50	St,Sc		L,M,Cs
QH2A	32/39-19dba1 40 37 59		117 37 48	1,490	-0.085	-0.28	134.00	441.27	32	1.25	St,C,c	R,T,G,G²,N	L,Cs
QH2B	-19dba2 40 37 59		117 37 40	1,490	-0.061	-0.2	152.92-153.38	501.71-503.22	38	1.50	St,Sc,c		
QH3A	31/38-14acd1 40 33 42		117 40 07	1,434.38	0.093	0.305	140.12	459.71	32	1.25	St,C,c	R,T,G,G²,N	L,Cs
QH3B	-14acd 40 33 42		117 40 07	1,434.74	0.258	0.845	153.82	504.66	38	1.50	St,C,c	R,T,G,G²,N	M,C
QH3C	-14acd3 40 33 42		117 40 07	1,434.74	0.401	1.316	63.45-63.91	208.17-209.68	38	1.50	St,Sc		M
QH3D	-14acd4 40 32 37		117 42 40	1,434.74	1.307	4.289	408.7-(410.2)4/	1,340-(1,345)4/			St	R,T,G,G²,N	L,Cs
QH4A	31/38-22caa1 40 32 40		117 42 40	1,519	0.168	0.55	123.58	405.45	32	1.25	St,C,c	R,T,G,G²,N	L,Cs
QH4B	-22caa2 40 32 39		117 42 40	1,519	0.290	0.95	127.27-127.73	417.55-419.06	38	1.50	St,Sc,c		M
QH5A	32/38-14acc1 40 38 53		117 40 14	1,390.93	0.396	1.30	130	425	32	1.25	St,C,c	R,T,G	L,Cs
QH5B	-14acc2 40 38 53		117 40 14	1,390.933	1.103	3.62	130	425	51	2.0	P,Sc,c		M,C
QH6A	32/38-21ada1 40 38 11		117 42 11	1,378.234	0.457	1.50	55	180	32	1.25	St,S,c	R,T,G	L,Cs
QH6B	-21ada2 40 38 11		117 42 11	1,379	0.351	1.15	55	180	51	2.0	P,Sc,c		M,C

TABLE 1 -- Data for wells and test wells in southern Grass Valley (Continued)

Name of test well	Location number	Latitude north	Longitude west	Altitude of land surface m	Height of measuring point above land surface m	Height of measuring point above land surface ft	Depth of screen or cap at bottom m	Depth of screen or cap at bottom ft	Nominal inside diameter of casing mm	Nominal inside diameter of casing in	Type of completion [1]	Geophysical logs available [2]	Other data available [3]
QH7A	31/38-3aac1	40 35 41	117 41 08	1,396.530	0.427	1.40	75	245	32	1.25	St,C,c	R,T,G	L,C$_s$
QH7B	-3aac2	40 35 41	117 41 08	1,396.530	0.792	2.60	75	245	51	2.00	P,Sc,c		W,C
QH8A	31/39-7aaa1	40 35 55	117 37 25	1,478.264	0.762	2.50	50	165	32	1.25	St,C,c	R,T,G	L,C$_{sE}$
QH8B	-7aaa1	40 34 55	117 37 25	1,478.264	0.088	0.29	50	165	51	2.00	P,Sc,c		W
QH9A	31/39-17abc1	40 33 55	117 36 41	1,478.554	0.702	2.60	91	300	32	1.25	St,C,c	R,T,G	L,C$_s$
QH9B	-17abc2	40 33 55	117 36 44	1,478.554	0.972	3.19	91	300	51	2.00	P,Sc,c	R,T,G	L,C$_s$
QH11A	31/38-16aca1	40 33 51	117 42 29	1,484	0.582	1.91	55	182	32	1.25	St,C,c	R,T,G	L,C$_s$
QH11B	-16aca2	40 33 51	117 42 29	1,481	0.396	1.30	55	182	51	2.00	P,Sc,c		W
QH12A	31/39-34bab1	40 31 23	117 34 49	1,512	0.396	1.30	53	173	32	1.25	St,C,c	R,T,G	L,C$_s$
QH12B	-34bab2	40 31 23	117 34 49	1,512	0.600	1.97	53	173	51	2.00	P,Sc,c		W
Q1	32/38-26bba	40 37 31	117 40 42	1,385.6	.30	1.0	188 (61.0)[4]	617 (200)[4]	32	1.25	St,C,c	G,G$_2$,N,T,R	L,C$_s$,W
Q2	31/39-12daa	40 34 25	117 38 25	1,419			162	532	32	1.25	St,C,c	G,G$_2$,N,T,R	L,C$_s$
Q3	31/39-28aad	40 32 16	117 35 15	1,491			175	575	32	1.25	St,C,c	G,G$_2$,N,T,R	L,C$_s$
Q4	31/38-24ccd	40 37 36	117 39 35	1,403			66	215	51	2.00	P,C	R,T,G	L,C$_s$
Q5	32/39-30bba	40 37 31	117 38 19	1,454			107	350	51	2.00	P,C	R,T,G	L,C$_s$
Q6	32/38-29bba	40 37 27	117 44 12	1,393	.61	2.0	59.7 (45.7)[4]	195 (150)[4]	51	2.00	P,C	R,T,G	L,C$_s$
Q7	31/38-4dab	40 35 17	117 42 10	1,402			75	245	51	2.00	P,C	R,T,G	L,C$_s$
Q8	31/38-8aac	40 34 47	117 43 22	1,437			75	245	51	2.00	P,C	R,T,G	L,C$_s$
Q9	31/38-10dcc	40 34 12	117 41 22	1,438			58	190	51	2.00	P,C	R,T,G	L,C$_s$

14

TABLE 1 -- Data for wells and test wells in southern Grass Valley (Continued)

Name of test well	Location number	Latitude north	Logitude west	Altitude of land surface m	Height of measuring point above land surface m	Height of measuring point above land surface ft	Depth of screen or cap at bottom m	Depth of screen or cap at bottom ft	Nominal inside diameter of casing mm	Nominal inside diameter of casing in	Type of completion 1/	Geophysical logs available 2/	Other data available 3/
Q10	31/38-12cdc	40 34 07	117 39 28	1,643			56	185	51	2.00	P,C	R,T,G	L,C$_s$
Q11	31/38-14ccc	40 33 18	117 40 34	1,466			83	272	51	2.00	P,C	R,T,G	L,C$_s$
Q12	31/38-23dca	40 32 32	117 40 05	1,463			67	230	51	2.00	P,C	R,T,G	L,C$_s$
Q13	31/39-24ddd	40 32 22	117 38 38	1,436			101	330	51	2.00	P,C	R,T,G	L,C$_s$
Q14	31/39-29bbb	40 32 15	117 37 19	1,447			87	285	51	2.00	P,C	R,T,G	L,C$_s$
Q15	31/39-28bcb	40 32 09	117 36 23	1,465			53	175	51	2.00	P,C	R,T,G	L,C$_s$
Q16	31/39-21dcb	40 32 34	117 35 43	1,496			82	270	51	2.00	P,C	R,T,G	L,C$_s$
Q17	31/39-27acc	40 31 55	117 34 28	1,527			76	250	51	2.00	P,C	R,T,G	L,C$_s$
Q18	32/38-18aba	40 39 10	117 94 37	1,375			64	210	51	2.00	P,C	R,T,G	L,C$_s$
Q19	32/38-34bbd	40 36 34	117 41 36	1,389			59	195	51	2.00	P,C	R,T,G	L,C$_s$
Q20	31/38-2dcc	40 34 56	117 40 12	1,405			72	235	51	2.00	P,C,	R,T,G	L
Q21	31/38-13cdd	40 33 12	117 39 12	1,433			64	211	51	2.00	P,C	R,T,G	L,C$_s$
Q22	31/39-20bbc	40 33 14	117 37 24	1,442			49	160	51	2.00	P,C	R,T,G.	L,C$_s$
Q23	31/39-6cca	40 35 09	117 38 19	1,433.5			152	500	51	2.00	St,C,c	T	L
Q24	31/39-35caa	40 31 00	117 33 29	1,518			152	500	51	2.00	St,C,c	T	L
QH13A	31/31-22abd1	40 33 00	117 34 25	1,548	0.503	1.65	55	180	32	1.25	St,C,c	R,T,G	L,C$_s$
QH13B	-22abd2	40 33 00	117 34 25	1,548	0.488	1.60	55	180	51	2.00	P,C,c		W,C
QH14A	32/38-32dbd1	40 36 16	117 43 39	1,407	0.213	0.70	85	280	32	1.25	St,C,c	R,T,G.	L,C$_s$,C
QH14B	-32dbb2	40 36 16	117 43 39	1,616	0.216	0.71	85	280	51	2.00	P,Sc,c		W

TABLE 1 -- Data for wells and test wells in southern Grass Valley (Continued)

Name of test well	Location number	Latitude north	Logitude west	Altitude of land surface m	Height of measuring point above land surface m	ft	Depth of screen or cap at bottom m	ft	Nominal inside diameter of casing mm	in	Type of completion 1/	Geophysical logs available 2/	Other data available 3/
T1	-----	40 33 59	117 40 52	1,440.2	----	---	---	--	---	---	P,C	T	---
T2	-----	40 33 48	117 40 19	1,433.5	----	---	---	--	---	---	P,C	T	---
T3	-----	40 33 40	177 40 19	1,439.3	----	---	---	--	---	---	P,C	T	---
T21	-----	40 32 11	117 34 24	1,540.3	----	---	---	--	---	---	P,C	T	---
T22	----	40 31 08	117 35 03	1,510.4	----	---	---	--	---	---	P,C	T	---
T23	----	40 34 51	117 39 24	1,408.5	----	---	---	--	---	---	P,C	T	---
T24	-----	40 34 22	117 39 42	1,415.2	----	---	---	--	---	---	P,C	T	---
T25	-----	40 33 09	117 40 29	1,461.9	----	---	---	--	---	---	P,C	T	---
T26	----	40 33 18	117 39 52	1,441.7	----	---	---	--	---	---	P,C	T	---
T27	-----	40 38 00	117 44 28	1,387.8	----	---	---	--	---	---	P,C	T	---
T28	----	40 38 44	117 44 45	1,380.4	----	---	---	--	---	---	P,C	T	---
T29	----	40 38 42	117 45 27	----	----	---	---	--	---	---	P,C	T	---
T30	----	40 39 13	117 45 28	----	----	---	---	--	---	---	P,C	T	---
T31	----	40 39 04	117 44 01	1,374.0	----	---	---	--	---	---	P,C	T	---
G2	32/38-26acb	40 37 14	117 39 59	1,396.3	----	---	152.4	500	38	1.50	St,C	T	---
G3	32/39-29dcc	40 37 09	117 37 23	1,521.3	----	---	152.4	500	38	1.50	St,C	T	---
G4	32/38-35bcd	40 35 57	117 40 17	1,397.8	----	---	152.4	500	38	1.50	St,C	T	---
G5a	32/39-32dbd	40 36 25	117 37 07	1,536.6	----	---	152.4	500	25	1.00	St,C	T	---
G7	32/39-32dbd	40 36 25	117 37 07	1,536.6	----	---	152.4	500	25	1.00	St,C	T	---
G8	31/39-8dda	40 34 52	117 37 15	1,493.9	----	---	152.4	500	38	1.50	St,C	T	---

16

TABLE 1 -- Data for wells and test wells in southern Grass Valley (Continued)

Name of test well	Location number	Latitude north	Longitude west	Altitude of land surface m	Height of measuring point above land surface m	ft	Depth of screen or cap at bottom m	ft	Nominal inside diameter of casing mm	in	Type of completion 1/	Geophysical logs available 2/	Other data available 3/
G9	31/39-14cda	40 33 32	117 33 46	1,603.6	-----	---	134.1	440	38	1.50	St,C	T	---
G10	31/39-20aad	40 33 03	117 36 25	1,469.5	-----	---	152.4	500	38	1.50	St,C	T	---
G11	31/39-29acd	40 32 01	117 36 49	1,457.3	-----	---	152.4	500	38	1.50	St, C	T	---
G12	31/39-28cba	40 31 36	117 35 42	1,487.8	-----	---	152.4	500	38	1.50	St,C	T	---
G13	31/39-33bac	40 30 50	117 35 19	1,503.0	-----	---	146.3	480	38	1.50	St,C	T	---
G14	30/39-4dcc	40 30 11	117 36 16	1,481.7	-----	---	152.4	500	38	1.50	St,C	T	---
G15	30/39-3caa	40 30 02	117 34 43	1,512.1	-----	---	152.4	500	38	1.50	St,C	T	---
G105	31/39-6bcc	40 35 30	117 38 31	1,436.9	-----	---	352.1,[4/] (139.3)[4/]	115 (457)[4/]	51	2.00	St,C	T	L,W
G106	31/39-18caa	40 33 33	117 38 02	1,434.4	-----	---	454.8	1,492	51	2.00	St,C	T	L
G108	31/39-27caa	40 31 48	117 34 32	1,525.0	-----	---	448.1	1,470	51	2.00	St,C	T	L,W
T4	-----	40 33 33	117 40 13	1,442.3	-----	---	---	---	--	----	P,C	T	---
T5	-----	40 33 35	117 39 52	1,435.0	-----	---	---	---	--	----	P,C	T	---
T6	-----	40 33 53	117 39 59	1,428.3	-----	---	---	---	--	----	P,C	T	---
T7	-----	40 33 22	11739 28	1,434.7	-----	---	---	---	--	----	P,C	T	---
T8	-----	40 32 12	117 36 58	1,451.8	-----	---	---	---	--	----	P,C	T	---
T9	-----	40 32 10	117 36 36	1,463.4	-----	---	---	---	--	----	P,C	T	---
T10	-----	40 32 05	117 35 49	1,487.8	-----	---	---	---	--	----	P,C	T	---
T11	-----	40 32 01	117 35 15	1,500.9	-----	---	---	---	--	----	P,C	T	---
T12	-----	40 31 57	117 34 51	1,512.8	-----	---	---	---	--	----	P,C	T	---

TABLE 1 -- Data for wells and test wells in southern Grass Valley (Continued)

Name of test well	Location number	Latitude north	Logitude west	Altitude of land surface m	Height of measuring point above land surface m	ft	Depth of screen or cap at bottom m	ft	Nominal inside diameter of casing mm	in	Type of completion [1]	Geophysical logs available [2]	Other data available [3]
T13	----	40 31 53	117 34 08	1,546.4	----	----	--	---	--	---	P,C	T	---
T14	----	40 33 15	117 34 00	1,573.2	----	----	--	---	--	---	P,C	T	---
T15	----	40 32 50	117 35 01	1,523.5	----	----	--	---	--	---	P,C	T	---
T16	----	40 32 53	117 36 09	1,487.2	----	----	--	---	--	---	P,C	T	---
T17	----	40 32 25	117 35 29	1,498.2	----	----	--	---	--	---	P,C	T	---
T18	----	40 31 32	117 34 16	1,537.5	----	----	--	---	--	---	P,C	T	---
T19	----	40 31 32	117 34 16	1,537.5	----	----	--	---	--	---	P,C	T	---
T20	----	40 31 30	117 34 35	1,519.8	----	----	--	---	--	---	P,C	T	---

Name of well	Location number	Latitude north	Longitude west	Altitude of land surface m	Altitude of measuring point m	ft	Depth of well or perforation m	ft	Nominal inside diameter of casing mm	in	Other data available	Description of well
Goldbanks windmill	30/39-16abb	40 29 20	117 35 51	-----	1,475.695	4,841.46	----	---	---	----	W	Windmill
Mine well (old)	31/39-4ccc	40 33 12	117 23 58	-----	1,562	5,125	----	---	---	----	W	Engine, Pump
------	31/38-26abb	40 32 14	117 40 12	1,473	1,473	4,831	60	117	153	6.00	W	Abandoned windmill
Quicksilver windmill	31/38-34ada	40 31 10	117 40 50	-----	1,406	4,875	----	---	---	----	W	Windmill
Mine well (new)	31/39-27bbb	40 32 17	117 35 00	-----	1,503	4,931	----	---	---	----	W	Engine, pump

TABLE 1 -- Data for wells and test wells in southern Grass Valley (Continued)

Name of well	Location number	Latitude north	Longitude west	Altitude of land surface m	Altitude of measuring point m	Altitude of measuring point ft	Depth of well or perforation m	Depth of well or perforation ft	Nominal inside diameter of casing mm	Nominal inside diameter of casing in	Other data available	Description of well
Mud Springs ranch (new)	31/39-29dcc	40 31 28	117 36 47	-----	1,460.781	4,792.53	90.2	296	406	16.00	W	Irrigation, engine, pump
Mud Springs Ranch (old)	31/39-32abc	40 31 18	117 36 48	1,460	1,460.403	4,791.29	----	----	---	-----	W	Irrigation, engine, pump
Turner	32/38-18acc	40 38 54	117 44 54	-----	1,378	4,521	38.1	125	153	6.00	W	Windmill
-----	32/38-33bcc	40 36 15	117 43 06	1,378	1,431	- 4,695	----	----	---	-----	W	--------
Hot Springs Ranch	32/38-36cba	40 36 12	117 39 28	1,397.139	1,397.766	4,585.71	24.4-	90-	305	12	W	Irrigation

Footnotes:

1/ St, galvanized-steel pipe; P, polyvinyl chloride (PVC) pipe; Sc, screen or wellpoint at bottom; C, capped at bottom and filled with water; c, cement seal in annulus (all other holes sealed with drill cuttings and/or surface materials).

2/ G, natural gamma log; G_2, gamma-gamma (density) log; N, neutron log; T, temperature log; R, resistivity log.

3/ L, lithologic log; W, water level measurements; T_p, temperature profile; C, chemical analysis of water; C_s, core sample (s).

4/ Wells were initally capped. The value in parentheses indicates the depth to perforations which were shot in June 1977 (QH3D, QH1B) May 1980. (Q1, Q6, G105, G108).

19

were fitted with well points. A T-prefix was assigned to a series of shallower wells (15-18 m) drilled to help define the detail around known anomalies and isolated deeper holes Several wells have also been drilled for Sunoco Energy Development Co. by Geotherm Ex Inc. as part of a geothermal exploration effort --these wells have been given an "G" prefix.

Conversion of Units

The metric system is used throughout this report, although some of the original measurements and data were reported in inch-pound units. Thermal parameters are given in the more familiar "working units" rather than in the now-standard SI (Systeme Internationale) units. Table 2 lists metric and equivalent inch-pound units, and "working units" and equivalent SI units for the thermal parameters.

TABLE 2.-- Conversion factors between units.

Metric units		Inch-pound units
Length		
millimeter (mm)	=	3.937×10^{-2} inch (in)
meter (m)	=	3.281 feet (ft)
kilometer	=	.6241 mile (mi)
Area		
centimeter^2 (cm^2)	=	.1550 inch^2 (in^2)
meter^2 (m^2)	=	10.76 feet^2 (ft^2)
hectare (ha)	=	2.471 acres
Kilometer^2 (km^2)	=	247.1 acres
	=	.3861 mile^2 (mi^2)
Volume		
centimeter^3 (cm^3)	=	6.102×10^{-2} inch^3 (in^3)
liter (L)	=	.2646 gallon (gal)
	=	3.531×10^2 foot^3 (ft^3)
meter^3	=	35.31 feet^3 (ft^3)
	=	8.107×10^{-4} acre-foot (ac-ft)
hectometer^3 (hm^3)	=	8.107×10^2 acre-feet (ac-ft)
kilometer^3 (km^3)	=	.2399 mile^3 (mi^3)

TABLE 2.-- Conversion factors between units (Continued).

Metric units		Inch-pound units

Flow

liter per second (L/s)	=	15.85 gallons per minute (gal/min)
	=	25.58 acre-feet per year (ac-ft/yr)
hectometer^3 per year (hm^3/yr)	=	8.107 x 10^2 acre-feet per year (ac-ft/yr)
kilogram per second (kg/s)	=	7.938 x 10^3 pounds per hour (lb/hr)

Mass

gram (g)	=	3.528 x 10^{-2} ounce (oz)
kilogram (kg)	=	2.205 pounds (lb)

Density

grams per centimeter^3 (g/cm^3)	=	62.43 pounds per foot^3 (lb/ft^3)

Pressure

bar	=	14.50 pounds per square inch (psi)

Temperature

degrees Celsius (°C)	=	(degrees Fahrenheit -32) ÷ 1.8 (°F - 32) ÷ 1.8

Permeability

micrometer^2 (μm^2)	=	18.4 gallons per day per foot^2 @ 60°F (gal/day x ft^2 @ 60°F)

22

TABLE 2.-- Conversion factors between units (Continued).

Metric units	Inch-pound units

<center>Thermal parameters</center>

Working units	International system of units (SI units)

<center>Thermal conductivity</center>

thermal conductivity unit (tcu) (mcal/cm x s x °C)	=	41.87 milliwatts per meter x degree kelvin (mW/m x °K)

<center>Heat capacity</center>

calories per gram x degree Celsius (cal/g x °C)	=	4.187 joules per gram x degree kelvin (j/g x °K)

<center>Heat flow</center>

heat flow units (hfu) (μ cal/cm^2 x s)	=	41.87 milliwatts per meter^2 (mW/m^2)

<center>Energy</center>

calorie (cal)	=	4.187 joules (J)
kilocalorie (kcal)	=	4,187 joules (J)

<center>Heat discharge</center>

calorie per second (cal/s)	=	4.187 watts (w)

HYDROGEOLOGIC FRAMEWORK

Location and Physiographic Features

Leach Hot Springs is in southern Grass Valley, approximately 50 km south of the city of Winnemucca, within a region of active and fossil geothermal systems (fig. 2). Grass Valley is a fairly typical alluviated basin within the Basin and Range province. The altitude within the study area varies from about 1,375 m NVGD (National Vertical Geodetic Datum of 1929) in the valley floor to about 2,680 m in the southern Sonoma Range to the east. The valley is bounded by the East Range to the west, the Sonoma Range to the east and the Table Mountain-Goldbanks Hills area to the southwest. It is bounded on the north by the Humboldt River and is separated from Pleasant Valley to the south by a low, subtle drainage divide. The mountains consist primarily of intensely deformed Paleozoic and Mesozoic igneous and metamorphic rocks (pl. 1).

The structural basin has been partly filled with as much as 2 km of mildly deformed to undeformed volcanic rocks and consolidated to semiconsolidated sedimentary rocks. Leach Hot Springs is at the base of a prominent fault scarp. The fault is part of a complex system along which large aggregate displacement has occurred. Other important features of southern Grass Valley include Spaulding and Sheep Ranch Canyons, which appear to provide significant ground-water recharge, and Panther Canyon, the site of a thermal anomaly.

The rock units in the southern Grass Valley area have been described by Johnson (1977), Noble (1975a), and in the vicinity of Leach Hot Springs by Olmsted, Glancy, Harrill, Rush and VanDenburgh (1975). The following description of the units and geologic structure has been derived primarily from these sources.

24
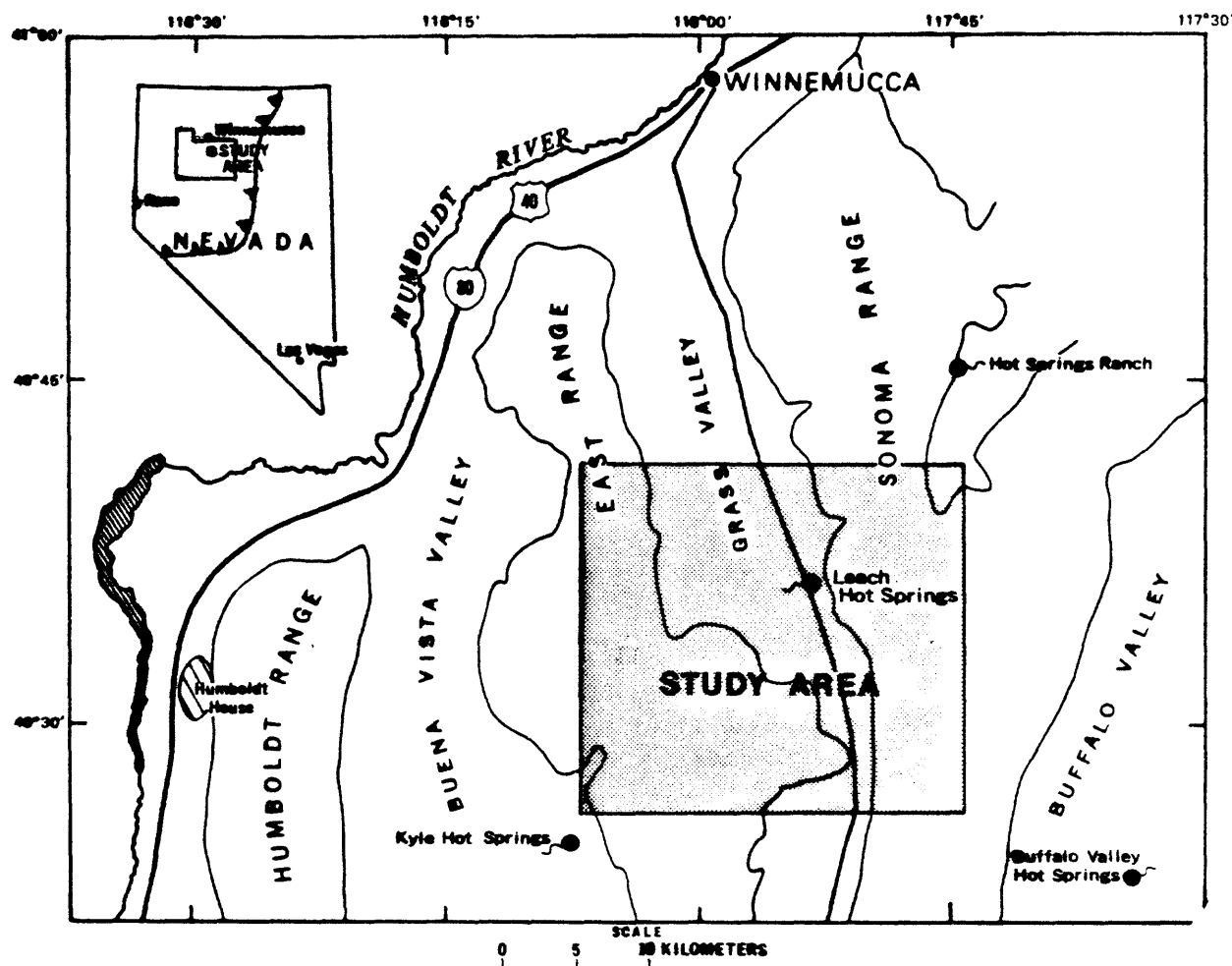
FIGURE 2. -- Index map showing location of study area. Inset map upper in the upper left corner shows the leading edge of the Roberts Mountain thrust with sawteeth on the upper plate, and the outline of Pershing County. Outline of mountain ranges based on 5,000 ft land-surface contour.

Rock Units and Physical Properties of Rocks and Deposits

The physical and chemical characteristics of the rock materials in southern Grass Valley control the flow of fluids and heat as well as the chemical composition of the ground water. A basic knowledge of the geology of the study area is therefore required in order to understand the geothermal system and its relationship to the shallower ground-water system. The general hydrologic and physical properties of the rocks exposed in the area are summarized in table 3, and the results of laboratory measurements made on core samples are presented in table 4. The areal distribution of the mapped rock units is shown on plate 1.

The pre-Tertiary rocks in the southern Grass Valley are lithologically inhomogeneous, structurally complex, and, slightly to moderately metamorphosed. Secondary permeability resulting from fractures and also from dissolution of the carbonate rocks probably controls most ground-water flow in these rocks. Large-scale, interbasin movement of ground water through thick sequences of Paleozoic carbonate rocks in the southern Great Basin has been demonstrated by Winograd and Friedman (1972) and Winograd and Pearson (1976). Thus, the possibility of interbasin flow in carbonate rocks should be evaluated. The thick carbonate assemblage exposed east and south of the study area represents miogeosynclinal deposition with contemporaneous eugeosynclinal deposition to the west. Although subsequent eastward movement of the eugeosynclinal rocks along the Roberts Mountain thrust (fig. 2) has concealed thick sequences of miogeosynclinal carbonate rocks in parts of central Nevada, some windows exist which suggest that a transitional facies composed of a relatively minor amount of carbonate rock types is present beneath the

TABLE 3 -- Physical and hydrologic properties of rock units

Geologic unit	Rock types 1/	Degree of deformation and lithification	Location and extent	Hydrologic Characteristics	Electrical resistivity 2/ (ohm - meters)	Other physical properties	
						Saturated bulk density 3/	Thermal conductivity (tcu)
Cenozoic erathem							
Quaternary alluvium	Unconsolidated fluvial deposits ranging from gravel to silt and clay. Primarily poorly sorted with local silicification.	Relatively undisturbed except near zone of active faulting along the margins of the valley. Unconsolidated except where hydrothermal activity has caused silicification.	Laterally extensive in the basin	Generally low hydraulic conductivity with a low horizontal to vertical permeability ratio due to dominately horizontal stratification. Porosities vary from moderate to high values.		Mean of 22 values 2.03	Mean of 10 values 3.04 standard deviation 0.63
Quarternary Tertiary alluvium	Coarse to fine grained sediments including tuff and volcanic clastics		Only minor exposures along the western base of the Sonoma range. Laterally extensive beneath the younger alluvium.	Similar to the overlying alluvium with somewhat lower permeabilities and porosities due to compaction and lithification. Minor vertical fracturing may allow greater vertical ground-water movement.	Terrestial sands claystone, and artosa 15-50	Mean of 3 values 1.68	Mean of 49 values 3.98 standard deviation 0.71
Tertiary sediments	Simiconsolidated deposits ranging from ash and tuff and tuffaceous sands to mudstone and siltstone. Primarily poorly sorted fanglo-morates which have undergone local silicifica-tion.	Locally these deposits have been faulted and eroded after deposition.	Minor exposures are present in the Goldbanks area. Probably laterally exten-sive beneath the younger sediments.				
Tertiary volcanics	Dark vesicular olivine basalt flows and shallow intrusive rhyolite.		A large part of the Goldbanks area is capped by relatively undisturbed basalt and a minor exposure is present 1.5 km southeast of Leach Hot Springs. Only minor exposures of rhyolite are present in the Sonoma Range.		10-200		mean of 3 values 2.61 standard divipation 0.57
Mesozoic erathem							
Jurassic grandiorite	Grandiorite		Occurs as scattered outcrops in the East and Sonoma ranges	Low primary porosity and permeability due to fracturing and solution cavit-ies in the carbon-ates.	500-2,000	2.67-2.79	6.2-8.3

27

TABLE 3 -- Physical and hydrologic properties of rock units (Continued).

Geologic unit	Rock types 1/	Degree of deformation and lithification	Location and extent	Hydrologic Characteristics	Electrical resistivity 2/ (ohm - meters)	Other physical properties	
						Saturated bulk density 3/	Thermal conductivity (tcu)
Minnemucca and Dun Glen Formations	Limestone, dolo-mite, sand-stone, and fine-grained clastic rocks.	Extensively folded and faulted due to several periods of tectonism.	Minor exposures are present on the eastern flank of the central East Range.	Vertical fractures allow downward movement of ground water which may be at least partially responsible for re-charging the geo-thermal system.	Limestone and dolo-mite 100-10,000	Limestone 2.58-2.72 Dolomite 2.77-2.80 Sandstone 2.17-2.70 Shale 2.06-2.66	Limestone 4.7-7.1 Dolomite 9.6-12.0 Quartzite 14.2-17.0 Sandstone 3.5-10.2 Shale 3.0-6.9
Grass Valley Formation	Mudstone and fine-grained sandstone	Metamorphism ranges from low grade to locally high grade near intrusive contacts.	A moderately large outcrop is pres-ent in the East Range west of Leach Hot Springs	Extensional faulting apparently creates zones of relatively high permeability	Marine sand, shale and graywacke 5-20 Volcanic rocks 20-500 Terrestrial sand, claystone, and arkose 25-100		
Triassic meta-sedimentary rocks	Metamorphosed limestone and shale						
Nachez Pass and Pride Formations	Limestone, dolo-mite, siltstone, and sandstone		Minor exposures are present in the central East Range				
Kiopato Group	Altered porphy-ritic andesite rhyolite, and tuffaceous sed-imentary rocks.		Occurs as scattered outcrops in Goldbanks Hills, East and Sonoma Ranges.				
Triassic leucogranite	Fine- to medium grained granite		One outcrop occures Goldbanks Hills			2.52-2.81	6.2-9.0
Paleozoic erathem							
Havallah Formation	Quartzite, chert, argillite, lime-stone, sandstone, and greenstone		Major parts of Goldbanks Hills, and the southern Sonoma and Tobin Ranges.		Limestone and dolomite 10,000-100,000 Marine sand, shale, and graywacke 40-200 Terrestrial sands, claystone, and arkose 100-500		Typical values given above
Pumpernickle Formation	Greenstone, dark-gray chert, quartzite, and argillite with, minor sandstone and limestone						
Inskip Formation	Sandstone conglom-erate, quartzite, sandy siltstone, and thin limestone		Moderately large area in the west-central East Range				
Valmy Formation	Argillite, chert, greenstone, and vitreous quartzite		Large outcrop area in the East Range				
Harmony Formation	Feldspathic quartz, sandstone, and conglomerate with lesser amounts of argillaceous rocks and limestone		Minor outcrop east of Spaulding canyon and a larger outcrop in the central Sonoma Range				

TABLE 3 -- Physical and hydrologic properties of rock units (Continued).

Footnotes:

1/ From Johnson (1977).

2/ Typical electrical resistivity values are for water-bearing rock types from Keller (1966).

3/ The saturated bulk density data are typical values from Daly and others (1966) for all pre-Cenozoic rock types. All other values are from the data given in table 2.

4/ The thermal conductivity data are typical values for the rock types from Clark (1966) for all pre-Cenozoic rocks with values determined at 20°C on dry samples. All other values are from saturated samples collected during this study. The individual measurements are listed in table 4.

TABLE 4. -- Physical properties of cores from southern Grass Valley.

Well	Depth ft	Depth m	Lithologic description	Grain density (g/cm³)	Saturated bulk density (g/cm³)	Dry bulk density (g/cm³)	Moisture content by weight	Moisture content by volume	Total porosity (percent)	Effective porosity at 2,000 psi (percent)	Thermal conductivity of solid (tcu)	Saturated bulk thermal conductivity (tcu)	Standard deviation	Computed thermal conductivity (tcu)	Computed porosity (percent)	Median size (mm)	Sorting Coefficient	Skewness	Kurtosis	Uniformity Coefficient	Vertical hydraulic conductivity at 60°F (15.5°C) (m/s)	Formation
0-1	172-210	52.2-64.0	Clay and silt; tan; rare pebbles of chert and quartzite	--	--	--	--	--	--	--	--	3.79	--	--	--	--	--	--	--	--	--	Qal or QT
	207	63.1	Homogeneous clay	2.71	--	1.64	--	--	39.5	--	--	--	--	--	--	--	--	--	--	--	--	Do.
	400-410	121.9-125.0	Clay and silt; tan; 5-20 percent medium to coarse sand	--	--	--	--	--	--	--	--	3.27	--	--	--	--	--	--	--	--	--	Do.
	405	123.5	Lithic graywacke	2.69	--	1.69	--	--	37.2	--	--	--	--	--	--	0.04	4.9	0.28	--	--	--	Do.
	406	123.8	Homogeneous silt and clay	2.62	--	1.40	--	--	46.6	--	--	--	--	--	--	0.02	4.4	0.73	--	--	--	Do.
	408	124.4	Moderately sorted silt and clay	2.69	--	1.46	--	--	45.7	--	--	--	--	--	--	0.08	20.	0.67	--	--	--	Do.
	550-552	167.6-168.1	Clay to very fine sand, tan	--	--	--	--	--	--	--	--	3.38	--	--	--	--	--	--	--	--	--	Do.
	550-555	167.7-169.2	Mudstone	2.76	--	1.70	--	--	38.4	--	--	--	--	--	--	0.03	3.3	1.5	0.07	20	--	Do.
	550-555	167.7-169.2	Lithic graywacke	2.67	--	2.23	--	--	16.5	--	--	--	--	--	--	0.01	5.1	2.0	--	--	--	Do.
0-2	205-209	62.5-63.6	Conglomerate, 20-40 percent matrix of tan clay and silt; ill-sorted	--	--	--	--	--	--	--	--	4.84	--	--	--	--	--	--	--	--	--	Do.
	208	63.4	Graywacke	2.72	--	2.03	--	--	25.4	--	--	--	--	--	--	0.27	5.0	0.71	0.08	925.	--	Do.
	402-411	122.5-125.2	Clay, silt, and "conglomerate," 5-50 percent of chert, quartzite pebbles	--	--	--	--	--	--	--	--	3.34	--	--	--	--	--	--	--	--	--	Do.
	410	12.5	Proto quartzite	2.67	--	1.55	--	--	41.9	--	--	--	--	--	--	0.02	3.7	0.75	--	--	4.4 x 10⁻⁶	Do.
0-3	212-216	64.6-66.0	Clay, silt and "conglomerate" 40-60 percent of chert, quartzite pebbles	--	--	--	--	--	--	--	--	4.78	--	--	--	--	--	--	--	--	--	Do.
0-3	214	65.2	Mudstone	2.70	--	1.98	--	--	26.7	--	--	--	--	--	--	0.67	7.2	0.31	0.18	1,060.	--	Do.

30

TABLE 4. -- Physical properties of cores from southern Grass Valley (Continued).

Well	Depth (ft)	Depth (m)	Lithologic description	Grain density (g/cm³)	Saturated bulk density (g/cm³)	Dry bulk density (g/cm³)	Moisture content by weight	Moisture content by volume	Total porosity (percent)	Effective porosity at 2,000 psi (percent)	Thermal conductivity of solid (tcu)	Saturated bulk thermal conductivity (tcu)	Standard deviation	Computed thermal conductivity (tcu)	Computed porosity (percent)	Median size (mm)	Sorting Coefficient	Skewness	Kurtosis	Uniformity Coefficient	Vertical hydraulic conductivity at 60°F (15.5°C) (m/d)	Formation
Q-3	428-429	120.0-120.6	Clay, silt, and conglomerate, some coarse sand	--	--	--	--	--	--	--	--	3.72	--	--	--	--	--	--	--	--	--	Qal or Qfg
	421	128.4	Graywacke	--	--	--	--	--	--	--	--	--	--	--	--	.06	--	--	--	--	--	Do.
	540-541	164.6-165.9	Conglomerate, ill-sorted, pebbles of chert, quartzite, and andesite	--	--	--	--	--	--	--	--	--	--	--	--	--	--	--	--	--	--	Do.
	541	16.5	Subgraywacke	2.65	--	1.75	--	--	34.0	--	--	--	--	--	--	0.56	11.	0.04	--	--	--	Do.
	548	167.1	Lithic graywacke	2.66	--	1.48	--	--	44.4	--	--	--	--	--	--	0.48	2.0	1.0	0.15	9.7	--	Qal
Q-4	170-175	51.8-53.3	Clayey sandstone, yellowish-brown, poorly sorted	2.72	2.10	1.74	0.204	0.355	41.8	--	5.54	3.49	--	3.12	0.330	--	--	--	--	--	--	Qfg or Ts
Q-5A	203-205	61.9-62.5	Clay, silty, and gravel, poorly sorted	--	--	--	--	--	14.6	--	7.0	4.52	--	5.53	.272	--	--	--	--	--	--	Qfg or Ts
Q-5A	250-251	76.2-76.5	Clay, silty, pebbly; buff-brown, poorly sorted	--	--	--	--	--	--	--	--	3.69	1.06	--	--	--	--	--	--	--	--	Do.
Q-6	110-115	33.5-35.0	Gravel (chert), and clay, silt, grit; and pebbles	--	--	--	--	--	--	--	--	4.33	1.95	--	--	--	--	--	--	--	--	Qal
Q-6	187-192	57.0-58.5	Conglomerate, very tight	2.66	--	--	--	--	23.7	--	6.22	4.12	.49	4.37	.276	--	--	--	--	--	--	Qal or Qfg
Q-7	106-112	32.3-34.1	Clay, sandy, and fine gravel	2.66	2.12	1.76	.203	.357	--	--	8.15	3.37	.31	4.49	.501	--	--	--	--	--	--	Qal
Q-8	190-195	57.9-59.4	Clay, silty and sandy.	2.69	2.28	2.03	.185	.376	28.0	16.7	6.3	4.17	.16	4.13	.274	--	--	--	--	--	--	Qfg or Ts
	190-195	57.9-59.4	Poorly sorted sandstone	--	--	--	--	--	21.3	16.7	--	--	--	--	--	--	--	--	--	--	--	Do.
Q-8	95-100	29.0-30.5	Tuff, light bluish-gray, bedded	2.44	1.44	.74	.035	.618	--	--	3.6	1.86	.07	1.66	.699	--	--	--	--	--	--	Tv (Ts)
	100-105	30.5-32.0	do.	--	--	--	--	--	--	--	3.6	--	--	--	--	--	--	--	--	--	--	Do.
	212-217	64.6-66.1	Clay, tuffaceous, yellowish-buff; some quartz grains	2.42	1.60	1.03	.576	.593	46.1	37.9	4.46	3.01	.13	2.55	.339	--	--	--	--	--	--	Do.

TABLE 4. -- Physical properties of cores from southern Grass Valley (Continued).

Well	Depth ft	Depth m	Lithologic description	Grain density (g/cm³)	Saturated bulk density (g/cm³)	Dry bulk density (g/cm³)	Moisture content by weight	Moisture content by volume	Total porosity (percent)	Effective porosity - 2,000 psi (percent)	Thermal conductivity of solids (tcu)	Saturated bulk thermal conductivity (tcu)	Standard deviation	Computed thermal conductivity (tcu)	Computed porosity (percent)	Median size (mm)	Sorting Coefficient	Skewness	Kurtosis	Uniformity Coefficient	Vertical hydraulic conductivity at 60°F (15.5°C) (m/d)	Formation
Q-8	212-217	64.6-66.1	Well sorted siltstone	--	--	--	--	--	58.4	37.9	--	--	--	--	--	--	--	--	--	--	--	Ts
Q-9	107-110	32.6-33.5	Clay, sandy, and gravel	--	--	--	--	--	--	--	--	4.68	.63	--	--	--	--	--	--	--	--	Qal? or QTg
	160-165	48.8-50.3	Gravel, silty, gravel, and sandy clay	2.68	1.98	1.56	.274	.427	42.0	--	10.057	3.49	.14	4.39	.537	--	--	--	--	--	--	Do.
Q-10	110-115	33.5-35.0	Siltstone, clayey, reddish-brown, few pebbles	2.65	2.00	2.05	.352	.722?	43.8	28.0	8.3	2.9	.09	3.81	.591	--	--	--	--	--	--	Qal?
	110-115	33.5-35	Well sorted mudstone	--	--	--	--	--	39.1	28.0	--	--	--	--	--	--	--	--	--	--	--	Do.
	160-165	48.8-50.3	Claystone, sandy	--	--	--	--	--	--	--	--	4.09	.18	--	--	--	--	--	--	--	--	Ts?
Q-11	250-255	76.2-77.7	Clay and sandy clay with gravel	--	--	--	--	--	--	--	--	4.87	.59	--	--	--	--	--	--	--	--	QTg or Ts
Q-12	152-157	46.3-47.0	Grit, clay, and angular gravel	--	--	--	--	--	26.0	--	8.3	4.39	45	5.23	.358	--	--	--	--	--	--	Do.
	190-195	57.9-59.4	Clay, gritty and sandy	2.78	2.19	1.86	.187	.348	--	12.6	5.16	3.35	.27	3.35	.331	--	--	--	--	--	--	Do.
	190-195	57.9-59.4	Conglomerate	--	--	--	--	--	24.1	12.6	--	--	--	--	--	--	--	--	--	--	--	Do.
Q-13	280-285	85.3-86.9	Clay, gravelly	2.60	2.18	1.89	.158	.299	36.8	--	7.1	4.38	.31	4.40	.298	--	--	--	--	--	--	Do.
Q-14	96-101	29.3-30.8	Clay, gravelly and gritty	2.76	2.19	1.87	.157	.294	--	--	6.8	4.93	1.03	4.87	.315	--	--	--	--	--	--	Do.
	153-156	46.6-47.6	Clay, gravelly and sandy	--	--	--	--	--	--	--	--	5.21	--	--	--	--	--	--	--	--	--	Do.
Q-15	95-100	29.0-30.5	Clay	2.66	1.54	.87	.719	.626	60.4	--	--	2.58	.09	2.13	.522	--	--	--	--	--	--	Qal
	140-145	42.7-44.2	Tuff, white, siliceous	2.76	2.13	1.77	.154	.273	--	--	5.03	2.97	.06	3.18	.412	--	--	--	--	--	--	Tv
Q-16	160-165	48.8-50.3	Silt, clayey, with gravel	2.72	2.24	1.96	.151	.290	--	--	7.01	3.16	.24	4.47	.495	--	--	--	--	--	--	Qal or QTg
	218-223	66.4-68.0	Sand, medium, well sorted	--	--	--	--	--	--	--	--	3.57	.37	--	--	--	--	--	--	--	--	Do.
Q-17	247-252	75.3-76.8	Gravel and gritty clay	--	--	--	--	--	26.9	--	7.4	4.63	.14	4.73	.282	--	--	--	--	--	--	QTg or Ts
	110-115	33.5-35.1	Clay, brown with sand and pebbles	2.74	2.22	1.92	.169	.206	--	--	6.6	4.06	.39	5.00	.413	--	--	--	--	--	--	Qal or QTg
	215-220	65.5-67.1	Clay, gravelly	--	--	--	--	--	--	--	--	4.61	--	--	--	--	--	--	--	--	--	QTg or Ts

32

TABLE 4. -- Physical properties of cores from southern Grass Valley (Continued).

Well	Depth ft	Depth m	Lithologic description	Grain density (g/cm³)	Saturated bulk density (g/cm³)	Dry bulk density (g/cm³)	Moisture content by weight	Moisture content by volume (?)	Total porosity (percent)	Effective porosity at 2,000 psi (percent)	Thermal conductivity of solids (tcu)	Saturated bulk thermal conductivity (tcu)	Standard deviation	Computed thermal conductivity (tcu)	Computed porosity (percent)	Median size (mm)	Sorting coefficient	Skewness	Kurtosis	Uniformity coefficient	Vertical hydraulic conductivity at 60°F (15.5°C) (m/d)	Formation
Q-10	90-95	27.4-29.0	Sand, clayey, brown	2.60	2.24	2.01	.4347	(?)	20.6	17.3	5.23	3.89	.24	3.88	.225	--	--	--	--	--	--	Qal or QTg
	98-95	27.4-28.9	Moderately sorted sandstone	--	--	--	--	--	18.9	17.3	--	--	--	--	--	--	--	--	--	--	--	Do.
Q-19	100-105	54.9-56.6	Clay, brown, sandy	2.69	1.90	1.43	.352	.503	21.4	--	6.09	4.03	.29	3.06	.281	--	--	--	--	--	--	Do.
	80-85	24.4-25.9	Clay and fine to medium gravel	--	--	--	--	--	--	--	--	4.12	.13	--	--	--	--	--	--	--	--	Do.
Q-21	81-85	24.7-25.9	Sandstone, silty, abundant pebbles	--	--	--	--	--	--	--	--	4.63	.57	--	--	--	--	--	--	--	--	QTg or Ts
Q-22	80-85	24.4-25.9	Clay, brown, silty; scattered pebbles	2.64	2.00	1.61	.247	.398	17.2	.228	8.1	3.41	.10	4.08	.493	--	--	--	--	--	--	Qal or QTg
	80-85	24.4-25.9		--	--	--	--	--	27.5	22.0	--	--	--	--	--	--	--	--	--	--	--	Do.
QH-1	191-192	58.2-58.5	Conglomerate; 30 percent matrix of light-green clay and silt	--	--	--	--	--	--	--	--	5.45	--	--	--	--	--	--	--	--	--	QTg or Ts
	192-196	58.5-59.7	Clay and silt, light-green; sheared; scattered pebbles	--	--	--	--	--	--	--	--	3.70	--	--	--	--	--	--	--	--	--	Ts
	195	59.47	Homogeneous clay	2.71	--	1.48	--	--	45.4	--	--	3.91	--	--	--	--	--	--	--	--	--	Do.
	392-398	119.5-121.3	Sand, fine to medium; clay and silt, ill-sorted	--	--	--	--	--	--	--	--	--	--	--	--	--	--	--	--	--	--	Do.
	393	119.0	Mudstone	2.74	--	0.55	--	--	79.9	--	--	--	--	--	--	0.01	4.7	0.71	0.24	--	--	Do.
	501-506	152.7-154.2	Clay and silt, brown; scattered pebbles of chert and quartzite	2.58²	2.32²	2.15²	--	--	16.6²	--	5.09c	4.11	--	--	--	--	--	--	--	13.	--	Do.
	503	153.4	Subgraywacke	2.69	--	1.97	--	--	26.8	--	--	--	--	--	--	0.03	--	--	--	--	--	Do.
QH-2	200-206	61.0-62.8	Clay and silt, light-green; indistinct intrabeds of very fine sand	--	--	--	--	--	--	--	--	2.74	--	--	--	--	--	--	--	--	--	Ts Tuffaceous?
	206	62.0	Argillite	2.71	--	1.59	--	--	41.3	--	--	--	--	--	--	0.01	--	--	--	--	--	Do.
	400-407	121.9-124.0	Clay and silt, light-green; scattered pebbles	--	--	--	--	--	--	--	--	2.74	--	--	--	--	--	--	--	--	--	Do.

TABLE 4. -- Physical properties of cores from southern Grass Valley (Continued).

34

TABLE 4. -- Physical properties of cores from southern Grass Valley (Continued).

Well	Depth ft	Depth m	Lithologic description	Grain density (g/cm³)	Saturated bulk density (g/cm³)	Dry bulk density (g/cm³)	Moisture content by weight	Moisture content by volume	Total porosity (percent)	Effective porosity at 2,000 psi (percent)	Thermal conductivity of solids (tcu)	Saturated bulk thermal conductivity (tcu)	Standard deviation	Computed thermal conductivity (tcu)	Computed porosity (percent)	Median size (mm)	Sorting Coefficient	Skewness	Kurtosis	Uniformity Coefficient	Vertical hydraulic conductivity at 60°F (15.5°C) (m/d)	Formation
QH-4	511	155.8	Indurated clay	2.53	--	1.25	--	--	--	--	50.6	--	--	--	--	--	--	--	--	--	--	--
QH-6	90-95	27.4-29.0	Clay, silty and sandy, brown	--	--	--	--	--	--	--	--	4.16	.19	--	--	--	--	--	--	--	--	Qol or QT
	135-140	41.2-42.7	Clay, sandy, with fine gravel	--	--	--	--	--	--	--	--	3.92	.24	--	--	--	--	--	--	--	--	Qa
QH-7	113-110	34.4-36.0	Clay and fine sand	2.62	1.02	1.33	0.360	0.477	--	0.305	5.6	3.43	.19	2.83	.354	--	--	--	--	--	--	Qol
QH-7	113-110	34.4-35.9	Siltstone	--	--	--	--	--	36.0	30.5	--	--	--	--	--	--	--	--	--	--	--	Qa
	200-205	61.0-62.5	Clay with coarse sand	2.66	1.76	1.21	.428	.519	54.9	6.2	7.9	3.07	.13	3.08	.546	--	--	--	--	--	--	Qa
QH-7	200-205	61-62.5	Well sorted mudstone	--	--	--	--	--	20.0	6.2	--	--	--	--	--	--	--	--	--	--	--	Qa
QH-8	113-110	34.4-36.0	Clay, pebbly, medium brown, subangular fragments of green stone	2.68	1.76	1.21	.469	.567	46.8	--	7.8	3.35	.18	2.89	.458	--	--	--	--	--	--	Qa
QH-8	145-150	44.2-45.7	Moderately sorted siltstone	--	--	--	30.3	16.1	30.3	--	--	--	--	--	--	--	--	--	--	--	--	Qa
	145-150	44.2-45.7	Clay, brown, with gravel	2.62	1.68	1.10	.560	.594	--	.151	5.33	2.90	.09	2.45	.455	--	--	--	--	--	--	Qa
QH-9	160-165	48.8-50.3	Clay, brown, gritty with gravel	--	--	--	--	--	--	--	--	3.51	.19	--	--	--	--	--	--	--	--	Qoc
QH-11	90-95	27.4-29.0	Gravel (mostly), wet and soft	2.68	2.33	2.12	.140	.247	32.7	.163	3.66	3.87	.51	4.81	.348	--	--	--	--	--	--	Qa
	130-135	39.6-41.1	Sand, clayey, layered brown and bluish-gray	2.51	1.61	1.02	.328	.734?	--	.160	4.14	2.31	.06	2.17	.538	--	--	--	--	--	--	Qol?
QH-11	130-135	39.6-41.1	Fine grained sandstone	--	--	--	--	--	59.6	46.0	--	--	--	--	--	--	--	--	--	--	--	Qa
	163-168	49.7-51.2	Clay, brown	2.43	1.53	.90	.579	.521	67.4	--	4.0	2.46	.07	2.06	.463	--	--	--	--	--	--	Qol or Qa
QH-12	130-135	39.6-41.1	Sandstone, fine, pebbly, brown siltstone	2.70	1.78	1.24	.432	.536	54.9	--	6.4	2.77	.11	2.81	.551	--	--	--	--	--	--	Qa
QH-13	115-120	35.1-36.6	Claystone, reddish-brown, with abundant rock fragments	2.66	2.24	1.99	.146	.290?	--	--	7.4	6.46	.47	4.86	.304	--	--	--	--	--	--	Qtg or Ti

TABLE 4. -- Physical properties of cores from southern Grass Valley (Continued).

Well	Depth ft	Depth m	Lithologic description	Grain density (g/cm³)	Saturated bulk density (g/cm³)	Dry bulk density (g/cm³)	Moisture content by weight	Moisture content by volume	Total porosity (percent)	Effective porosity at 2,000 psi (percent)	Thermal conductivity of solids (tcu)	Saturated bulk thermal conductivity (tcu)	Standard deviation	Computed thermal conductivity (tcu)	Computed porosity (percent)	Median size (mm)	Sorting Coefficient	Skewness	Kurtosis	Uniformity Coefficient	Vertical hydraulic conductivity at 60°F (15.5°C) (m/d)	Formation
QH-13 180-185	48.8-50.3		Clay, silty, brown, with abundant angular pebbles	--	--	--	--	--	--	--	--	5.09	.66	--	--	--	--	--	--	--	--	Qtg or Ts
BH-B 92-93	28.1-28.3		Sand, silty, and gravel; nearly dry	--	--	--	--	--	--	--	--	.50	--	--	--	--	--	--	--	--	--	Qal
BH-11 106-122	32.2-37.3		Mudstone, bluish-gray	--	--	--	--	--	--	--	--	4.23	--	--	--	--	--	--	--	--	--	Ts
BH-12 10-17	3.0-5.3		Silt to coarse sand; scattered pebbles	--	--	--	--	--	--	--	--	2.64	--	--	--	--	--	--	--	--	--	Qal
BH-13A 30-31	9.1-9.4		Sand, soft, clayey; gravel unsaturated	--	--	--	--	--	--	--	--	2.29	--	--	--	--	--	--	--	--	--	Qo
133-134	40.4-40.8		Mudstone, variegated	--	--	--	--	--	--	--	--	3.78	--	--	--	--	--	--	--	--	--	Ts

1. 1 tcu = 1 mcal/cm.S.°C.
2. Sample from 154:2 a measured by Menlo Park Lab; saturated bulk thermal conductivity 4.13 mcal/cm.S.°C.
3. Sample from 154:5 a measured by Menlo Park Lab; saturated bulk thermal conductivity 3.51 mcal/cm.S.°C.

36

autochthon (Stewart and McKee, 1977). This suggests that if carbonate rocks are present beneath the thrust, they are probably not as thick as those seen to the east and south of the Roberts Mountain thrust. Subsequent tectonism would then have made the carbonate units discontinuous, which would largely prevent interbasin flow through these units.

The Tertiary volcanic rocks and associated sedimentary rocks in Pershing County can be separated into two major sequences consisting of an older Oligocene to Miocene sequence and a younger sequence coincident with the onset of Basin and Range tectonics. Although the older Oligocene to Miocene group is not exposed in the area covered by plate 1, Noble (1975a) concluded on the basis of their presence in the central Tobin Range, that a significant thickness (from about 100 to more than 300 m) unconformably overlies the Mesozoic and Paleozoic units beneath Grass Valley. Subsequent drilling and interpretation of geophysical data indicate that the actual thickness may be closer to the lower limit of this estimate.

Relatively minor exposures of Tertiary sedimentary rocks, chiefly fanglomerate, have been mapped in the Table Mountain and Goldbanks Hills area (see pl. 1). Fanglomerate was derived from rapidly rising pre-Tertiary bedrock and records the beginning of Basin and Range tectonics. Conformably overlying the fanglomerate are volcanic rocks extruded about 12 to 15 million years ago. Both the sedimentary and the volcanic rocks are considered Miocene. In the vicinity of Leach Hot Springs coarse- to fine-grained nonmarine sedimentary rocks including volcanic clastic rocks and fresh-water limestone were deposited. These sedimentary rocks are overlain by a gravel derived from the pre-Tertiary rocks in the adjacent Sonoma Range. Although not shown as a map unit, the fanglomerate has undergone chalcedonic and opaline silicification in the Goldbanks Hills and Table Mountain area. The silicified fanglomerate is associated with mercury mineralization and is overlain by unaltered

lake sediments and volcanic rocks.

Basalt and minor associated rhyolite about 12 to 15 million years old are exposed in the Table Mountain and Goldbanks Hills area (Noble 1975a). A small basalt outcrop about 1.5 km southeast of Leach Hot Springs is probably associated with this suite of Miocene basalts as indicated by age dating, lithology, and trace element abundance (Noble, 1975a). Although the outcrop has been interpreted as a dike by Noble (1975a), we believe the basalt is in fault contact with the alluvium to the west. However, contact relations are obscured by poor exposure, and the nature of the contact of the basalt and the pre-alluvial sediments is unknown.

Unconsolidated alluvium covers older rocks and deposits throughout most of southern Grass Valley. This poorly sorted and obscurely bedded alluvium ranges downward in grain size from gravel to silt and clay. Caliche in the form of coatings on pebbles and fragments was observed at the surface and in drill cuttings. The alluvial cover ranges in thickness from 1 to about 200 m, with a maximum toward the axis of the valley.

Silicified alluvium is exposed on the upthrown side of the fault at Leach Hot Springs and downgradient westward from the springs (pl.1 and fig. 25). The alteration products along the fault scarp consist of dense chalcedonic sinter and kaolinized alluvium. White and yellow deposits near orifices at the base of the scarp (orifices 12, 15, and 16 of fig. 7) are believed to be sulfur compounds. The flow from the springs has apparently caused the formation of the fragmental sinter of the springs. The fragments consist of white to light-gray opaline sinter and range in size from pebbles to sand. This sinter is younger than that exposed in the fault scarp.

-

Structural Geology

The pre-Cenozoic structural history of the Grass Valley area comprises three major periods of deformation. The oldest recognized period of deformation is the Late Devonian and Early Mississippian Antler orogeny. The Antler orogeny generally consisted of large-scale eastward thrusting of thick siliceous-volcanic sequences over a Paleozoic carbonate assemblage (Johnson, 1977). This movement, which took place along the Roberts Mountain thrust, displaced the lower Paleozoic Harmony and Valmy Formations 145 km to the east. In the East and Sonoma Ranges, these formations are complexly faulted and folded, resulting in significant secondary permeability. The lithology of the lower plate of the thrust cannot be definitely determined because of lack of exposures. The closest recognized exposures of the lower plate are known as the Goat and Horse Mountain windows, approximately 65 km southeast of Leach Hot Springs, exposing quartzite, limestone, and shale (Stewart and McKee, 1977).

The Havallah and Pumpernickel Formations were deposited west of their present locations in relatively deep ocean, and the Inskip Formation was disconformably deposited on the Valmy Formation. The deposition of these rocks followed the Antler orogeny and was in turn followed by the Sonoma orogeny. Tectonic features of the Sonoma orogeny are similar to those of the Antler orogeny with large-scale eastward movement of deep-water sedimentary rocks onto previously deformed lower Paleozoic rocks.

Following the Sonoma orogeny, Triassic and Jurassic marine and nonmarine rocks were deposited unconformably on the older, deformed units. The Nevadan orogeny occurred during Jurassic and Cretaceous time and affected all the pre-Tertiary rocks. This episode is characterized by east-to-west movement of a few kilometers, northeasterly folds, and low-grade regional metamorphism.

The orogeny culminated in the intrusion of granodiorite into metasedimentary rocks resulting in contact metamorphic aureoles and minor local folding and faulting.

Cenozoic deformation and volcanism occurred during two distinct periods. The first period consisted of volcanic activity in a generally stable region. Although the volcanic rocks are not exposed in the southern Grass Valley area, they may be present beneath the sedimentary rocks filling the valley.

The onset of Basin and Range extensional tectonics and associated volcanic activity began about 15 million years ago. In southern Grass Valley, a major basin bounding fault occurs on the eastern side of the basin. Noble (1975a, b, and c) presented a complex picture of the faults that affect the basin filling sediments. He separates the faults into three systems consisting of a east-side system, a central-graben system, and a transverse system. The east-side system is the result of uplift of the southern Sonoma Range. Tertiary rocks exposed to the east of Leach Hot Springs have been rotated to dips of as much as 30 to 50 degrees to the east. Leach Hot Springs is on one of the prominent transverse faults near an intersection with one of the faults of east-side system. A warm spring about 0.5 km southwest of Leach Hot Springs is also along this same transverse fault. The southwestern part of this fault appears to be acting as a barrier to the northward movement of ground water as will be discussed in a later section. The central-graben system is interpreted as being a result of localized crustal extension at depth. If this relatively narrow central system extends into bedrock, then enhanced permeability should be expected. The transverse system, which consists of those faults that are alined at a high angle to north, may be at least in part due to differential subsidence. At present the most likely locations for permeable zones within the basement appear to be at the intersection of the major transverse faults with major north-trending faults. Although the

40

faulting has locally enhanced the permeability, concurrent displacement of possibly high permeability units, such as the Paleozoic carbonate rocks, decreases the probability of interbasin flow in the Grass Valley area.

The Panther Canyon area is an area of complicated faulting and is on a regional northeast-trending lineament (Beyer and others, 1976). The fault along which the Pleasant Valley earthquake of 1915 (magnitude of 7 to 8) resulted in about 5 m of displacement (Page, 1933) apparently terminates in the Panther Canyon area.

Thickness of the valley fill of Tertiary and Quaternary age in southern Grass Valley is poorly known because of the lack of test-hole data in the deeper parts of the valley. Goldstein and Paulson (1977, fig. 8) used a gravity survey to construct a map showing depth to apparent density contrast, which commonly is interpreted as depth to so-called "bedrock" or thickness of valley fill. Depths so interprested are inversely related to the assumed density contrast between the Tertiary and Quaternary valley-fill deposits and the pre-Tertiary rocks (bedrock) for a given gravity survey: the greater the density contrast, the smaller the depth to bedrock. Goldstein and Paulson (1977, p. 5) used a density con-trast, DP, of 0.6 g/cm^3 (incorectly given in the paper as 0.06 g/cm^3: Goldstein, oral communication, 1980) in constructing their map; they noted also (p. 7) that the depth interpreted from the gravity data is approximately 200-300 m less than the depth interpreted from electrical surveys, but they re-garded the estimate from gravity as the more reliable.

Our map (fig. 3) is based on the map of Goldstein and Paulson (1977, fig. 8). but the thickness of fill, or depth to bedrock, is everywhere 17 percent less than that shown by Goldstein and Paulson. The adjustment is based on the depth to bedrock actually found in test wells QH3D and G105, as compared with
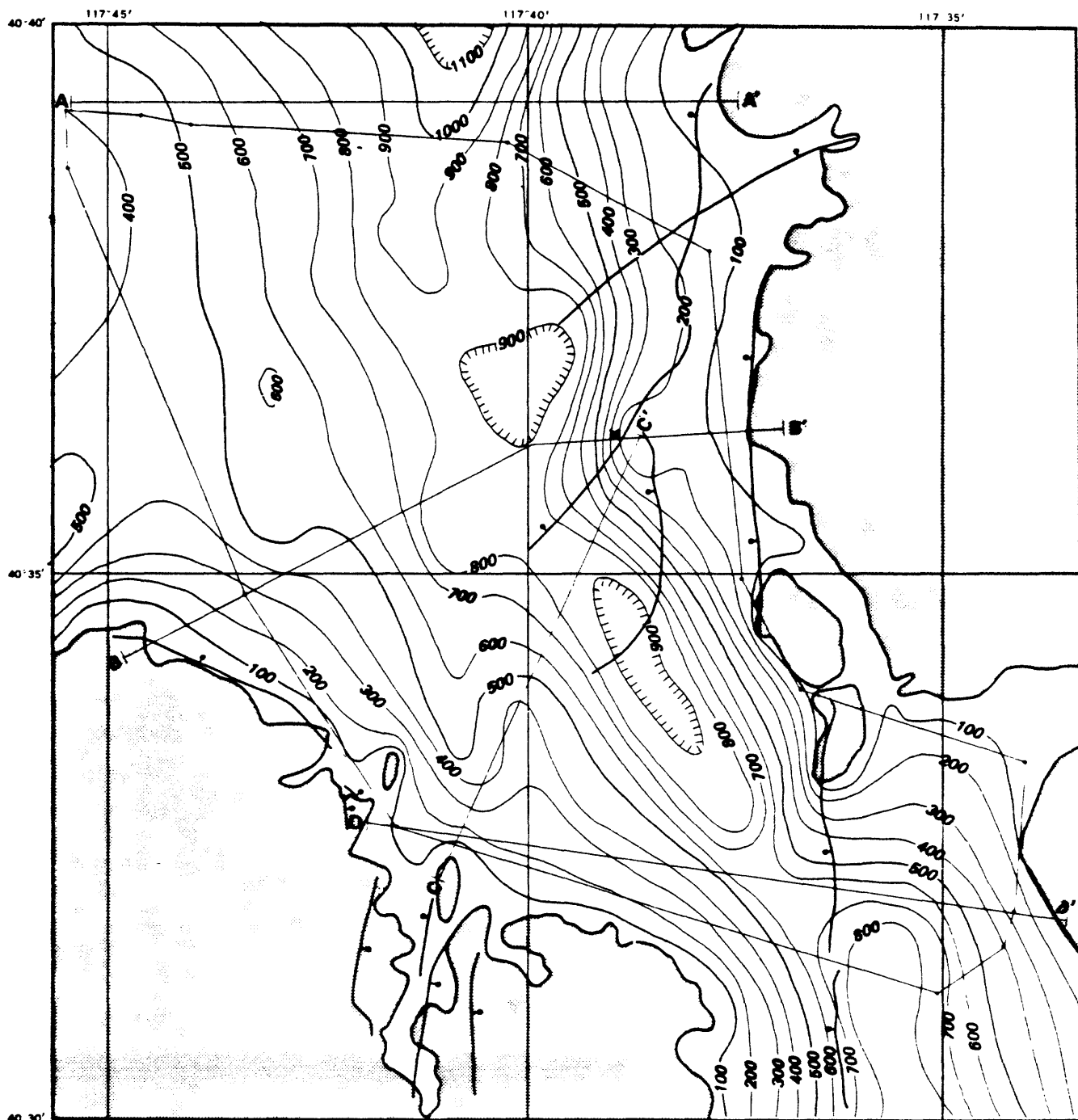
EXPLANATION
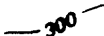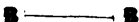
▢ Edge of pre-Tertiary bedrock outcrop

⌒300⌒ Line of equal depth to base of valley fill, in meters

B———B' Location of geologic cross section

⌒•⌒ Principal faults, bar and ball on downthrown side

✕ Leach Hot Springs

FIGURE 3. — Map showing thickness of fill in southern Grass Valley. Contour interval, 100 meters.

the greater depth indicated for the those locations by Goldstein and Paulson (1977, fig. 8). Thus, our map (fig. 3) implies a density contrast between bedrock and valley fill greater than 0.6 g/cm^3. Saturated bulk density of valley-fill deposits averages 1.99 g/cm^3 for 28 samples from test wells; if this mean value is truly representative of all the valley fill, the average density of the pre-Tertiary bedrock exceeds 2.7 g/cm^3.

Although data are not available to refine our present estimate of valley-fill depths shown in figure 3 and used later in calculations of nonthermal ground-water flow and advective heat discharge beyond the study area (see fig. 6, table 6), we believe the thickness of fill in the center of the valley may be substantially greater than shown in figure 3. The reasons for this belief are enumerated as follows:

(1) The shallower-than-expected bedrock penetrated in test well QH3D represents a buried high on which only a minor thickness of Tertiary sedimentary rocks is present. Therefore, the density contrast between the valley fill and the bedrock is larger at this location than it is in the deeper parts of the valley trough where greater thicknesses of relatively dense Tertiary sedimentary (and volcanic?) rocks overlie the pre-Tertiary bedrock.

(2) At test well G105, the other point used in adjusting the thickness interpreted by Goldstein and Paulson (1977), the "bedrock", although probably considerably denser than most valley fill, actually is a Tertiary rhyolite. However, the density of the rhyolite almost certainly is much less than 2.7 g/cm^3; moreover, it might overlie Tertiary sedimentary rocks rather than pre-Tertiary bedrock. The true depth to bedrock at the site of G105, therefore may be greater than shown by Goldstein and Paulson (1977, fig 8), not less.

In summary, the valley-fill thicknesses shown on figure 3 should be regarded as minimum values in the deeper parts of the valley. More reliable

estimates of thickness must await the drilling of deep wells that penetrate the pre-Tertiary rocks in the axial parts of southern Grass Valley.

HYDROLOGIC SETTING

Climate and precipitation

The main factor controlling the climate of Grass Valley is the effect of the Sierra Nevada on eastward-moving storms. As warm, moist air masses from the Pacific Ocean cross these mountains, they are forced to greater altitudes resulting in a large loss in moisture through precipitation. The eastward-moving air masses are relatively dry and yield fairly small amounts of precipitation. The Basin and Range topography also causes these orographic effects so that the valleys tend to be arid to semiarid and the mountains subhumid.

Climatological data have been only sparsely collected in Nevada making detailed analysis of the southern Grass Valley area impossible. Analysis of precipitation is a particular problem as most of the weather stations are in the lowlands, whereas the mountains receive greater amounts of precipitation, which is the major source of ground-water recharge.

The station closest to southern Grass Valley where climatological data have been collected is at Winnemucca Airport about 45 km north of Leach Hot Springs. A mean annual precipitation of 213 mm per year has been observed, most of which (66 percent) occurrs between December and May in the form of rain or snow. The mountains receive a greater amount of precipitation, estimated to exceed 510 mm per year in the higher peaks of the Sonoma Range (Cohen, 1964). An annual evaporation rate from free-water surfaces in the valley lowlands has been estimated to be about 1,200 mm (Kohler and others, 1959), which is more than five times the annual precipitation. Temperature data show large diurnal fluctuations of as much as $25^{o}C$ and average monthly values ranging from -2 to $22^{o}C$. The climatological data are used in the analysis of the heat flow and recharge to the ground-water system, discussed later.

Surface Water

Although some of the streams in Grass Valley flow for short distances during most of the year, the majority flow only during times of rainfall or snowmelt. Flows from the mountains, even during intense rainfall or warm rain on frozen ground, probably do not leave the valley as streamflow. Hansen (1963) reported that even a large peak flow of 320,000 L/s from Clear Creek (in the central Sonoma Range) did not reach the Humboldt River, which borders Grass Valley on the north.

Rapid infiltration of water as it traverses the coarse-grained alluvial fans supplies a significant source of ground-water recharge as indicated by the disappearance of surface water and by the temperature of the ground water (as is discussed in a later section). The temperature data, size of watershed area, and the presence of surface water through much of the year indicate that the streams in Sheep Ranch, Spaulding and Pollard Canyons, in addition to Clear Creek, are supplying significant ground-water recharge. Surface water recharges the alluvial aquifers and may also supply some of the water to the geothermal system. However the sources of recharge to the geothermal system are as yet poorly known.

Shallow Ground-Water System

The hydrologic system can be separated into two separate, but not necessarily distinct, flow systems. The flow within the valley-fill sediments and adjacent mountain-forming bedrock will be referred to as the "shallow ground-water system." The flow of the thermal water, deep within the bedrock underlying the basin and upward along faults in the sediments, will be termed the "deep ground-water system." The two systems are interrelated, which presents a problem in rigorously defining boundaries; however, the concept is believed to be useful for discussion purposes.

Information on the shallow ground-water system has been obtained from both test wells drilled during this study, from existing wells in the area, and from previous studies. A list of the holes drilled specifically for this study showing construction details and the types of information collected is presented in table 2. The history of the drilling program has been discussed by Olmsted, Glancy, Harrill, Rush, and Van Denburgh (1975); Sass and others (1976), and Beyer and others (1976).

The flow of ground water in the shallow system is primarily through intergranular pores in the unconsolidated valley sediments and fractures in the consolidated bedrock. The available data on the shallow ground-water system, which consists of water-level measurements (table 5) and mapping of phreatophytes, has been used to construct figures 4 and 5. The water-table contour map is greatly generalized, owing to the scarcity of data in most of the area studied. This lack of information also prevents the documentation of the effect that faulting of the unconsolidated sediments has on the flow of ground water. In the vicinity of Leach Hot Springs, the water-table altitude is about 10 m lower on the downthrown (northwestern) side of the fault that causes the scarp than it is to the southeast. This style of a large difference in the water-table altitude across recent faults is believed to

47

TABLE 5.--Water-level data for wells in southern Grass Valley

Location	Well	Date	Depth to water below land surface m	ft	Altitude of water level m	ft
	DH1	77 06 07	12.674	41.58	1394.161	4574.24
	DH3	75 09 18	26.1 [1/]	85.6 [1/]	1429.2	4888
	DH4	75 09 18	24.1 [1/]	78.7 [1/]	1405.4	4611
	DH6	77 06 07	16.404	53.82	1409.542	4624.71
	DH7	77 06 06	26.530	87.04	1369.402	4493.01
	DH8	77 06 08	23.354	76.62	1370.707	4497.29
	DH9	77 06 07	36.436	119.55	1380.710	4530.11
	DH10	77 06 15	5.870	19.26	1423.703	4671.17
	DH11	77 06 07	29.331	96.24	1371.225	4498.99
	DH12	77 06 07	25.127	83.11	1376.045	4514.80
	DH13A	77 06 15	17.317	56.82	1422.927	4668.62
	DH14A	77 06 15	32.004	105.01	΄1383.182	4538.22
	DH15	75 09 17	34.0 [1/]	111.5 [1/]	1420.8	4661
	QH1B	77 06 15	32.44	106.4	1413	4634
	QH2B	77 06 07	74.917	245.80	1415	4643
	QH3B	77 06 06	61.967	203.31	1372.77	4504.06
	QH3C	77 06 06	61.271	201.03	1373.47	4506.36
	QH3D	77 06 28	4.98	16.34	1429.76	4691.04
	QH4B	77 06 07	45.870	150.50	1473	4833
	QH5B	77 06 06	30.397	99.73	1360.536	4463.92
	QH6B	77 06 06	16.990	55.74	1362	4466
	QH7B	77 06 06	30.144	98.90	1366.386	4483.11
	QH8B	77 06 07	45.557	149.47	1432.707	4700.71
	QH9B	77 06 07	65.718	215.62	1412.836	4635.51

TABLE 5.--Water-level data for wells in southern Grass Valley (continued)

Location	Well	Date	Depth to water below land surface m	ft	Altitude of water level m	ft
	QH11B	77 06 06	38.106	125.03	1446	4744
	QH12B	77 06 07	31.429	103.12	1481	4859
	QH13B	77 06 07	45.635	149.73	1502	4928
	QH14B	77 06 06	45.717	150.00	1361	4465
	Q1	80 06 18	21.3 [2]	70 [2]	1364	4475
	Q6	80 07 31	31.6 [2]	103.6 [2]	1362	4466
	Q23	77 07 18	21.0 [3]	69 [3]	1413	4636
	Q24	77 07 18	65.5 [3]	215 [3]	1514	4965
30/39 16dbb	Goldbanks windmill 77 03 07		4.80 [4]	15.73 [4]	1471.26	4825.73
31/37 4ccc	Mine well (old) 77 03 08		16.5	54	1546	5070
31/38 26abb		77 03 10	49.4	162	1423	4668
31/38 34ada	Quicksilver windmill 77 04 29		27.4	89.8	1459	4785
31/39 27bbb	Mine well (new) 80 5 17		20.1	66	1489	4884
31/39 32abc	Mud Springs Ranch (old) 77 03 08		44.2	145	1416	4646
32/38 18acc	Turner well 55 09 22 [5]		24 [4]	79 [4]	----	----
		73 10 29 [5]	39	128	----	----
		77 04 26	25.3	83	1353	4438
32/38 36cba	Hot Springs Ranch 73 06 14 [5]		25	82	----	----
		77 03 11	28.7	94	1369	4490

TABLE 5.--Water-level data for wells in southern Grass Valley (continued)

Location	Well	Date	Depth to water below land surface m	ft	Altitude of water level m	ft
	G5a	79 10 15	79.3 [1]	260 [1]	1413	4636
	G105	80 07 31	2.4 [6]	7.8 [6]	1439.3	4720.8
	G108	80 07 31	32.4 [2]	106.2 [2]	1493	4896

Footnotes:

[1] Based on neutron and gamma-gamma logs, or temperature log.

[2] Wells gun perforated after completion.

[3] Water level in unscreened heat-flow well responding to slug test.

[4] Depth below measuring point.

[5] Data from Cohen (1964, table 8) and files of Nevada State.

[6] Height above land surface.
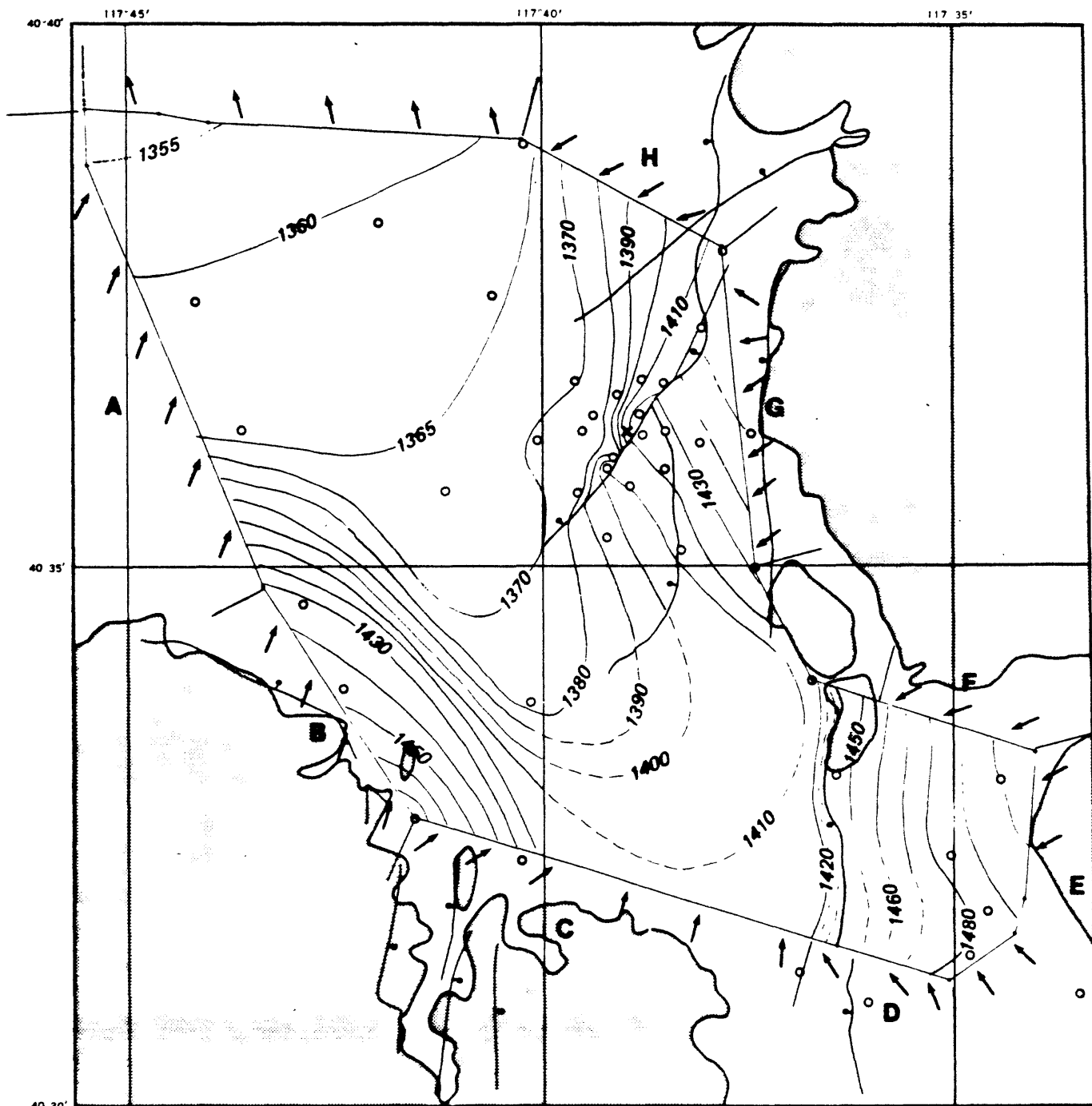
EXPLANATION
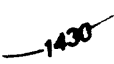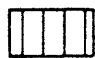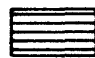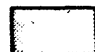
Edge of pre-Tertiary bedrock outcrop

Water table contour, dashed where a location is uncertain. Contour interval, 10 meters, except as marked.

Subsection for computing groundwater inflow and outflow through valley fill. Directions of flow indicated by arrows.

Principal faults, bar and ball on downthrown side

○ Control points, wells and springs

✕ Leach Hot Springs

FIGURE 4. — Map of southern Grass Valley showing water-table contours and direction of groundwater flow.

51
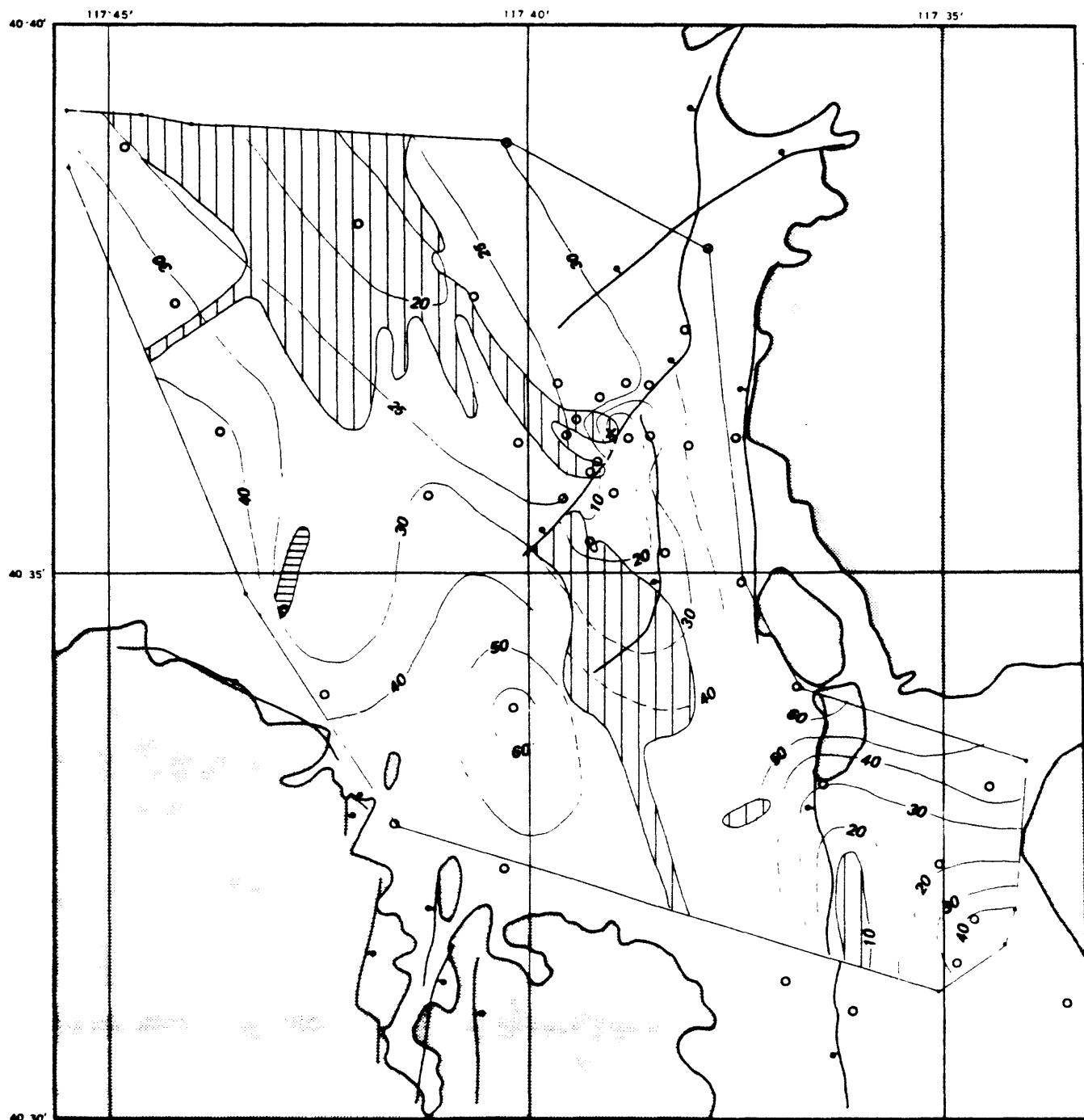
EXPLANATION

Phreatophyte distribution

| | Greasewood
| | Greasewood and rabbit brush
| | Edge of pre-Tertiary bedrock outcrop

Line of equal depth to water table below land surface, dashed where uncertain. Interval, 10 meters, except as marked

Principal faults, bar and ball on downthrown side

o   Control points, wells and springs

×   Leach Hot Springs

FIGURE 5. — Map of southern Grass Valley showing depth to water table and phreatophyte distributions.

occur along many of the basin-bounding faults although it cannot be shown throughout most of the southern Grass Valley area because of a lack of data. The presence of phreatophytes in the southeastern part of the study area is probably due to infiltration of intermittent runoff rather than to the ground-water-barrier effect of faults, as indicated by the relatively large depth to the water table (fig. 5). In general, the presence of phreatophytes where the water table is deeper than about 20 m appears to be due to infiltrated runoff. The phreatophytes in most of the area are not vigorous and are widely spaced, which indicates that either the water-table altitude has been declining or that about 20 m may be the maximum depth from which the plants can extract water.

Physical properties measured on cores from southern Grass Valley (table 4) reveal a heterogeneous assemblage of primarily fine-grained, poorly sorted sediments. The interlayering of sediments having variable hydraulic conduct-ivity indicates that there is a high ratio of overall horizontal to vertical hydraulic conductivitity in the valley fill. This is in marked contrast to the probable conditions in the consolidated rocks, where ground water movement is primarily in vertical fractures. As will be discussed in the following section, these vertical fractures may be responsible for the deep circulation that allows recharge to the thermal system.

The general, northerly ground-water flow direction is complicated locally by significant vertical components of flow. Although the vertical component is generally small, it is significant in the vicinity of Leach Hot Springs and wells QH3.and G105. Comparison of water-level and neutron-log data indicate a strong upward gradient in the vicinity of well DH9 and a downward gradient around well DH6. Thus, an upward flow along the fault with a downward flow downgradient from the hot springs is indicated. There is apparently little vertical flow at the locations of wells DH1, 7,8, and 11, where the water-table

53

indications from the neutron logs and the measured water level coincide. The data for wells QH3 and G105 will be discussed in a later section.

The volumetric flow rate northward from the study area has been estimated using two separate methods. The first method uses the observed hydraulic gradient across an east-west cross section of valley fill whose configuration is estimated from drill-hole and gravity data. The second method is based on a water-budget calculation for the study area using the general procedure and the potential recharge estimated for the entire Grass Valley basin by Cohen (1964). Each of the methods is described below.

The ground-water flow estimated by the first method is used to calculate the amount of heat advected northward beyond the area used to calculate a heat budget, as discussed in the section on heat flow (p. 99). Section A-A' shown in figure 6, at the north edge of the budget area, was constructed using the depth to the apparent density interface calculated by Goldstein and Paulson (1977), multiplied by a factor of 0.83 to agree with the depth to the interface actually penetrated in test well QH3D and G105. The flow normal to section A-A' and the advected heat was calculated using Darcy's law and the following assumptions:

(1) The apparent density interface can be interpreted as the contact of the Cenozoic valley fill and pre-Cenozoic "bedrock", and northward ground-water flow occurs only in the valley fill.

(2) The valley fill can be represented by five rectangular subsections occupying the central part of section A-A' (fig. 6)-- the part through which almost all the ground water is moving northward (fig. 4). The upper boundary of the top subsection is a horizontal line at 1,360 m altitude NVGD.

(3) The hydraulic conductivity at a reference temperature of 15.6°C

(60^OF) is 1 m/day at the water table and decreases linearly to 0.1

m/day at a depth of 1,000 m below the water table. Using the average

temperature for each subsection, the hydraulic conductivity at 15.6^OC

by the ratio of the kinematic viscosity of water at 15.6^OC to that at

the average temperature in the subsection. The temperature distribution

in each cross section can be represented by extrapolating the temperature

gradients measured in test wells Q18, QH6 and QH5 to the base of the

fill. The average temperature for each subsection is estimated from the

resulting temperature pattern shown in figure 6.

(4) The lateral hydraulic gradient of the water table applies to the

entire transmitting section. The gradient normal to the transmitting section

(fig. 4) used in the calculation is 0.0019.

The ground-water flow through each subsection is computed using a form of

Darcy's law

$$Q = KIA$$

where Q is the volumetric flow rate (m/day)

K is the temperature-adjusted hydraulic

conductivity (m/day)

I is the component of the hydraulic

gradient normal to the transmitting

section (dimensionless)

A is the area of subsection (m^2).

The advected heat flux through each subsection is computed using the equation

$$q = Q_m C \ (T-T_s)$$

where q is the advected heat discharge (cal/s)

Q_m is the mass flow rate (g/s)

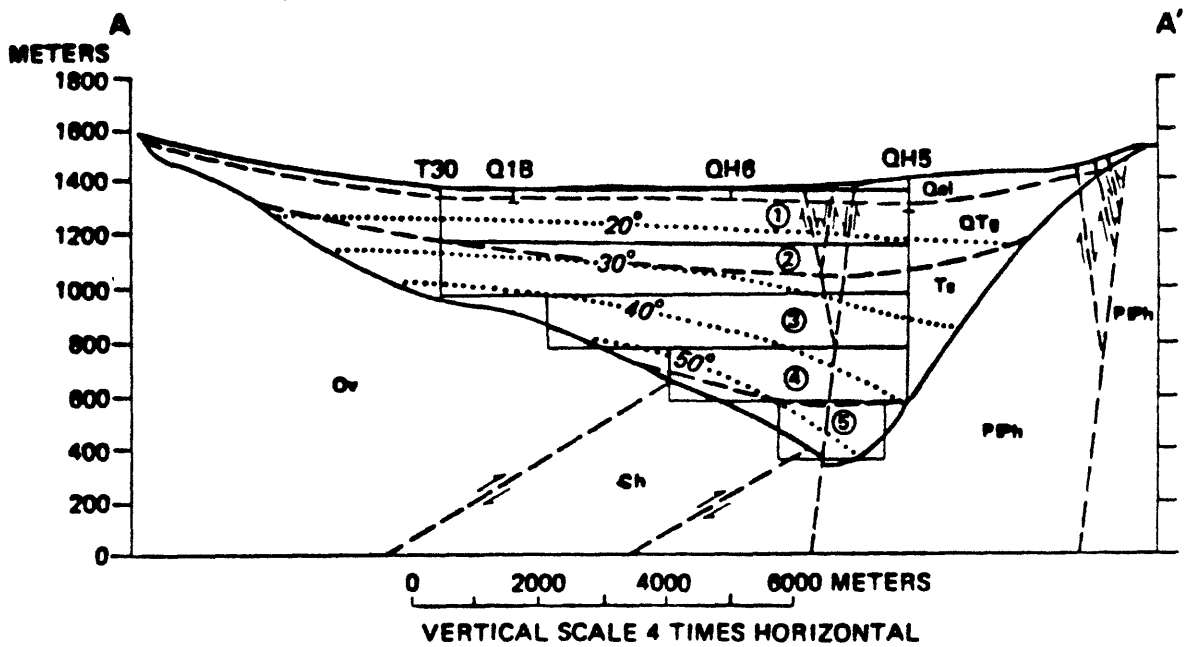C is the specific heat of water (1.0 cal/g.^{O}C was

used)

55

FIGURE 6. -- Generalized geologic section A-A', showing inferred temperature distribution in valley fill. Also shown are subsections 1-5, listed in Table 4 and described in text, and used to compute northward ground-water outflow and advective heat discharge from budget area. Explanation of symbols is on plate 1. Location of section is shown on figure 3.

56

T is the average temperature in the subsection (^{o}C)

T_s is the average annual temperature at the land surface (11.5^{o}C was used)

The mass flow rate is computed by adjusting the volumetric flow rate for the density of water at the average temperature in the subsection and converting the units from m^3/day to g/s. The values of advective heat flux for the subsections are summed to obtain the total advective heat flux (table 6).

In the second method, a simple calculation of water balance indicates that ground-water discharge from the study area is approximately equal to the ground-water recharge. Ground-water recharge is computed using the procedure and the precipitation that Cohen (1964) used for the entire Grass Valley basin (table 7). The outflow is estimated by summing the amounts of discharge across cross section A-A' and the losses due to phreatophyte evapotranspiration and evaporation from the thermal water at the surface. The total outflow is estimated to be about 4.73 x 10^6 m^3/yr, or about 5.8 percent greater than estimated ground-water recharge. It is interesting to note that if the discharge from Leach Hot Springs is added to the local recharge (which would be appropriate if interbasin movement were supplying the thermal water) then the inflow would equal the outflow. Unfortunately, the calculation is not precise enough to support or refute this possibility. In any case, the calculations do indicate a general internal consistency even if not accuracy so that the outflow volume probably is not greatly in error.

The volumes of ground-water flow estimated using the two different methods show general agreement indicating that the estimated advected heat flux is probably a good value within a factor of 2. The advected heat flux will be evaluated further in the section on heat flow.

TABLE 6.--Estimated ground-water outflow and advective heat discharge through valley fill in section A-A' near northern edge of budget area.

(See figs. 3, 4, and 6. Hydraulic gradient normal to section A-A').

Subsection	Area (x10^{6}m^2)	Average hydraulic conductivity (m/day)	Average temperature (°C)	Adjusted hydraulic conductivity (m/day)	Ground-water outflow (x10^{3}m^3/day)	Heat discharge (x10^{6}cal/s)
1	1.48	0.91	19.1	0.99	2.78	0.24
2	1.48	.73	29.5	1.01	2.84	.59
3	1.14	.55	38.1	.91	1.97	.60
4	.77	.37	43.3	.67	.98	.36
5	.34	.19	49.5	.38	.24	.11
Rounded totals	5.2		[1] 30.1		8.8	1.9

Footnote:

[1] Weighted average

TABLE 7. -- Estimate of potential ground-water recharge based on altitude
(precipitation) zones in southern Grass Valley south of line A-A'
(fig. 3).

Zone (m)	Area (km^2)	Precipitation (m/yr)	Precipitation (m^3/ x 10^6)	Percentage of precipitation	Recharge (m^3/yr x 10^6)
Above 2,438	0.518	0.533	0.276	25	0.069
2,134-2,438	8.13	.445	3.62	15	.543
1,829-2,134	79.75	.341	27.19	7	1.90
1,542-1,829	258.1	.253	65.30	3	1.96
Below 1,524	229.6	.152	34.90	0	0
Total					4.47

Deep Ground-Water System

Information on the deep hydrothermal flow system is limited to the geophysical data and direct measurements at Leach Hot Springs and wells QH3 and G105. Although some limits can be placed on the character of the deep system through the use of appropriate numerical modelling, as discussed in a later section, the lack of data make it impossible to provide a complete description of this system.

On the basis of the discovery of a heat-flow high in the vicinity of well QH3 as discussed by Sass and others (1977), a decision was made to drill an additional, deeper well (QH3D) at this location. The well casing was perforated at a depth of about 409-410 m-below the land surface, which the geophysical logs indicate is a zone of high porosity and low clay content within the pre-Tertiary rocks. The water level in well QH3D rose to within 5 m of the ground surface, which indicates a strong vertical component of flow when compared to a static water level in well QH3B of about 62 m below the ground surface. The strong gradient of about 0.22 m/m between the depths of about 155 and 410 m does not exist in the shallower part of the sedimentary fill, where a very slight downward component exists between wells QH3B and 3C. As will be discussed in a later section, the water at well QH3B is chemically and isotopically similar to the thermal waters in the area. This indicates that the vertical hydraulic gradient is causing an upward flow of water from the pre-Tertiary rocks into the unconsolidated deposits.

A hydraulic gradient for upward flow was also observed at well G105 located 1.7 km south by southeast of Leach Hot Springs. The temperature profile on this well, which penetrates Tertiary rhyolite at a depth of 323 m, shows a nearly isothermal interval with temperatures near 93°C within the rhyolite (fig. 16). The well was perforated at a depth of 139 m, following

which the the water level rose to 2.4 m above land surface. The water

table at this site is near 20 m below land surface, indicating that a

gradient for upward flow exists in the fill at this location of 0.18 m/m.

The chemical characteristics of water from the perforated interval in well

G105 have not been determined.

The only area other than at wells QH3 and G105 where the geothermal water

has been definitely found is in the vicinity of Leach Hot Springs. The flow

from the springs, which represents the outflow from the geothermal system, is

given in table 8 and the orifice designations are shown in figure 7. The

springs consist of two roughly linear arrays of orifices parallel to the fault

scarp. Most of the flow (almost 80 percent) is from six of the western

orifices. Intermittent measurements of the flow from orifices 1-29 pre-

sented in figure 8 show distinct changes in flow rate with time. These

fluctuations are not obviously correlated with rainfall and, unfortunately,

temperature was not measured concurrently with the flow. The variations in

temperature measured at each orifice (table 8) may be related primarily to

variations in flow rate and water-surface area.

The exact hydrologic relationship between Leach Hot Springs and the

thermal waters at wells QH3D and G105 cannot be determined owing to lack of

data on ground-water-flow directions in the pre-Tertiary bedrock. The hydro-

static heads at the perforated intervals in wells QH3D (1,430 m) and G105

(1439 m) is greater than that at the orifices of Leach Hot Springs (1422 m).

Whether this difference indicates a potential for flow toward the springs at

depth is unknown. Such a determination would require a measurements of head at

depths in the spring conduit system corresponding to the altitudes of the

perforations in these wells. The temperature logs indicate slight de-

creases in temperature near the bottom of each well. If this represents

actual undisturbed conditions, unaffected by the construction of the well, the thermal water must lose heat at both locations, and be flowing away from rather than toward a heat source. The temperature-gradient reversal would imply that either this is a transient condition or a cooler water is flowing beneath the zone of highest temperature in order to supply the heat sink necessary to maintain the reversal. Definitive conclusions as to the significance of the relations of temperatures and hydrostatic heads at wells QH3D and G105 and Leach Hot Springs must await the acquisition of more data.
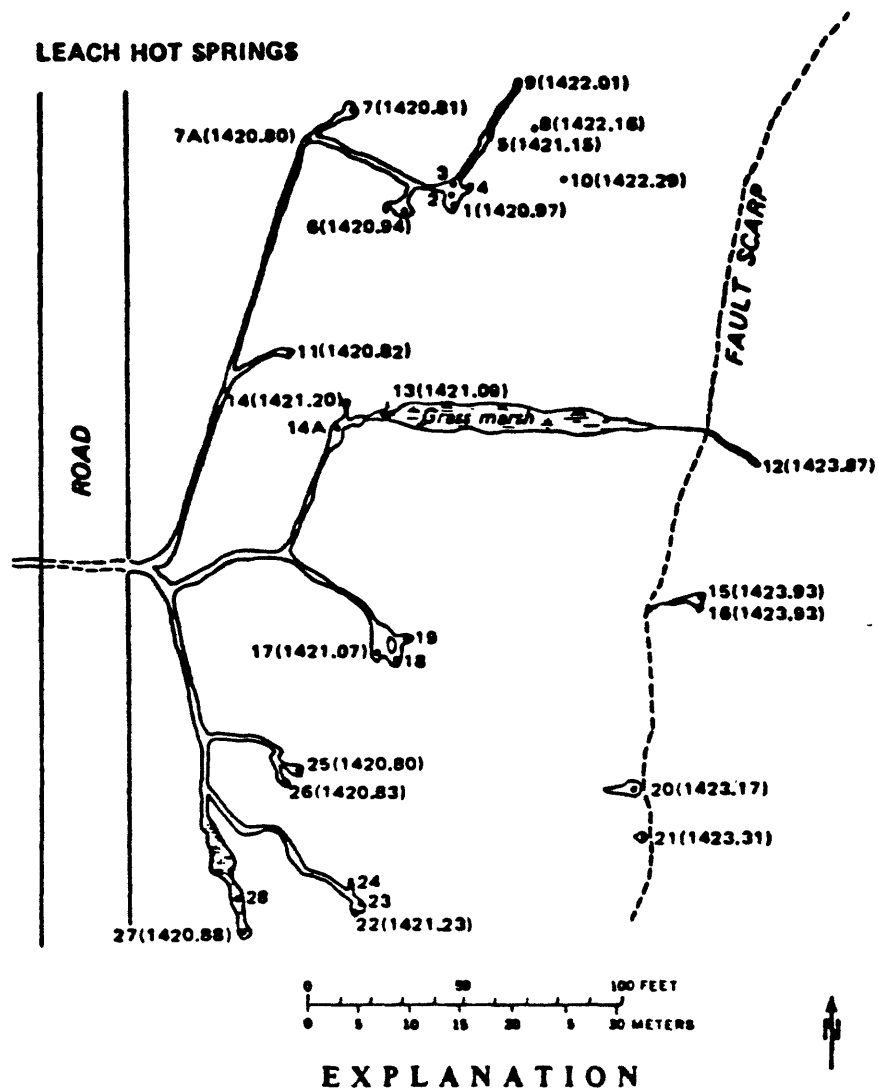
TABLE 8.-- Data for individual orifices at Leach Hot Springs

Orifice	Temperature [1] 1938	1973-4 (°C)	Discharge Nov. 1973 [2]	1974-8 [3] (L/sec)	Date sampled	Specific conductance (umhos/cm)	Chloride (mg/L)	Boron (ug/L)
1	85	83.3-85.0	1.7	1.26	78 01 09	780	27	1,200
2	--	83.3-85.0	4/	4/	-- -- --	---	--	-----
3	--	77.5-78.8	2.1d	1.56	-- -- --	---	--	-----
4	--	81.9-83.6	.42	.31	78 01 09	781	27	1,200
5	83.5	82.2-83.6	<.01	<.01	78 01 09	779	27	1,200
6	75.5	72.5-80.8	.34	.25	78 01 09	820	28	1,200
7	73	62.8-70.0	.34	.25	78 01 09	780	27	1,200
7A	--	73.6	5/	5/	-- -- --	---	--	-----
8	--	33.9	<.01	<.01	-- -- --	---	--	-----
9	67	43.3	<.01	<.01	-- -- --	---	--	-----
10	67	43.3	<.01	<.01	-- -- --	---	--	-----
11	73.5	65.3-66.4	.06	.04	78 01 09	800	27	1,200
12	94	91.1-92.3	.06	.04	78 01 09	802	--	1,300
13	95.5b	86.9-93.6	.71d	.53	-- -- --	---	--	-----
14	--	70.3-72.8	.01	.01	72 06 17 6/	811	29	1,200
14A	--	75.0-75.4	.23d	.17	-- -- --	---	--	-----
15	91	94.2-95.6b	.01	.01	78 01 09	558	10	350
16	--	91.7-95.0	.01	.01	-- -- --	---	--	-----
17	78	74.2-77.8	.59d	.44	78 01 09	810	27	1,200
18	--	80.8-82.8	.06	.04	-- -- --	---	--	-----
19	--	71.9-83.4	.06	.04	-- -- --	---	--	-----
20	--	38.1-47.2	<.01	<.01	73 02 11	919	--	-----
21	--	47.2	<.01	<.01	-- -- --	---	--	-----
22	79.5	80.6-81.4	2.0d	1.48	78 09 14	---	25	1,300
23	--	78.6-80.6	2.0d	1.48	78 01 09	778	27	1,200
24	--	78.1-79.2	.11	.08	-- -- --	---	--	-----
25	--	66.9-68.1	.08	<.01	78 01 09	795	28	1,300
26	--	66.9-68.1	<.01	<.01	78 01 09	795	28	1,300
27	71	47.2-56.1	<.01	<.01	-- -- --	---	--	-----
28	--	70.6-71.4	.03d	.02	73 02 11	795	--	-----
29	--	41.5-48.6	.40	.30	73 02 112	890	30	-----
Total or average, orifices 1-29		78.8	11.3	8.37		795	27	1,200
30	--	34.5-39.0	.59	.44	73 11 14	812	28	-----
Total or average, orifices 1-30		76.8	11.9	8.81		796	27	

63

TABLE 8.-- Data for individual orifices at Leach Hot Springs (Continued).

Footnotes:

[1] Temperatures for 1938 measured by Dreyer (1940, p. 22) sometime between
September 1 and October 15; are probably accurate to $\pm$ 1/2 °C. Temp-
eratures for 1973-74 measured one or more times from May 6, 1973 to
September 24, 1974. Measurements in 1973-74 were made using a single
maximum thermometer, lowered as deeply as possible in the orifice. The
accuracy was probably about $\pm$ 0.3°C. Boiling is indicated by "b".

[2] Discharge measured, estimated, or calculated by the difference; (the
latter values are indicated by "d").

[3] More accurate measurements than those for November 1973 indicate that the
total flow for the period June 1974 to October 1978 (shown in fig. 8)
averaged 74 percent of that for November 1973. Flows from individual
orifices for the latter period are estimated by assuming that the flow
from each orifice is 74 percent of that measured, estimated, or calculated
for November 1973.

[4] Included in discharge from orifice.

[5] Included in discharge from orifice 7.
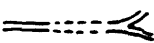
[6] From Mariner,Rapp, Willey, and Presser, (1974).

LEACH HOT SPRINGS

9(1422.01)
7(1420.81)
7A(1420.80)
8(1422.18)
5(1421.15)
3
2 4
8(1420.94)
1(1420.97)
10(1422.29)

FAULT SCARP

ROAD

11(1420.82)

4(1421.20)
14A
13(1421.08)
Grass marsh
12(1423.87)

15(1423.93)
16(1423.93)

17(1421.07)
19
18

25(1420.80)
26(1420.83)
20(1423.17)

21(1423.31)

28
24
23
27(1420.88)
22(1421.23)

0   50   100 FEET
0   5   10   15   20   5   30 METERS

N

EXPLANATION

15(1423.93) Spring pool and orifice. Number indicates
             orifice referred to in table 8 ; dot indicates
             location of orifice. Number in parentheses is
             elevation of orifice pool, in meters

Channel carrying hot-spring discharge; dashed
where in culvert beneath road

Pool or marsh with grass or tules

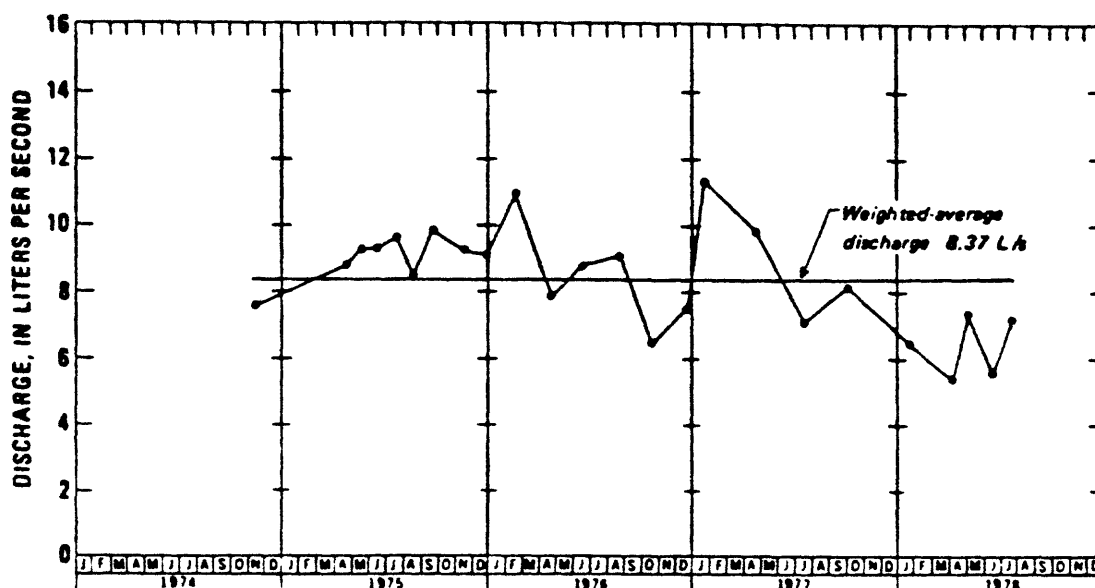FIGURE 7. — Sketch map of Leach Hot Springs showing location
of orifices

65

FIGURE 8. — Discharge from orifices 1-29 at Leach Hot Springs,
November 1974 to July 1978

GEOCHEMISTRY

Sampling Techniques

Geochemical sampling of wells and springs included the analysis of
selected unstable constituents in the field and sample preservation. Prior
to sampling, each well was pumped and (or) bailed several times over a period
of several months. During the pumping and bailing effort, the total water
discharge was recorded and samples were collected for specific conductance
determination. These data were used to determine whether the water quality
was reasonably stable after at least several well-bore volumes of water had
been removed. Final sampling for laboratory analysis began only after
the specific conductance in several successive samples was found to be virtu-
ally constant. Results of chemical and isotopic analyses of water from
wells and and springs are listed in table 9.

Because of the small diameter of the wells, the substantial depth to the
water table, and the desirability of being able to sample at a specified
depth, a special pumping apparatus was designed. The device, as shown in
figure 9, basically consists of a gas source (nitrogen was used during the
final sampling) and two lines connected to a one-way-flow valve. A larger
diameter hose positioned immediately above the one-way-flow valve was found to
increase the pumping rate by acting as a larger reservoir. The operation
consisted of setting a pressure with the regulator, opening the gas valve
(with the gas relief valve closed) and allowing the water to be forced up the
hose and discharged at the surface. After the lines were free of water, the
gas valve was closed and the gas relief valve opened to vent the gas. When
the gas in the lines was at or near atmospheric pressure, the water rose in
the hose and again was forced out. This device provided a higher pumping rate

TABLE 9.-- Chemical and isotopic analysis of samples from southern Grass Valley and vicinity (chemical analysis was performed by the U.S. Geological Survey Central Laboratory, Arvada, Colorado (except where otherwise specified).

Location number	Sample site	Letter desig-nation	Latitude north	Longitude west	Date of sample	Water temper-ature ($^{\circ}$C) [1]	Specific conduct-ance (micro-mhos) [2]	pH	Carbon dioxide dissolved (mg/L as CO_2)	Alka-linity (mg/L as $CaCO_3$) [3]	Bicar-bonate (mg/L as HCO_3) [3]	Car-bonate (mg/L as CO_3) [3]	Calcium disolved (mg/L as Ca)
	Leach Hot Sp.												
32/38 36dba1	Orifice 1	a	40 35 36	117 39 28	77 06	85.0	827	7.18	41	320	390	0	9.7
32/38 36dba1	Orifice 1	a_1	40 35 36	117 39 28	78 09 14	86.0	810	6.70	123	316	385	0	11
32/38 36dba12	Orifice 12	b	40 35 36	117 39 28	79 03 20	92.0	842	8.97	.5	271	324	3	9.6
32/38 36dba13	Orifice 13	c	40 35 36	117 39 28	72 06 17 [2]	92.0	811	7.40	22	300	366	0	8.8
32/38 36sba15	Orifice 15	d	40 35 36	117 39 28	78 12 13	92.0	578	5.90	6.0	2	3	0	8.6
32/38 36dba22	Orifice 22	e	40 35 36	117 39 28	77 06	81.0	825	7.03	58	320	390	0	10
32/38 36dba22	Orifice 22	e_1	40 35 36	117 39 28	78 09 14	81.0	802	6.60	148	303	369	0	11
32/38 36daa	Well DH 13A	f	40 36 31	117 38 44	78 08 23	52.5	1250	8.65	1.5	313	365	8	8.5
32/38 36ada	Well DH 10A	g	40 36 24	117 38 44	78 09 14	86.2	815	8.50	1.8	326	383	7	11
31/38 14abc2	Well DH30	h	40 33 42	117 40 06	78 08 29	58.1	803	8.25	4.2	381	456	4	11
32/38 14abc2	Well DH30	h_1	40 33 42	117 40 06	78 09 15	58.1	825	8.10	5.9	380	457	3	13
32/38 36abb	Well DH14A	i	40 36 34	117 39 02	78 08 30	28.9	810	8.50	2.1	337	399	6	12
30/39 30ddd	Coyote Sp.	j	40 25 05	117 38 23	77 06	22.0	959	6.97	82	394	480	0	73
31/38 14abc1	Well DH38	k	40 33 42	117 40 06	78 08 29	24.5	388	6.15	17	67	82	0	14
32/39 17add	Sheep Ranch Sp.	m	40 38 28	117 36 47	77 06	13.0	720	7.60	7.4	172	210	0	72
32/39 17add	Sheep Ranch Sp.	m_1	40 38 28	117 36 47	78 08 22	17.0	742	7.50	---	---	---	0	72
3138 03acc	DH 78	l	40 35 40	117 41 07	78 08 23	16.3	376	8.65	1.6	117	137	3	18
32/37 23bbd	Point Sp.	a	40 37 49	117 47 58	77 06	10.0	1250	7.55	14	246	300	--	150
31/40 18adc	Petain Sp.	a	40 32 48	117 31 22	77 06	12.0	541	7.61	8.2	172	210	--	67
31/40 18adc	Patain Sp.	a_1	40 32 48	117 31 22	78 08 22	16.0	515	7.85	4.9	178	217	--	65
31/39 33ccc	Mud Sp.	p	40 31 45	117 36 51	77 06	14.0	619	7.26	18	164	200	--	66
31/39 33cba	Well near Mud Sp.	q	40 31 49	117 36 43	77 06	15.0	675	7.66	6.7	156	190	--	68
32/38 35dba	DH8	r	40 36 09	117 40 03	78 08 23	14.8	542	8.30	1.7	169	202	2	56
31/39 22abc	DH13A	s	40 33 00	117 34 25	78 34 25	18.4	535	8.30	1.7	174	208	2	47
31/38 09bcd	Sp. in SW Grass Valley	t	40 33 57	117 43 32	77 06	20.0	1220	7.64	6.6	148	180	--	91
31/38 01dbbc	DH1	u	40 35 15	117 39 10	78 08 24	15.5	474	8.40	1.1	144	172	2	45
31/37 27dac	Sp. in Spulding Canyon	v	40 31 35	117 47 53	77 06	13.0	962	7.17	31	238	290	--	99
33/38 13cac	Clear Creek	w	40 43 51	117 39 21	79 03 20	5.0	371	8.20	1.6	127	153	1	42
33/39 30ddc	Grand Trunk Sp.	x	-- -- --	--- -- --	-- -- --	---	---	---	---	---	---	--	--
31/39 36ccc	Pollard Canyon	y	-- -- --	--- -- --	-- -- --	---	---	---	---	---	---	--	--

TABLE 9.-- Chemical and isotopic analysis of samples from southern Grass Valley and vicinity (Continued)

Letter desig-nation	Magne-sium dis-solved (mg/L as Mg)	Sodium dis-solved (mg/L as Na)	Posas-sium dis-solved (mg/L as K)	Chlo-ride dis-solved (mg/L as Cl)	Sul-fate dis-solved (mg/L as SO4)	Fluo-ride dis-solved (mg/L as F)	Silica dis-solved (mg/L as SiO2)	Boron dis-solved (µg/L)	Alum-inum dis-solved (µg/L as Al)	Lith-ium dis-solved (µg/L as Li)	Solids residue at 180°C dis-solved (mg/L)	Solids sum of consti-tuents dis-solved (mg/L)	Alti-tude of land surface datum (m of NGVD 1929)	δO (°/oo)[4]	δ18O (°/oo)[5]	δ13C
a	0.8	170	12	26	53	8.2	115	1300	---	870	571	588	1420.97	(-1291)	-15:7	---
a1	1.1	180	13	26	56	9.0	105	1300	<10	870	---	593	1420.97	-129	-16.0	---
b	.1	180	16	32	57	2.7	115	1300	---	940	---	577	1423.87	-127	-15.4	---
c	.5	160	13	29	53	7.8	135	1200	9	1700	584	591	1421.09	(-128.6)	-15.7	-9.13(g)[8]
d	.2	85	12	13	200	2.7	180	480	---	450	---	504	1423.93	-124	-14.0	---
e	1.0	170	12	28	50	8.5	100	1300	---	860	564	573	1421.32	-130.5	-16.45	---
e1	1.2	170	11	25	52	9.0	95	1300	<10	830	---	558	1421.23	-131	-16.9	-16.9
f	2.0	270	14	140	110	6.2	17	1800	20	810	---	758	1440.24	-134	-16.4	---
g	1.5	180	12	27	43	8.8	49	1300	<10	810	---	530	1429.57	-131	-16.6	---
h	1.8	180	11	24	30	3.9	16	600	<10	240	---	507	1434.74	-133	-16.8	---
h1	2.1	180	12	23	26	4.3	8.3	540	<10	240	---	498	1434.74	---	----	-7.4
i	2.3	180	11	24	49	8.1	79	1300	<10	910	---	570	1407	---	----	---
j	17	130	8.2	70	65	1.4	40	630	---	220	551	641	----	---	----	---
k	2.0	57	3.5	59	41	1.5	16	440	<10	110	---	267	1434.74	-129	-16.1	---
m	32	29	2.5	59	110	0.2	21	110	---	10	430	429	1535	(-124.5)	----	---
m1	34	31	3.5	62	110	.3	20	120	---	20	---	---	1535	---	----	---
l	6.2	53	4.5	39	15	.6	4.6	410	<10	50	---	212	1396.53	-125	-16.2	---
n	61	65	6.5	110	350	.5	19	170	---	30	818	910	----	(-124.2)	----	---
o	9.1	29	4.6	39	38	.3	58	80	---	4	365	349	1780	(-124.40) (-124.50)	-16.45	---
o1	9.6	29	4.2	36	39	.2	54	190	<10	9	---	344	1780	-124,-123	-15.8	---
p	18	32	1.8	56	59	.2	22	100	---	8	351	354	1474	(-122.7)	-16.00	---
q	19	38	2.3	81	53	.1	20	110	---	8	390	375	1481	-122.25	-15.90	---
r	12	39	3.1	36	53	.3	19	300	40	30	---	320	1417.15	-123	-16.5	---
s	12	52	3.0	39	48	.8	21	260	10	30	---	328	1548	-124	-16.4	---
t	32	110	4.7	180	190	.7	26	360	---	60	734	723	1535	-123.65 (-125.3)	-15.15	---
u	12	38	3.2	39	43	.4	25	140	10	30	---	293	1406.83	-125	-16.9	---
v	32	65	3.8	86	150	1.0	19	230	---	60	562	599	1512	-123.75 (-124.4)	-15.75	---
w	13	15	2.0	14	36	.4	17	70	---	3	---	215	1463	-121.5	-15.8	---
x	---	---	---	--	--	---	--	---	---	---	---	---	1682	(-125.7)	-16.48	---
y	---	---	---	--	--	---	--	---	---	---	---	---	1594	(-119.5)	----	---

TABLE 9.-- Chemical and isotopic analysis of samples from southern Grass

Valley and vicinity (Continued).

Footnotes:

1/ Well water temperatures are bottom-hole values from down-hole temperature measurements.

2/ Specific conductance was determined in the laboratory.

3/ Bicarbonate and carbonate species were mathematically distributed using field pH and titration data.

4/ Isotopic analysis of samples collected by R. H. Mariner were performed by two laboratories The values not in parentheses are from a commercial Laboratory which also performed the analysis of other samples. The values in parenthesies were performed by a U.S. Geological Survey Laboratory.

5/ Oxygen isotope analyses were performed by a commercial laboratory except for the samples collected by R. H. Mariner which were performed by a U.S. Geological Survey Laboratory.

6/ All samples collected in June were collected by R. H. Mariner.

7/ From Mariner and others, 1974; Mariner and others, 1975.

8/ Gas sample.
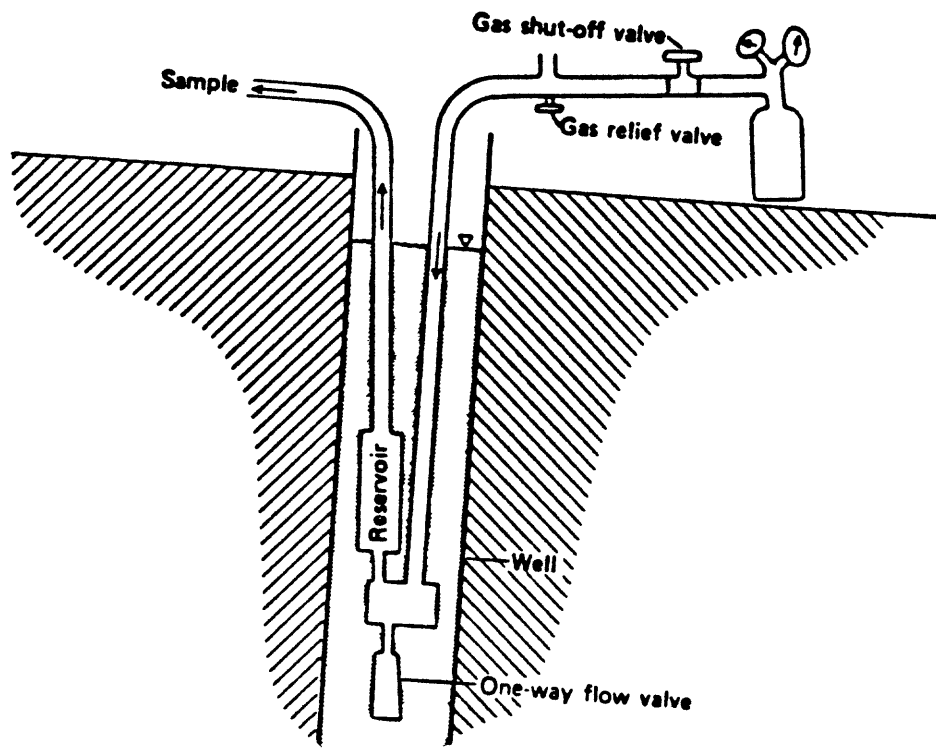
FIGURE 9. — Pumping system used in test wells of small diameter

than could be obtained by bailing and also allowed sampling at a predetermined depth.

Field determinations were made of pH and alkalinity using the methods of Wood (1976, p. 12-18). The water was filtered through a 0.45-μm pore-size membrane (142-mm diameter), with acidification of samples collected for cation analysis. Unacidified filtered samples were collected for anion and isotopic analysis. Samples for silica analysis were diluted with distilled water to prevent polymerization where oversaturation with respect to quartz was suspected. One separate sample was also collected after a second filtration through an 0.1-um pore-size filter for the aluminum analysis. All samples collected for chemical analysis were placed in plastic bottles which had been washed with acid. Glass bottles were used on samples collected for isotopic analysis.

Major Constituents and Chemical Types of Water

The chemical and isotopic composition of the sodium bicarbonate type hot-springs water is virtually the same for all of the sampled orifices with high flow rates (table 8). The chemistry of this water is unusual for near-boiling hot springs with moderate to high discharges. Such water is characterized by "high contents of alkali chlorides, SiO_2, B, and As" (White and others, 1971, p.77). The hot springs water by comparison, has unusually small concentrations of both chloride and arsenic. The chemistry of this water is similar to that found in a metamorphic terrain in Taiwan, as recently reported by Cherng (1979). The thermal water from Taiwan, which is believed to be meteoric, has a low chloride concentration even though the estimated reservoir temperature is 195-220°C. In contrast to the sodium bicarbonate type water of the orifices with the high flow rates, orifice 15 discharges a dilute, acid-sulfate type water. This orifice does not have a visible surface discharge. Instead, the low chloride and and dissolved-solids concentrations

72

indicate subsurface flow. The two contrasting chemical types of water have been discussed by White, Muffler, and Truesdell (1971, p. 77) who concluded that the low discharge acid-sulfate waters are a result of boiling and condensation near the water table. Orifice 15 is topographically higher than the orifices with larger discharges, which is consistent with the conclusion that the water coming from this orifice has boiled and condensed.

The major- and minor-element chemistry as well as the stable-isotope data allows the sampled water to be separated into two reasonably distinct groups. For purposes of discussion, the two groups will simply be referred to as "thermal" and "nonthermal" Waters from Leach Hot Springs, QH3B and 3D, DH10A, DH13A, and DH14A will be called thermal, whereas the other well and spring water will be called nonthermal.

In selecting sampling locations for the nonthermal waters an attempt was made to obtain data on waters that may recharge the geothermal system or mix with ascending thermal fluids. The two most probable sources of recharge are precipitation at the higher altitudes and subsequent downward movement through the mountain blocks and infiltration of surface water as it traverses the alluvial fans. The selection of cold springs for sampling was also made to obtain a reasonable range in altitude, and thereby detect any changes due to variation in isotopic composition of precipitation with temperature.

Diagrams similar to those used by Piper (1944) have been used to graphically display the major-constituent chemistry of natural waters. Back (1961, 1966, p.14) described the concept of hydrochemical facies and identified fields for different water types as shown in figure 10. Data reduction consists of first converting the data from milligrams per liter to milliequivalents per liter and then plotting the percentages of total cation or anion milliequivalents represented by each constituent. Although the

diagrams do not unambiguously indicate the types of geochemical processes that may be causing particular relations, they are useful in demonstrating trends. The information derived from the plots can then be combined with other hydrologic, geologic, and hydrochemical data to determine the processes causing chemical changes and the relations between different chemical types of water. This method has been particularly useful in evaluating systems where mixing and ion exchange are controlling the hydrochemistry.

The major-element compositions of the thermal waters are different from those of most of the nonthermal waters in southern Grass Valley, as demonstrated in figure 11. The major cations show a distinct grouping of the thermal samples in the high sodium-plus-potassium area of the diagram. All the thermal waters, with the exception of that from QH3B, have more than 90 percent sodium plus potassium, whereas all the nonthermal samples have less than 65 percent. This dominance of sodium is consistent with the mechanism suggested to explain the sodium-potassium-calcium geothermometer by Fournier and Truesdell (1973). This mechanism, one involving high temperature reaction of water with silicate minerals, would also explain this observed dominance of sodium and potassium. The cation plot also indicates that the water at Coyote Spring, well QH7B, and well QH3B is intermediate in composition between most of the thermal and nonthermal waters. The exchange by clays of calcium and magnesium for sodium in the shallow ground-water system may be at least partly responsible for this relation. The possible explanations for this observation will be discussed in a later section.

The anion plot in figure 11 also shows a distinct grouping of the thermal as opposed to the nonthermal waters. The thermal waters, with the exceptions of Leach Hot Springs orifice 15, well QH3B, and well DH13A, are primarily bicarbonate type waters. Although the major anions show a grouping similar to

74
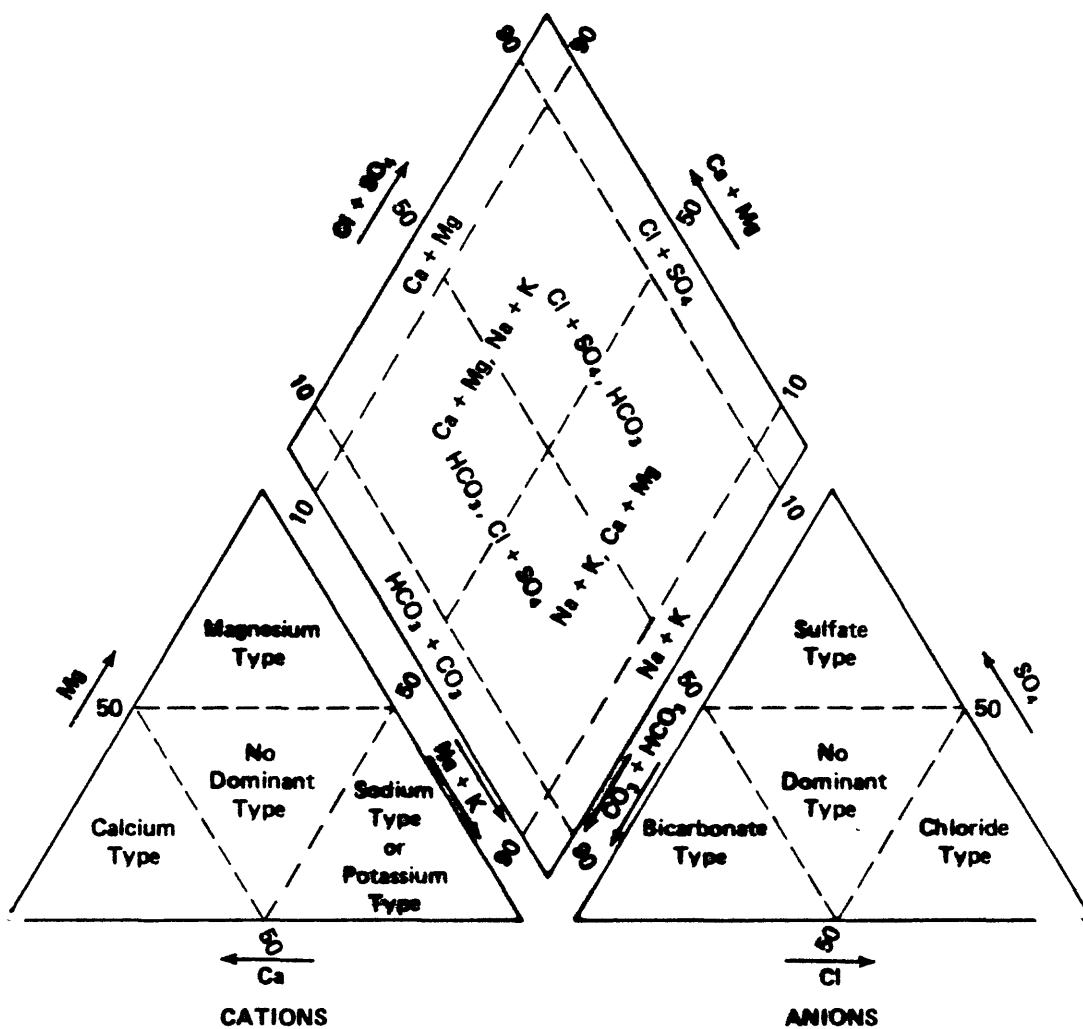
FIGURE 10. — Trilinear diagram showing hydrochemical facies
(from Back, 1966)

75
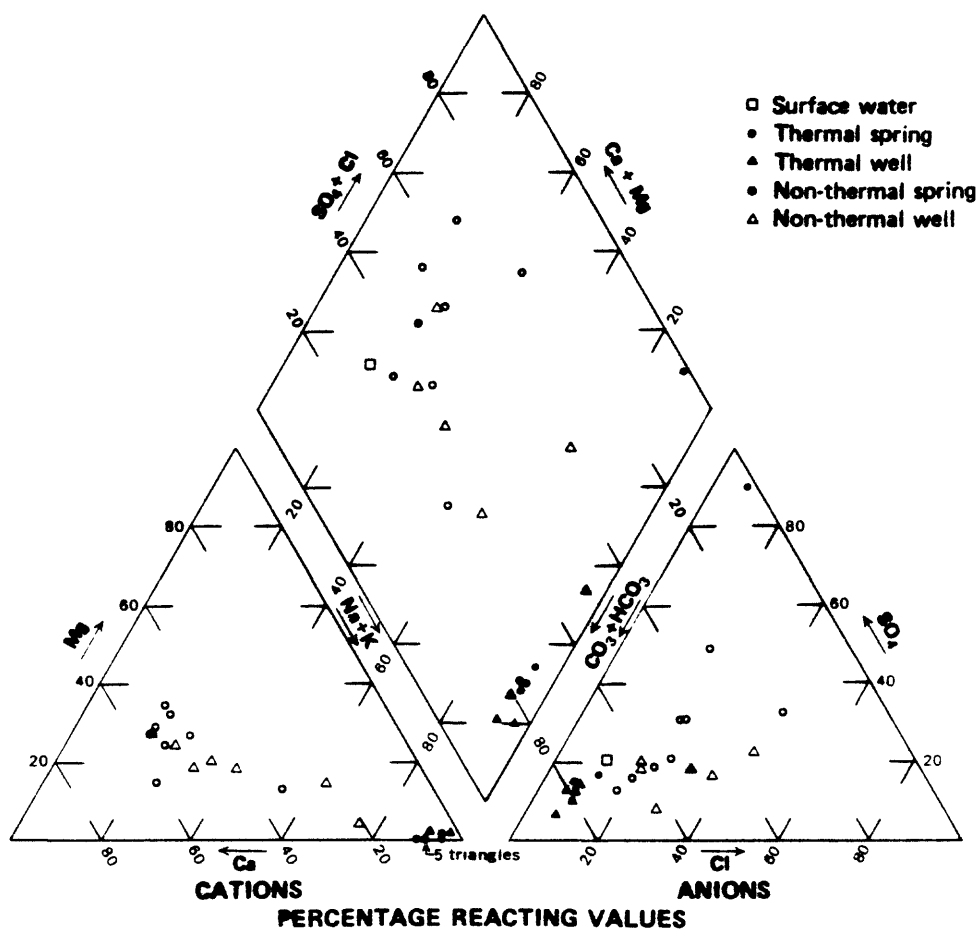
FIGURE 11. -- Trilinear diagram showing chemical composition of water from selected wells and springs.

that seen for the cations, the exceptions require further explanation.

The application of the concept of chemical evolution of ground water is often useful in obtaining an understanding of a suite of chemical analyses (see Freeze and Cherry, 1979,p. 237-302 for a general discussion of the subject). The concept attempts to describe the change in the dominant anion along a flow path. The sequence from a bicarbonate- to a sulfate- to a chloride-dominated water generally corresponds to increasing age or "maturity" within a flow system. The relative maturity of a water can be illustrated using a variety of plots such as those shown in figure 12. The relative maturity in the (carbonate alkalinity/chloride) versus Cl plot increases from the upper left to the lower right, whereas the log (Cl/total anions) versus log Cl indicates increasing maturity from the lower left to the upper right. Both plots demonstrate that in general the thermal water is less mature than the nonthermal water. As can be seen, the thermal water is lower in chloride and has a lower total carbonate alkalinity-to-chloride ratio than the nonthermal water. The water at well DH13A is an exception, appearing relatively mature and having the highest dissolved-solids concentration of any of the thermal samples. This high dissolved-solids concentration, which is primarily a result of higher Na, SO_4, and Cl, may be due to relatively slow movement of ground water immediately east of the hot springs (which is consistent with the relatively flat water-table configuration), resulting in the dissolution of solids within the valley fill. One other possibility for the genesis of the water at well DH13A would be mixing of a small amount of water with high concentrations of Na,SO_4, and Cl with rising thermal water having a composition similar to that at Leach Hot Springs. The Na, SO_4 and Cl rich water might be formed by evaporative concentrations of these constituents with $CaCO_3$ precipitation due to boiling at the water
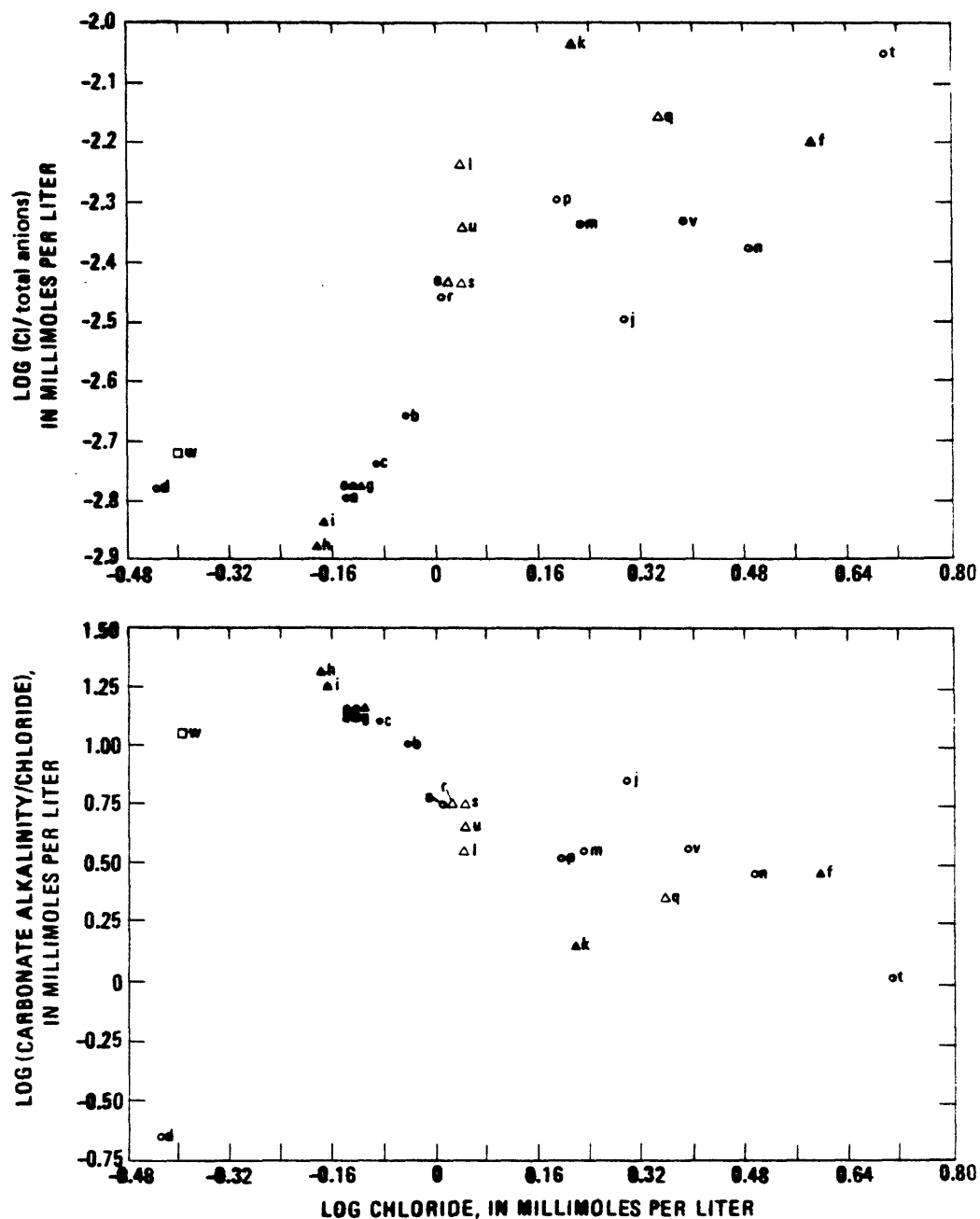
FIGURE 12. -- Plots of total carbonate and carbonate alkalinity versus chloride. Symbols are the same as in figure 11. Letters designate sampling locations listed in table 9. Values plotted for samples with multiple analyses represent average concentrations.

table. The anion composition of the water sampled at well QH3B also is similar to that of the nonthermal water, which may be due to upward movement of thermal water through overlying basin-fill deposits.

Because chloride is normally considered a conservative or non-reactive constituent, particularly in the case of the low concentrations observed in this thermal system, some mechanism for obtaining lower chloride values would be required to allow a simple model of recharge of the nonthermal water. One possible mechanism is mixing of the typical nonthermal water with another nonthermal water having a chloride concentration lower than that of even the thermal water. The source of such a nonthermal water of low chloride concentration may be represented by a sample from Clear Creek in the central Sonoma Range (table 9). This sample was collected during a period of high flow during spring runoff, and therefore may represent about as dilute a recharge source as is available in this area. Recharge of this water, perhaps along a fault zone, as has been suggested by Wollenberg (1976, 1979), might be the source of low-chloride water for the hydrothermal system, provided that very little additional chloride be brought into solution. Although nonthermal ground water with chloride concentrations close to that in the Clear Creek sample were not found during this study, shallow ground water beneath the inferred recharge areas at the mouths of the creeks, where they leave the mountains, might have much lower dissolved-solids and chloride concentrations than most other ground water in the area. Careful sampling from stratigraphically placed shallow test wells would be required to test this possibility. Such water has, in fact, been found in a similar setting near Yuma, Arizona. (See Olmsted and others, 1973, p. H139) Alternatively, the immaturity of thermal waters relative to present-day nonthermal waters sampled and the stable-isotope data discussed in a later section suggest that the thermal waters in Grass Valley represent paleowater recharged at least 8,000 years ago.

Geothermometry

Geochemical and isotopic data have been used to estimate the temperature of geothermal reservoirs. The two most widely applied methods are the silica (Fournier and Rowe, 1966) and the Na-K-Ca (Fournier and Truesdell, 1973) geothermometers. More recently, a method using oxygen-isotope data has been applied to Basin and Range geothermal systems in particular (Nehring and Mariner, 1979, and Nehring and others, 1979). The application of these techniques is based on certain assumptions summarized by Fournier and Truesdell (1974) as: (1) Temperature-dependent reactions occur at depth; (2) all constituents involved in a temperature-dependent reaction are sufficiently abundant; (3) water-rock equilibration occurs at the reservoir temperature; (4) little or no re-equilibration or change in composition occurs at lower temperatures as the water flows from the reservoir to the surface; and (5) the hot water coming from deep in the system does not mix with cooler shallow ground water. The effect of violating the assumptions varies among the group of assumptions and also from one hydrologic setting to another. Models have also been developed to account for mixing with cold ground water as discussed by Truesdell (1975). Temperature estimates using mixing and nonmixing models will be discussed for previously published data and additional values generated during this study.

Silica and cation geothermometry (Mariner and others, 1974) as well as the sulfate-water oxygen isotope method (Nehring and Mariner, 1979, and Nehring and others, 1979) have been used to estimate reservoir temperatures at Leach Hot Springs. A set of data from Basin and Range hot springs including Leach Hot Springs has also shown a correlation between tungsten contents of the water and the estimated reservoir temperatures (Wollenberg and

others, 1977). Additional estimates have been generated using a FORTRAN version of SOLMNEQ (Kharaka and Barnes, 1973), a mineral-solution program similar to WATEQ (Truesdell and Jones, 1974). A summary of the estimated reservoir temperatures is presented in table 10.

As recommended by Fournier and Truesdell (1974), the adiabatic quartz value is presented rather than the conductive value because of the boiling and near-boiling temperatures found at these hot springs. The values for the water from orifices 12 and 15 should be considered suspect, owing to the low flow and unusual chemical composition. Orifice 15 had no surface outflow at the time of sampling, although the boiling and low dissolved-solids concentration require that subsurface flow be present to prevent a salt buildup, which is not observed. The high pH at orifice 12 makes the quartz temperature too high as the method is based in part on the distribution of silica species as follows:

$$H_4SiO_4 \longrightarrow H_3SiO_4^- + H^+ \tag{1}$$

$$H_3SiO_4^- \longrightarrow H_2SiO_4^{2-} + H^+ \tag{2}$$
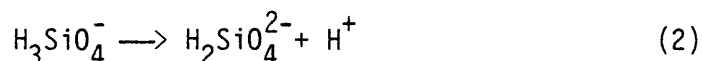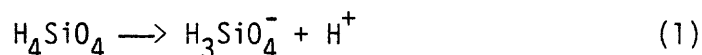
Only equation (2) is important at the pH value found at orifice 12 and the effect is a greater temperature estimate than is justified. Although a correction can be made to account for the disassociation, this was not done because even a corrected value would be suspect as discussed above.

Examination of the estimated values obtained from data on the hot springs with the largest flows (orifices 1, 13, and 22) shows a consistently lower value for the quartz technique than that found using the cation technique. This is consistent with the geophysical evidence of a greater density in the subsurface (Goldstein and Paulsson, 1977) and surface observations of silica

TABLE 10.-- Geothermometry for Leach Hot Springs.

Orifice	Date sampled	Calculated temperature, °C Quartz (adiabatic)	Na-K-ca (B = 1/3)	SO_4-H_2O	Source of sample
1	78 09 14	135	170	---	This study
	77 06 --	139	168	---	R. H. Mariner, unpublished data
12	79 03 20	139	182	---	This study
13	72 06 17	147	176	---	Mariner and others (1974)
	72 06 17	---	---	160	Nehring and Mariner (1979); Nehring and others (1979)
15	78 12 13	164	195	---	This study
22	77 06 --	133	168	---	R. H. Mariner, unpublished data
	78 09 14	130	163	---	This study

deposition which indicate the assumption concerning no re-equilibration at a lower temperature is being violated. Therefore, the cation estimates of 163-176°C are probably more accurate than those obtained using the silica technique, although the values obtained for orifices 12 and 15 are not reliable because of the unusual compositions discussed above.

Although measured temperatures do not exceed about 100°C in the valley-fill sediments there is little reason to suspect that the geothermometer estimates are invalid, considering the correspondence shown below for deep drill hole temperatures and chemically estimated temperatures in other Basin and Range areas in Nevada (Brook and others, 1978).

Location	Best chemical geothermometer estimate of reservoir temperature (°C)	Drill-hole temperature (°C)
Beowawe Hot Springs	229 + 8	211
Desert Peak area	221 + 5	>200
Brady Hot Springs	155 + 6; 246 (deep reservoir)	214
Soda Lake area	157 + 5	144
Stillwater area	159 + 8	156

Estimates of reservoir temperatures have been made using models which account for mixing of thermal water with shallower ground water (see Truesdell, 1975, for a discussion of mixing models). These models can be useful; however, the results should be considered valid only when mixing can be independently demonstrated or inferred. Mixing is indicated when thermal waters associated with a single system have differing concentrations of chloride (or some other non-reacting constituent). This type of situation has been interpreted as being a result of mixing variable proportions of high-chloride thermal water with low-chloride shallow ground water. Available chloride data in Grass Valley do not show a significant difference in the chloride concentration among samples from orifices with the larger flow rates. A

second indication of mixing would be a varying chloride concentration that corresponds to a change in flow rate. As has been shown (fig. 8), the total flow rate has changed over the period of observation. If varying amounts of shallow ground water were mixing with a constant input of thermal water (perhaps due to wetter and dryer periods of time) then a change in composition would be expected. The available data do not indicate that this is occurring. However, sampling did not correspond with the times of flow measurement so that the sampling may have occurred during periods when the flow was nearly the same. The data show that the chloride, silica, lithium, and boron concentrations in particular are not uniformly higher or lower for one sample when compared to the other for a particular orifice. The chloride concentration has been nearly constant; for example, analyses of four samples collected at orifice 1 over a five-year period showed only a 2 mg/L (about 8 percent) difference between the highest and lowest values. With lack of any good evidence of mixing, mixing-model calculations would not seem valid.

Minor Constituents

Minor and trace constituents have been used as qualitative geothermometers or geothermal "tracers." Three constituents were chosen for use in the Leach Hot Springs. The choices are based on the sensitivity of present analytical procedures and concentrations in the hot springs as indicated by previous analyses reported by Mariner, Rapp, Willey, and Presser (1974); Mariner, Rapp, and Willey (1975); and Wollenberg, Bowman, and Asaro (1977). The three constituents, that are consistently higher in the thermal as opposed to the nonthermal water, are lithium, boron, and fluoride. All the thermal water has a fluoride concentration equal to or greater than 1.5 mg/L,(maximum, 9.0 mg/L) whereas Coyote Spring is the only nonthermal sample having a concentration greater than 1.0 mg/L. Similarly, the lithium and boron concentrations in the

84

thermal water are consistently greater than in the nonthermal water, with the exception of Coyote Spring. The elevated levels of these constituents in Coyote Spring are consistent with slightly elevated temperature, silica, and sodium concentrations. The location of Coyote Spring at the base of Goldbanks Hills indicates that there may be anomalously high heat flow related to the earlier thermal activity associated with mineralization and siliceous sinter near Squaw Butte.

The values found for boron, fluoride, and lithium correlate reasonably well; that is, when a high value for one of the constituents is found then the other two are also likely to be high (see fig. 13). On the basis of these data it does not appear that there is a need to analyse for all three constituents in an exploration effort.

Stable Isotopes

The available $\delta^{18}O$ and $_{\delta}O$ data for the Leach Hot Springs area are plotted in figure 14 using the standard del unit, permil (o/oo) relative to "Standard Mean Ocean Water" (SMOW) A noticeable feature of the data is the fact that the thermal water has consistently more negative deuterium values than those for the nonthermal water. The more negative values, which indicate a lower deuterium content, or lighter water, can be caused by several different mechanisms:

1. The thermal water is partly metamorphic or primary magmatic water.
2. The thermal water is a product of boiling at depth
    with subsequent condensation.
3. The source of recharge for the thermal water is at a higher altitude,
    and therefore, colder than for the nonthermal waters.
4. The thermal water was originally recharged during a period of colder
    precipitation.
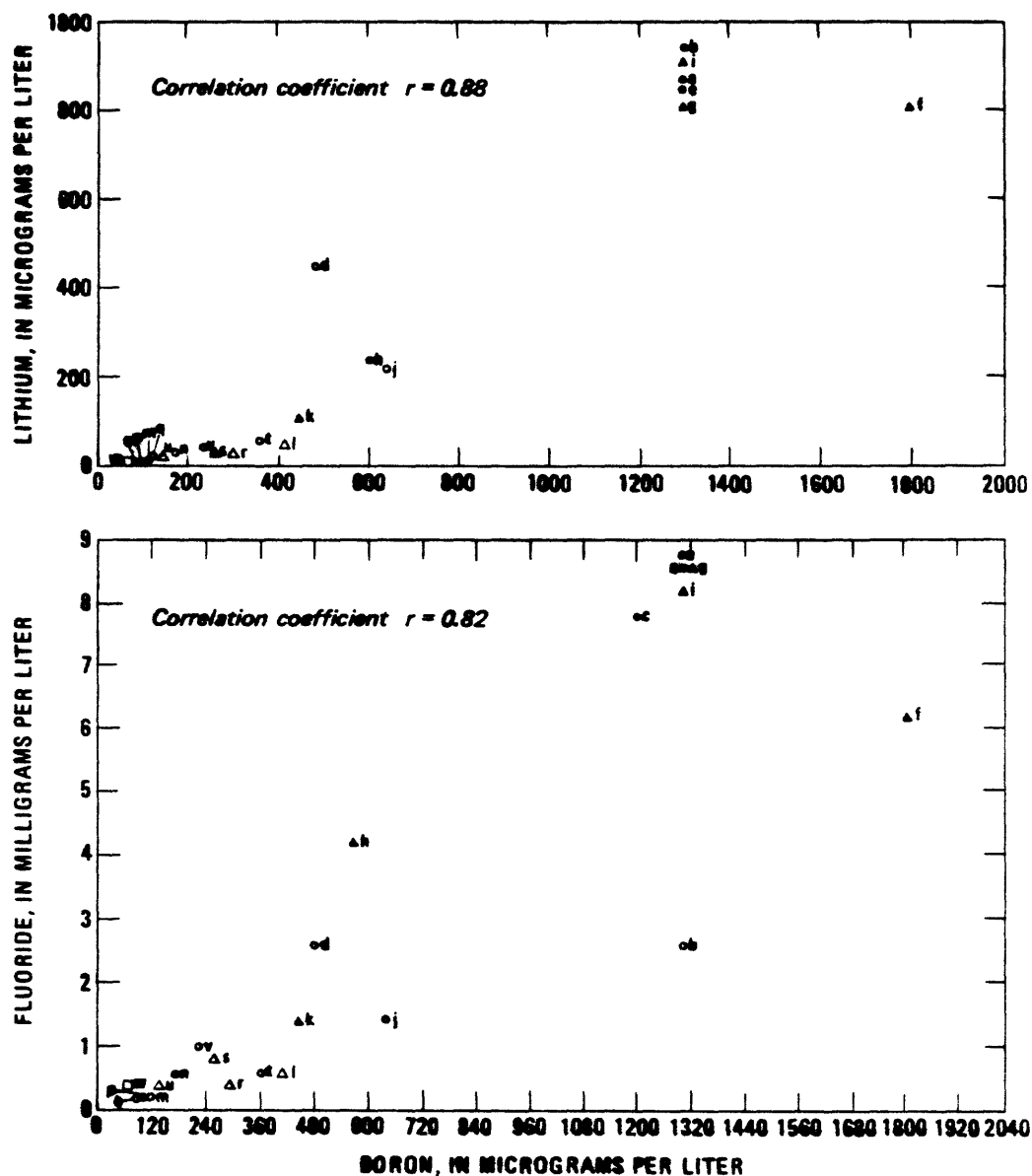
FIGURE 13. -- Plots of fluoride and lithium versus boron. Symbols are the same as in figure 11. Letters designate sampling locations listed in table 9. Values plotted for samples with multiple analyses represent average concentrations.
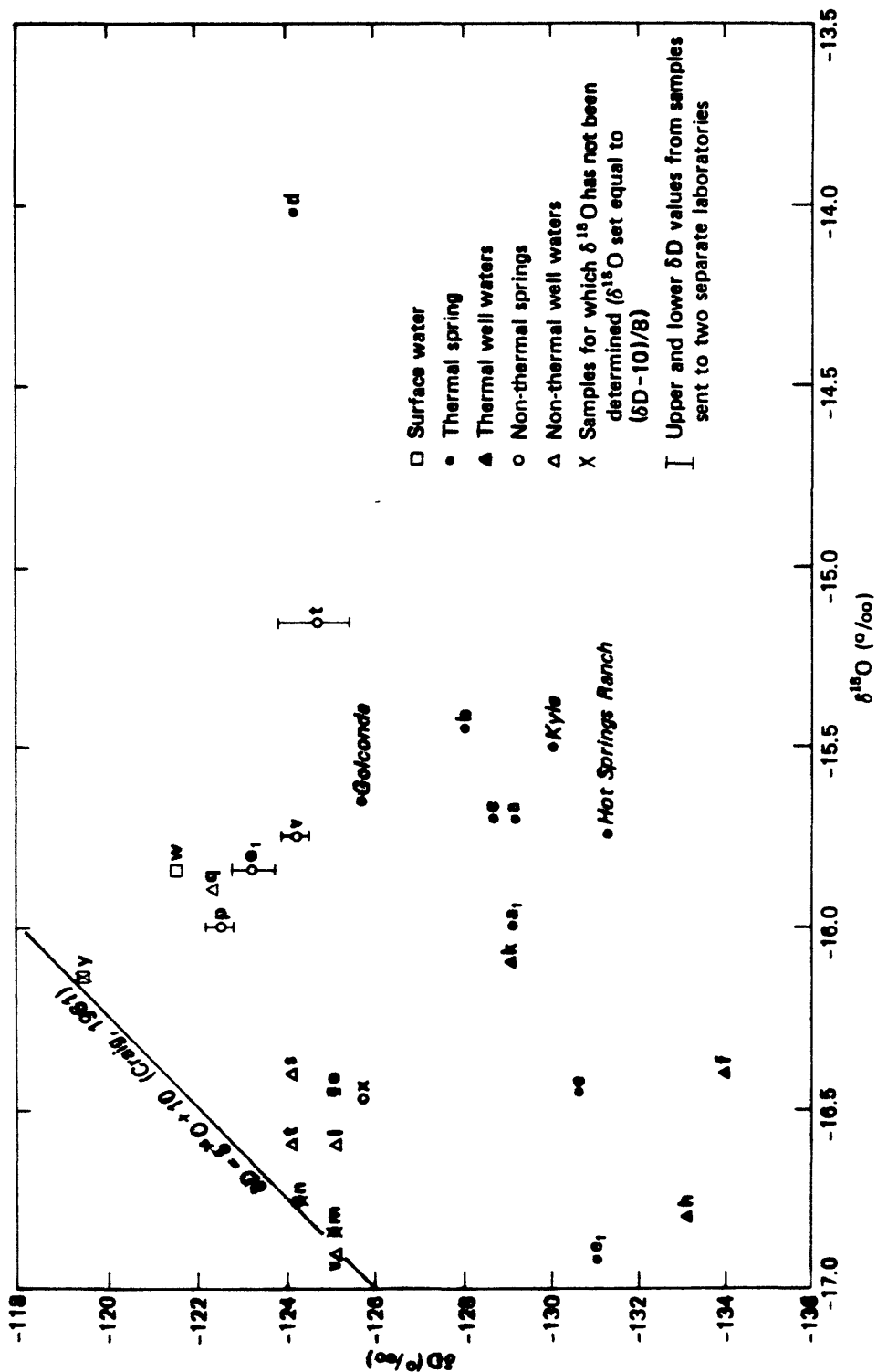
FIGURE 14. -- Isotopic composition of some thermal and non-thermal waters in southern Grass Valley compared with data for three hot springs in adjacent valleys and trend line for meteoric water. Letters correspond to sampl-ing locations shown on table 9. Kyle, Hot Spring Ranch, and Golconda values are from Mariner and others, 1975, p. 23-24.

The proposition that the lower deuterium content in the thermal water is caused by presence of some magmatic or metamorphic water is untenable because of the relative isotopic composition of these waters. The mixing of meteoric waters, as represented by the nonthermal waters, with the composition of metamorphic or magmatic water, as plotted in figure 15, would show an increased deuterium content rather than the observed lighter composition.

Boiling of water can result in a higher concentration of deuterium in the liquid phase and therefore a lower concentration in the vapor phase for temperatures below about 200°C (Friedman and O'Neil, 1977, fig. 35). Subsequent condensation of this vapor could then produce a liquid with a lower deuterium concentration than the original liquid. There are problems with the scenario that make this process very unlikely at Leach Hot Springs. Assuming the existence of a deep thermal water with a deuterium content equal to that of the nonthermal water, then a residium with an even greater deuterium content would be produced. Although such a water could be present, no data support its existence. The depth at which boiling would have to occur makes this process appear even more unlikely. The heat-flow studies (p. 149) indicate that the estimated reservoir temperature of about 163°-176°C would require a circulation depth of at least 3.0 km. If the geothermometry is valid, then equilibration must occur after the boiling-condensation process, which would then require very high temperatures (>350°C) to create a vapor pressure great enough to overcome the hydrostatic pressure. The boiling-condensation process therefore seems unrealistic.

The possibility of recharge from recent precipitation at a much higher altitude ,such as the Ruby and Toiyabe Ranges (which are the closest areas with significantly higher altitudes), should also be considered. The proposal that the thermal system is being recharged at a greater altitude than has been sampled is based on the observation in other areas that precipitation becomes
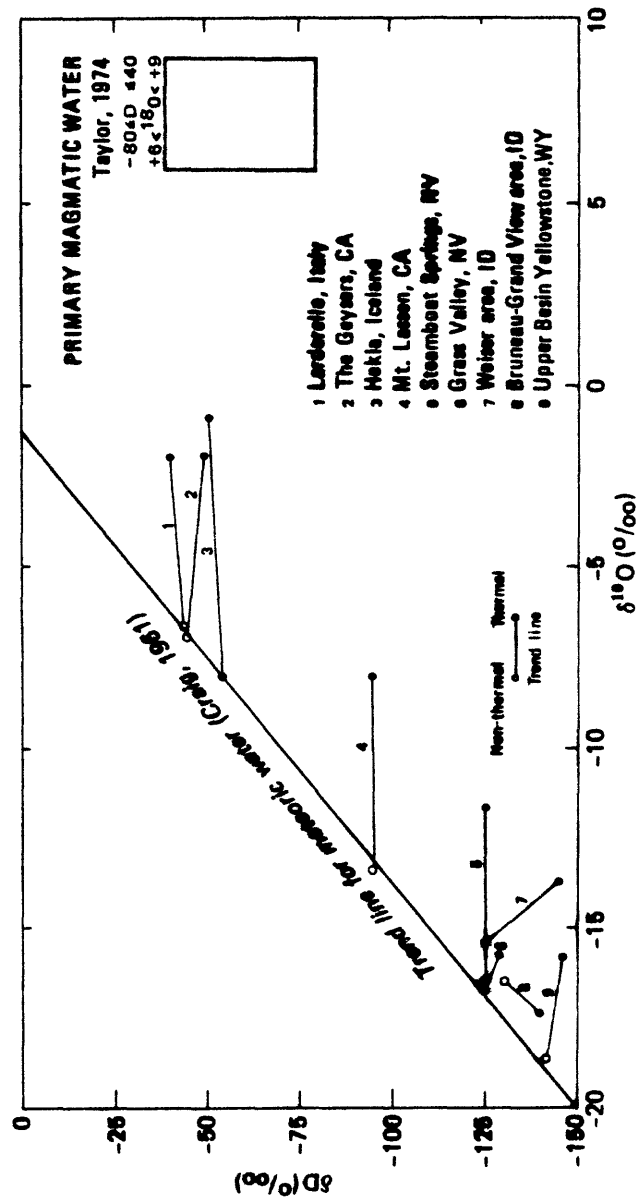
88

FIGURE 15. -- Comparison of thermal and non-thermal waters from southern Grass Valley and other areas of the world. Data for Idaho from Rightmire and others (1976); data for other areas except Grass Valley from White and others (1973).

isotopically lighter with increasing altitude. Although stable-isotope data are not available for these higher altitude areas, the large distances to these mountains make this possibility very unlikely. The central Toiyabe Range, which is closer than the Ruby Mountains, is about 160 km to the southeast. Even assuming a relatively high ground-water flow rate of 10 m per year, it would still take 16,000 years for infiltrating precipitation to reach Leach Hot Springs. It is therefore apparent that even if the recharge source is at high altitude, it would be "paleowater" (mechanism 4). The present data include samples from cold springs that range in altitude from about 1,430 to 1,780 m and appear to drain areas at altitudes up to 2,440 m. However, as the surrounding mountains have only a minor surface area above about 2,100 m, the potential for lighter precipitation to be deposited as a supply for the thermal reservoir appears small. In addition, available deuterium values from the cold springs and stream flow draining the mountains (Pollard Canyon and Clear Creek) do not show a trend with altitude that would indicate a source of lighter water from precipitation on the higher parts of the local mountains.

The use of stable-isotope data to identify water that was recharged during a cooler climatic period has been discussed by Gat (1971) on the basis of arid-zone data from North Africa and the Middle East. Using stable-isotope data for the paleowater from several areas, Gat (1971) noted the following relationships between the isotopic composition of present-day and past precipitation:

1. The meteoric-water line, that is, $\delta D = \delta^{18}O + d$ of Craig (1961) has a lower d value (named "the deuterium excess" parameter by Dansgaard, 1964) for the paleowater than the more recently recharged ground water.

2. The paleowater has a lower deuterium content than recently recharged ground water.

The thermal and nonthermal water in Grass Valley show the same two relations noted for old and recently recharged ground water in the Middle East and North Africa. This suggests the possibility that the recharge for the thermal system occurred during a cooler, and perhaps wetter, period. The occurrence of isotopically lighter paleowater found in arid regions has not been observed in more humid regions or areas closer to oceans which supply water to storm systems. Pearson (1975) has noted that the deuterium- and oxygen-isotope contents of both young and relatively old water (on the order of tens of thousands of years old) are very similar in the Carrizo Sand of south Texas and the London Chalk in England. Because both of these aquifers have recharge areas relatively close to an ocean, the magnitude of the difference in the isotopic composition between the present and glacial periods may not be nearly as great as in the arid to semi-arid regions of the Basin and Range province in North America, the Middle East, and North Africa. A lack of shift for near-ocean areas may be reasonable if earlier climatic temperatures were not greatly different from today, because the isotopic composition of ocean water does not appear to have changed significantly since at least the Paleozoic (Taylor, 1974).

Two areas in southern Idaho also have thermal water that is lower in deuterium than the nonthermal water (fig. 15). The difference between the thermal and nonthermal water is much greater for the Idaho examples (about 10 to 20 permil) than at Grass Valley (5 permil)..This could be related to differences in storm-track patterns or temperature differences between the individual areas during the last glacial (pluvial) period. A storm that passes over a continental mass has a progressively lighter isotopic composition owing to preferential loss of the heavier fraction of water as precipitation. The storm tracks during the time of precipitation that supplied the now-thermal

91

water in Idaho may have traversed the continent for a much greater distance (perhaps coming from the north) in comparison to the storm track passing over Grass Valley (which may have been from the west). Alternatively, the difference in deuterium shifts between the thermal and nonthermal water could be a result of recharge from cooler precipitation. The relation developed by Dansgaard (1964) between δD and the mean annual air temperature at the land surface indicates that a 5 permil shift could result from a temperature difference of about $1^\circ C$. Mifflin and Wheat (1979) estimate that only about a $2.8^\circ C$ difference from modern temperatures could account for the climate in Nevada during a pluvial period. However, the complicating factor of changes in storm-track pattern makes it difficult to account for the differences in δD shift observed between the Idaho and Nevada systems.

These considerations suggest that the thermal water in Grass Valley is at least 8,000 years old, as climatic conditions greatly different from those at present have not occurred since late Wisconsin time. Stable-isotope data from the Greenland ice cap (Epstein and Gow, 1970) show that significant shifts in δD and $\delta^{18}O$ in the ice occurred between 10,000 and 15,000 years ago, but that the isotopic composition has remained nearly constant since about 8,000 years ago. This estimate of 8,000 years for the age of the thermal water in Grass Valley is compared with residence times calculated for different models of the hydrothermal system in a later section.

Comparisons of oxygen-isotope ratios are useful in geothermal investigations as a result of the exchange of oxygen with carbonate and silicate minerals at the high temperatures reached in geothermal systems (Craig, Boata, and White, 1956). The change in oxygen isotopic composition in thermal fluid, which is commonly called the oxygen shift, depends upon the temperature, flow rate, and the relative quantities of rock and fluid. Where small quantities of fluid are moving past a large amount of aquifer material, a large oxygen

shift would be expected, and this has been observed at the Salton Sea geothermal system, by Craig (1963, 1966). In contrast, White (1970) has noted a small shift at the Wairakei system where the quantity of water moving through the system is much larger. The oxygen shift at the Leach Hot Springs system is small compared to other systems (fig. 15), indicating that the thermal fluid at Leach Hot Springs has been in contact with a relatively small amount of aquifer material. Although it is not possible to quantify a "small amount of aquifer" on the basis of the available data, a conceptual flow model that involves a small amount of aquifer or long period of flow would be preferred to one which involves a large amount of aquifer or a short time period. The above discussion has assumed that oxygen is in isotopic equilibrium between the water and aquifer material. This assumption is probably not violated as oxygen isotopic equilibrium has been observed to at least 150°C and possibly as low as 100°C by Clayton and others (1968).

Oxidized carbon species in hydrothermal fluids can be derived from igneous, metamorphic, sedimentary, and atmospheric sources. The origin of the carbon can sometimes be determined using data on stable isotopes just as the origin of the water can at times be deduced using oxygen and hydrogen isotope ratios. The present data indicate that a deep source is most likely for the carbon observed at Leach Hot Springs. The ratios for stable carbon isotopes are known for two aqueous samples and one gas sample as shown in table 9. The $\delta^{13}C$ value of -9.13 permil obtained for carbon dioxide in the gas sample corresponds to a bicarbonate value of -7.74 permil (bicarbonate being the dominate aqueous carbon species) assuming equilibrium at 100°C and using a value of 1.4 for $10^3 \ln V$ where V is the isotopic fractionation factor (Friedman and O'Neil, 1977).

The similarity of carbon-isotope values for water from Leach Hot Springs and QH3D (-7.4 and 7.9 per mil) indicates that the carbon at Leach Hot Springs and QH3D may have derived from the same source.

Shallow ground water in an arid environment might be expected to have a carbon-isotope ratio in the range of that observed for the thermal water in the Leach Hot Springs system. The source of carbon in many ground-water systems is a mixture of $CO_2(g)$ derived from the soil zone and carbon from the dissolution of carbonate minerals. A $\delta^{13}C$ value for the soil CO_2 of -12 has been suggested by Pearson (1975); the value may be less negative in sparsely vegetated areas (Lerman. 1970), whereas more negative values are typically found in more humid areas. A 1:1 mixture of soil CO_2 with calcium carbonate is indicated by the following dissolution reaction:

$$CO_2(g) + H_2O + CaCo_3(s) \leftrightarrow Ca^{2+} + 2HCO_3^-.$$
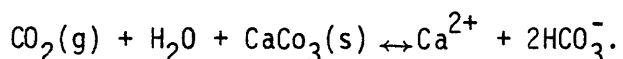
Most marine limestones have $\delta^{13}C$ values of about 0 permil. A 1:1 mixture could therefore result in a carbon isotope composition similar to that observed in the thermal water, and it could yield the same composition if a more negative value for atmospheric carbon were used. Although the dissolution process could account for the $\delta^{13}C$ values observed, only a limited amount of oxidized carbon can be brought into solution. The amount is limited by the amount of acid which is involved in the dissolution of the common carbonate minerals. One primary source of acid in groung water, carbonic acid, is restricted by the partial pressure of $CO_2(g)$ in the soil zone, as represented by the reaction:

$$H_2O + CO_2(g) \leftrightarrow HCO_3^- + H^+.$$
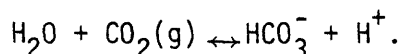
Assuming that the ground-water is in a nearly neutral pH condition after the dissolution, and that carbonic acid is the primary source of hydrogen ion, then the total amount of the carbon species would be equal to only about

twice as much as was introduced in the soil zone. This follows from examination of the reaction:

$$H^+ + CaCO_3 \leftrightarrow Ca^{2+} + HCO_3.$$
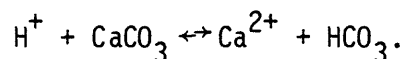
The partial pressure of $CO_2(g)$ at depth in the Leach Hot Springs system has been calculated using a version of SOLMNEQ (Kharaka and Barnes, 1973) which computes a pH value at a specified temperature using a mass balance approach for H^+ (Y.K. Kharaka, U.S. Geological Survey, oral communication 1980). At a temperature of $175^\circ C$ (the estimated approximate value at depth) a $CO_2(g)$ partial pressure of about 0.25 atmosphere was calculated for the most recent sample at orifice 22 (table 9). This value is much greater than could be achieved solely by the inroduction of soil CO_2 with subsequent dissolution of calcite. This conclusion is valid even if additional acid, from the conversion of pyrite to sulfuric acid, is responsible for all the observed sulfate in the thermal water. Therefore, an additional process must be producing most of the carbonate species present.

Although carbonate minerals can also supply CO_2 in hydrothermal fluids through decarbonation reactions at high temperatures (Ohmoto and Rye, 1979), this type of reaction does not appear to be important at the Leach Hot Springs system. This conclusion is based on the assumption that any limestone present at depth is of marine origin. The resulting $\delta^{13}C$ value of CO_2 from a decarbonation reaction would be about +5.0 permil which is distinctly different from the values observed in the thermal water.

Mantle carbon-isotope values measured by Moore, Bachelder, and Cunningham (1977), and Pineau, Javoy, and Bottinga (1976), are in the same range as observed at Leach Hot Springs. The carbon-isotopic composition of CO_2-charged springs

has been compared to the mantle values and used as evidence by Barnes and McCoy (1979) for a mantle source of CO_2 in some springs. As the carbon-isotope values observed at Leach Hot Springs are in this same range, the carbon in the hot springs appears to be a result of mantle outgassing. The carbon source at well QH3D is less certain as the CO_2 partial pressure is in the range which could be supplied by the soil atmosphere--the source could be from either the mantle or a soil and marine limestone carbon mixture.

Age of Leach Hot Springs System

The age of the geothermal system is an important parameter in evaluating alternative conceptual flow models. It should be emphasized that methodology for routine dating of hydrothermal systems does not exist so that the results of efforts to determine the age of this system must be considered somewhat specu-lative. Age estimates have been based upon several different lines of reasoning. Bodvarsson (1979) suggested that at least some of the Basin and Range hydro-thermal systems were created as a result of upwarping caused by the disappea-rance of large pluvial lakes. He argues that this deformation may have resulted in fracturing which allowed deeper circulation of fluids. Although this isostatic rebound may have caused deep vertical fracturing, there has been fracturing due to extensional tectonics for about the last 15 million years. It is difficult, then, to understand why the fracturing caused by isostatic rebound would allow deep circulation whereas fracturing due to deep seated extensional tectonics would not. Additionally, this system is beyond the margin of Lake Lahontan, which should make any rebound effects minimal.

The apparent amount of deposited silicic material in the vicinity of Leach Hot Springs may be used to estimate the age of the system. Goldstein and Paulsson (1977) have estimated that about 2.5×10^8 metric tons of precipitated material is present on the basis of an excess-mass calculation derived from

gravity data. Assuming that the aqueous silica is near equilibrium with respect to quartz at a reservoir temperature of about 175°C then about 175 mg/L should be in solution at depth. Measured concentrations in hot-spring waters at the land surface average 110 mg/L of SiO_2. The 65 mg/L difference between the two equilibrium values is the amount of silica per liter which is estimated to be precipitating from the thermal water before it reaches land surface. Assuming that the present flow rate of 8.4 L/s represents the long-term value for the thermal water discharging from the system and that all the silica precipitates in the vicinity of the hot springs (the precipitated silica is deposited in the zone where the excess mass is detected), then an age can be estimated. The result of 14×10^6 years appears unrealistically large, suggesting that the excess mass estimate is too high, that the long-term average spring flow exceeds the present-day rate, or the system has decreased in temperature. As dimensions of the channel carrying thermal water from the hot springs do not suggest significantly greater flow in the past and heat-budget calculations show approximate thermal equilibrium with the present-day convective heat discharge, the present flow rate may be a resonable value to use in the calculation. On the other hand, it is possible that some or most of the gravity anomaly attributed to excess mass of silica could instead be due to the presence of shallow bedrock in the vicinity of Leach Hot Springs. Hence, the above estimate for the age of hot-spring activity is of questionable validity..

An estimate of the age of hot-spring activity has also been made by Wollenberg (1977) using the uranium-238 decay series. His estimate of 3.1×10^5 years, although not unrealistic, was based on a number of assumptions including uranium being in secular equilibrium with its daughter products. According to the model, the equilibrium would be established between dissolved

uranium and its daughter products during transport in the hydrologic system. If no radiogenic thorium were initially present in the water, then about 200,000 years would be required to reach secular equilibrium, which represents an unrealistic residence time for the fluid. Furthermore, the method proposed yields very young ages for Beowawe and Lawton Hot Springs (161 and 307 years, respectively) on the basis of a recharge water uranium concentration of 2.0 mg/L and the thermal water data of O'Connell and Kaufmann (1976). These ages are probably not valid for high-temperature systems such as Beowawe, so that the age calculated by Wollenberg (1977) for Leach Hot Springs should not be considered reliable.

Other lines of evidence do give less ambiguous indications that the Leach Hot Springs system is considerably older than, say, 10,000 years. Low chloride concentrations and small δO^{18} shifts in the thermal water tend to suggest a well-flushed circulation system, implying long times and/or large flow rates. Heat-budget calculations discussed in later sections for the southern Grass Valley area as a whole and for the thermal anomaly surrounding Leach Hot Springs indicate approximate thermal equilibrium between a regional conductive heat flow near 3 hfu and the present-day conductive and convective heat discharge at the land surface. This in turn, suggests more-or-less continuous fluid circulation at near present-day rates for times sufficient to establish the heat-flow balance. For depths of circulation of several kilometers, periods of 100,000 years or more are required.

SUBSURFACE TEMPERATURE AND HEAT FLOW

Purpose of Subsurface-Temperature and Heat-Flow Studies

Determination of the patterns of subsurface temperature and heat flow was an important part of the present investigation for several reasons. First, the discharge of heat from areas affected by hydrothermal convection, principally at Leach Hot Springs and near Panther Canyon, and the weighted-average heat flow from the entire southern Grass Valley provide information about the characteristics of both the shallow and the deep ground-water systems and about the nature of the underlying heat sources. Second, patterns of subsurface temperature and heat flow help to outline areas of ground-water recharge and discharge, and areas where convective heat transport is significant. Third, although the available thermal data are based on measurement to depths of only 0.5 km, the analysis of these data yields insight as to the characteristics of the deeper parts of the hydrothermal system within which exploitable high temperature resources may exist.

Present Approach and Its Relation to Earlier Studies

In the present study, total heat discharge is estimated from a polygonal area occupying most of southern Grass Valley. This area, designated the "budget area", is enclosed by a series of straight-line segments connecting the outermost of 82 test wells used to estimate conductive heat flow. (See fig. 22) As thus conservatively defined, the budget area has an extent of 125.5 km^2, as contrasted with the area of 200-300 km^2 for the "hydrothermal convection system supported by regional heat flow" described by Sass and others (1977, p.55).

In deriving the estimate of conductive heat discharge, the present study uses essentially the same basic data but somewhat different methods of analysis from those used by Sass and others (1977). These differences are described in a later section "Conductive Heat Discharge". In addition, data from 16 test wells drilled by Geothermex Company in 1979 were used in the present study.

The present estimate of convective heat discharge is about three-fourths that estimated by Olmsted, Glancy, Harrill, Rush, and VanDenburgh (1975, p. 199), which was used also by Sass and others (1977, p. 60). The dominant item-- the measured discharge of Leach Hot Springs-- was 12.5 L/s in 1973-74 (Olmsted and others, 1975, p. 189, 199), whereas the weighted-average of 24 measurements from November 1974 to July 1978 made for the present study was 8.8 L/s (table 8). Some of this sizable difference results from measurement error, but some of it probably represents a real decrease in flow of the springs from 1973 to 1978. (See fig. 8.) We believe that the measurements made for the present study are more accurate than those reported by Olmsted, Glancy, Harrill, Rush, and VanDenburgh (1975).

The present study considers advective heat discharge from the budget area, a component not included by Sass and others (1977) in their estimate of total heat discharge. This component, which is difficult to estimate but probably is a significant fraction of the total, consists of the heat carried by ground water moving northward out of the area minus the heat brought in by ground-water inflow from the western, southern, and eastern sides of the area.

In spite of the difference in approach, the present estimate of 3.8 hfu for the average heat flow in southern Grass Valley is in fair to good agreement with the estimate of 3.3 to 3.7 hfu of Sass and others (1977, p.60).

Subsurface Temperature Distribution

With few exceptions, temperature profiles in test wells in southern Grass Valley are linear within zones of fairly uniform thermal conductivity. Below the water table, gradients in some wells exhibit notable changes with depth, but most of these changes are obviously related to changes in thermal conductivity: Zones of high conductivity have relatively small gradients, and zones of low conductivity have relatively large gradients. In a few wells, temperature gradients in the uppermost 10-20 m of the saturated zone are less than they are below these depths or are even reversed locally. This suggests hydrologic disturbance caused by shallow ground-water flow. However, at some places, as at test well QH3D, the anomalous gradients to 10-20 m below the water table may be an artifact of well construction; casing at these depths was not grouted to prevent upward or downward movement of water in the annulus between the casing and the walls of the drill hole.

Above the water table, gradients tend to decrease with depth as the water table is approached, caused by the increase in water content and corresponding increase in thermal conductivity with depth.

Temperature profiles to a depth of 14 m were measured periodically in several test wells near Leach Hot Springs in order to define average annual temperatures within the zone of seasonal fluctuation. In these wells the average ratio of the temperature gradient from 0 to 14 m to that from 14 to 20 m is 1.4. Using this value for all the test wells in which temperture gradients from 14 to 20 m (or 14 to 18 m) were measured, the average annual temperature at the land surface was calculated by extrapolation. The average for 72 wells was $11.5^{o}C$; the standard deviation was $0.8^{o}C$. Areal variation in this temperature has no obvious pattern related to land-surface altitude or other factors. The value of $11.5^{o}C$ is therefore used as a

102

surface boundary condition for all the heat-flow estimates.

Most test wells in southern Grass valley penetrate only a small fraction of the total thickness of valley fill. However, as shown in figure 16, linear gradients continue to greater depths in test wells that penetrate either to the base of the fill or more than three-fourths of its thickness. The drilled depth of these wells ranges from 60 to 457 m. Apparently, vertical and horizontal ground-water flow at most places is too slow to modify significantly a conductive heat-flow regime.

Exceptions to linear temperature gradients throughout the valley fill probably are limited mainly to the area within about 0.5 km of Leach Hot Springs, especially west of the hot springs fault. For example, a sharp decrease in temperature gradient below a depth of 7 m in test well DH10 (only 430 m northeast of Leach Hot Springs), and evidence of hydrologic disturbance at greater depths is indicated by the fact that extrapolation of the gradient in DH9 to the inferred base of the valley fill at that site gives a temperature of 269°C (table 11) -- well above geothermal reservoir temperature indicated by hydrochemical evidence. Other areas of decreased gradients with depth, gradient reversals, or other irregularities caused by hydrologic disturbance may exist within the valley fill in southern Grass Valley, but this possibility cannot be confirmed with present data.

The pattern of ground-water circulation within the upper part of the bedrock is revealed by projecting temperature gradients measured in the test wells to the inferred interface between the valley fill and the bedrock. The gradients used in this calculation are given in table 11; the inferred depths to bedrock are shown in figure 3 and listed in table 11; and the calculated temperature distribution at the base of the valley fill is shown in figure 17 and listed in table 11.
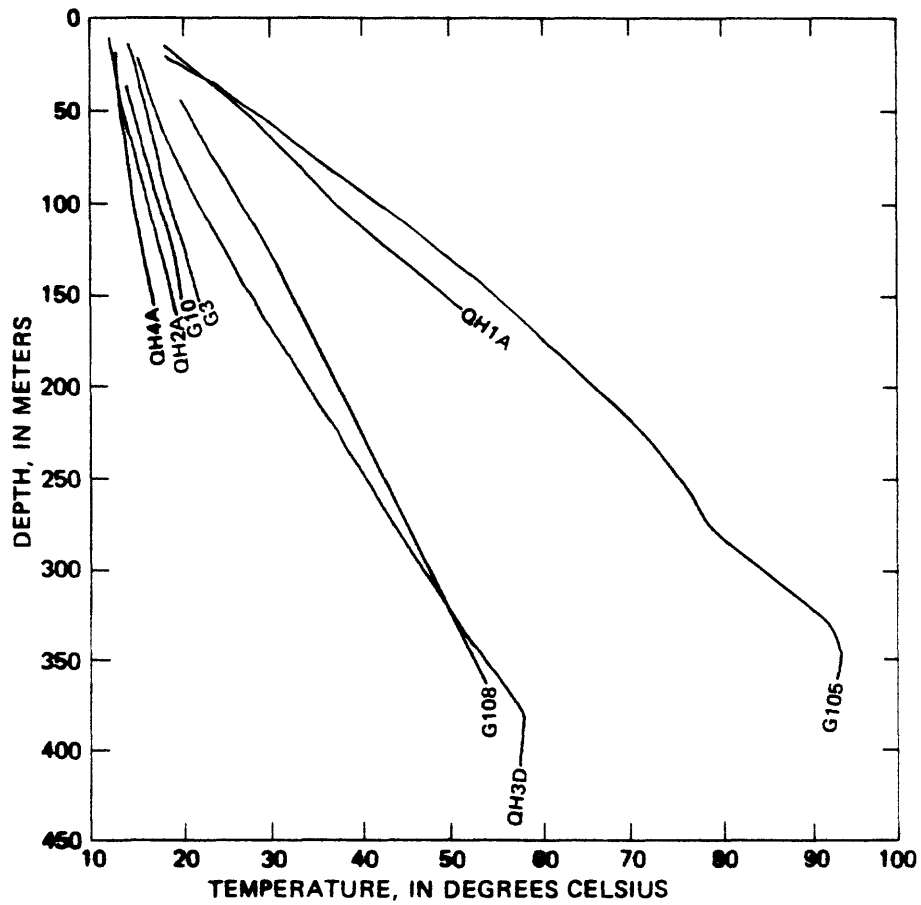
FIGURE 16. -- Temperature profiles in test wells penetrating all or most of valley fill.

TABLE 11.—Temperature gradient in test wells and estimated temperature at base of valley fill.

Test well	Reference depth (m)	Temperature (^{o}C)	Depth range (m)	Temperature gradient (^{o}C/km)	Depth to base of Valley fill (m)	Temperature at base of valley fill (^{o}C)	Remarks
DH1	39	15	30-44	74	800	71	
DH2	38	15.4	42-50	36	180	21	
DH3	44	40	38-46	508	150	94	
DH4	34	26	24-48	251	280	88	
DH5	24.5	17.4	24-27	128	150	33	
DH6	40.5	22	31-41	170	410	85	
DH7	50	19.8	33-39	107	900	111	
DH8	39.5	14.5	31-44	72	900	77	
DH9	38.5	44	37-41	641	390	269	
DH11	40	23.6	35-44	233	620	159	
DH12	30	14	28-42	81	710	69	
DH13	0	16.3	42-50	663	150	116	

TABLE 11.--Temperature gradient in test wells and estimated temperature

at base of valley fill (continued.)

Test well	Reference depth (m)	Temperature (°C)	Depth range (m)	Temperature gradient (°C/km)	Depth to base of Valley fill (m)	Temperature at base of valley fill (°C)	Remarks
DH14A	0	17.7	34-42	257	410	123	
DH15	0	16.9	40-44	296	200	76	
QH1A	132	45	80-155	224	220	65	
QH2A	150	20	25-130	52	150	20	
QH3D	378	58	--	--	378	58	Measured temperature
QH4A	150	16.5	125-155	42	155	17	
QH5A	92	16	55-128	37	750	40	
QH6A	33	14	17-50	51	770	52	
QH7A	58	16	30-73	45	820	50	
QH8A	42	16	41-49	69	170	25	
QH9A	54	16	67-75	40	200	22	
QH11A	50	14	40-55	52	180	21	
QH12A	59	16	38-48	110	600	76	

TABLE 11.--Temperature gradient in test wells and estimated temperature
at base of valley fill (continued.)

Test well	Reference depth (m)	Temperature (°C)	Depth range (m)	Temperature gradient (°C/km)	Depth to base of Valley fill (m)	Temperature at base of valley fill (°C)	Remarks
QH13A	107	16	46-52	116	160	28	
QH14A	43	14	46-73	30	500	28	
Q1	100	18	50-200	65.5	870	68	
Q2	110	17	50-160	55.5	950	63	
Q3	100	22	50-170	120	520	72	
Q4	41	14	33-56	51	750	50	
Q5	56	16	54-107	41	250	24	
Q6	45.5	15	39-55	45	470	34	
Q7	44	14	35-73	35	500	30	
Q8	60	17	44-66	59	290	31	
Q9	30	13	49-57	30	500	27	
Q10	39	14	38-55	52	660	46	
Q11	72	15	46-78	37	490	30	

TABLE 11.--Temperature gradient in test wells and estimated temperature

at base of valley fill (continued.)

Test well	Reference depth (m)	Temperature (°C)	Depth range (m)	Temperature gradient (°C/km)	Depth to base of Valley fill (m)	Temperature at base of valley fill (°C)	Remarks
Q12	55	15	51-62	45	220	22	
Q13	80	15	38-82	39	350	26	
Q14	98	14	51-116	21	660	26	
Q15	46	15	42-50	95	600	68	
Q16	71	18	54-81	78	400	44	
Q17	52	23	44-75	134	380	67	
Q18	47	16	38-53	71	460	45	
Q19	41	14	32-55	45	730	45	
Q20	52	15	38-69	42	750	44	
Q21	50	14	49-61	37	490	30	
Q22	38	13	39-49	20	780	28	
Q23	122	26.8	57-124	144	490	80	
Q24	119	18	87-151	45	240	23	

TABLE 11.--Temperature gradient in test wells and estimated temperature
at base of valley fill (continued.)

| Test well	Reference depth (m)	Temperature (°C)	Depth range (m)	Temperature gradient (°C/km)	Depth to base of Valley fill (m)	Temperature at base of valley fill (°C)	Remarks
T1	64	17.06	---	55	600	47	
T2	63	20.52	---	101	440	59	
T3	65	19.91	---	83	430	50	
T4	65	20.93	---	92	390	51	
T5	60	18.27	---	71	390	42	
T6	56	17.39	---	65	440	42	
T7	54	15.89	---	54	460	38	
T8	43	13.78	---	41	620	37	
T9	44	14.12	---	43	610	38	
T10	47	16.19	---	71	690	62	
T11	40	17.30	---	97	650	76	
T12	37	20.08	---	145	510	89	
T13	55	25.42	---	172	260	61	

TABLE 11.--Temperature gradient in test wells and estimated temperature

at base of valley fill (continued.)

Test well	Reference depth (m)	Temperature (°C)	Depth range (m)	Temperature gradient (°C/km)	Depth to base of Valley fill (m)	Temperature at base of valley fill (°C)	Remarks
T14	215	33.32	---	70	80	24	
T15	51	17.26	---	74	290	35	
T16	57	17.44	---	81	230	31	
T17	47	16.42	---	74	500	50	
T18	41	19.83	---	132	440	72	
T19	48	18.02	---	85	400	48	
T20	36	18.05	---	120	490	73	
T21	51	25.12	---	164	290	64	
T22	29	13.83	---	68	700	59	
T23	28	12.88	---	43	860	49	
T24	42	14.77	---	48	680	45	
T25	61	15.68	---	39	430	30	

TABLE 11.--Temperature gradient in test wells and estimated temperature
at base of valley fill (continued.)

Test well	Reference depth (m)	Temperature (°C)	Depth range (m)	Temperature gradient (°C/km)	Depth to base of Valley fill (m)	Temperature at base of valley fill (°C)	Remarks
T26	61	16.66	---	54	380	34	
T27	33	15.23	---	71	440	44	
T28	30	15.43	---	88	410	49	
T29	30	15.30	---	83	380	44	
T30	26	14.99	---	70	400	41	
T31	23	14.87	---	73	530	52	
G2	138	23	99-151	77	900	82	
G3	84	18	80-150	56	50	16.0	Measured temperature
G4	113	18	120-150	70	870	71	
G7	80	17.5	60-80	43	110	19	
G8	42	16	40-60	73	50	16.6	Measured temperature
G9	34	15	---	--	40	15.8	Measured temperature
G10	57	15	40-80	54	100	17.3	Measured temperature
G11	123	16	120-150	47	650	41	

TABLE 11.--Temperature gradient in test wells and estimated temperature
at base of valley fill (continued.)

Test well	Reference depth (m)	Temperature (°C)	Depth range (m)	Temperature gradient (°C/km)	Depth to base of Valley fill (m)	Temperature at base of valley fill (°C)	Remarks
G12	143	27	110-152	112	840	105	
G13	147	22	100-147	78	800	73	
G14	150	17.7	60-150	52	620	42	
G15	150	18.8	30-150	46	700	44	
G105	--	--	--	--	323	94	Measured temperatures; rhyolite at 323 m
G106	270	20	250-400	47	910	50	Measured temperatures
G108	225	40	100-360	104	440	62	Measured temperatures

The temperature pattern shown in figure 17 is characterized by two promi-
nent highs: (1) A large northwest-trending high centered at Leach Hot Springs
and occupying much of the northern two-thirds of the area; and (2) a high near
Panther Canyon in the southeastern part of the valley and extending southward,
beyond the budget area. A secondary high, superimposed on the southwest flank of
the Leach Hot Springs high, is centered at test well QH3D, about 5 km south-south-
west of the hot springs, on the Quicksilver Mine Road. Temperatures at the base of
the valley fill range from less than 20°C along some of the margins of the valley
to more than 150°C in the central part of the Leach Hot Springs area and more than
100°C southwest of Panther Canyon. The maximum measured temperature at the high
at well QH3D is about 58°C.

One of the most significant features of the temperature pattern exhibit-
ed in figure 17 is that it differs from the pattern that would be expected
from a conductive regime and the buried bedrock topography shown in figure 3.
In a temperature regime unaffected by hydrothermal convection , the tempera-
ture at the base of the valley fill (top of the bedrock) would be expected
to be highest where the valley fill is thickest . Comparison of figures 3 and
17 indicates, however, that although to a limited extent this relationship is
true, there are notable departures from it. One striking example of such a
departure is the area of relatively low temperature in the south-central part
of the valley, between test wells Q22 and Q14 (pl. 1, fig. 17). This thermal
low lies near the axis of the trough in the bedrock surface where the valley
fill is 600-800 m thick (fig. 3).

In order to highlight this anomaly and other cold or warm areas, fig-
ure 18 shows the difference in temperature at the base of the valley fill
between the estimated or measured temperature at this surface and the projected
temperature that would exist at this surface if an average temperature grad-
ient of 48.2^{o}C/km, which corresponds to the estimated average conductive
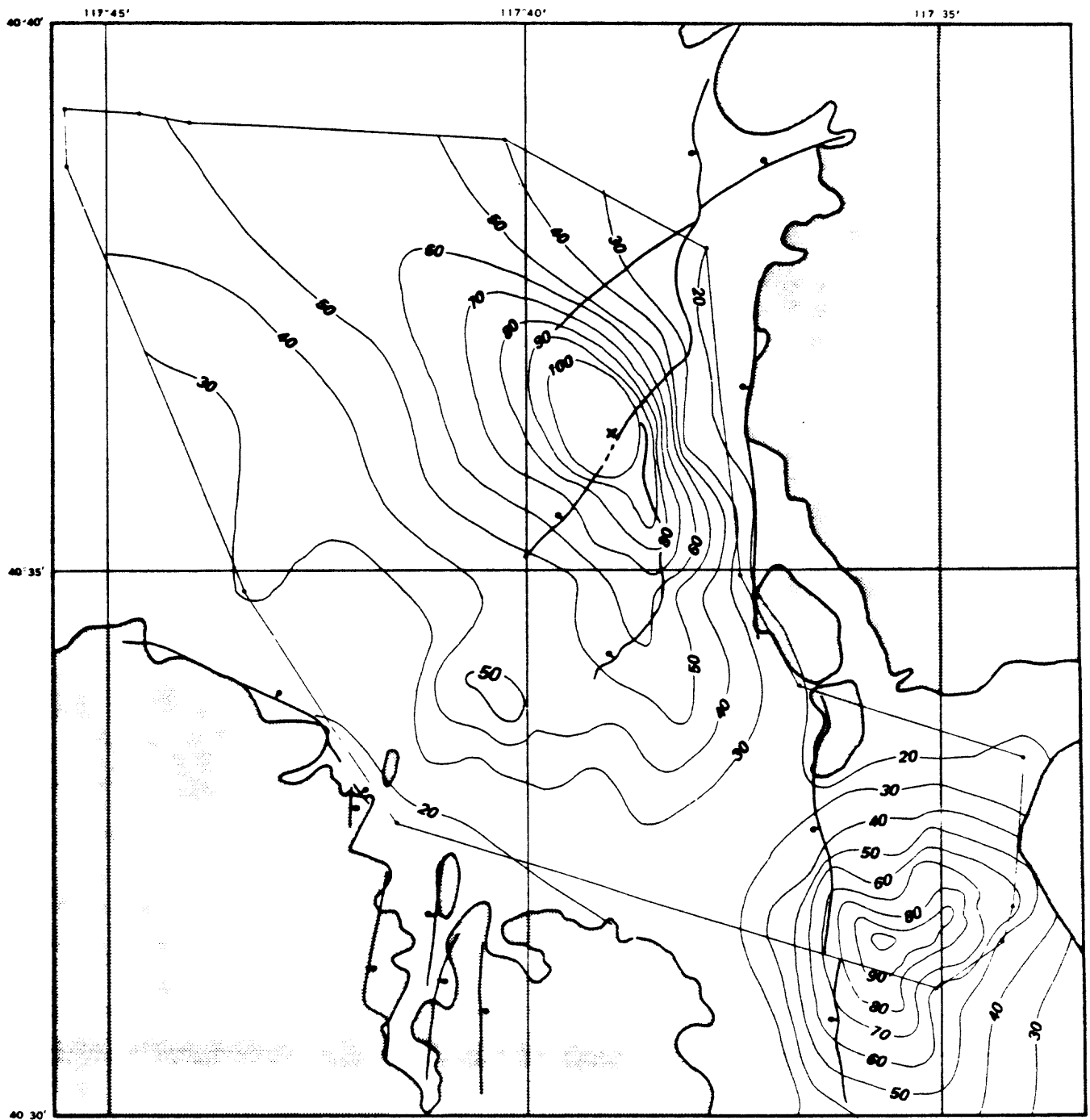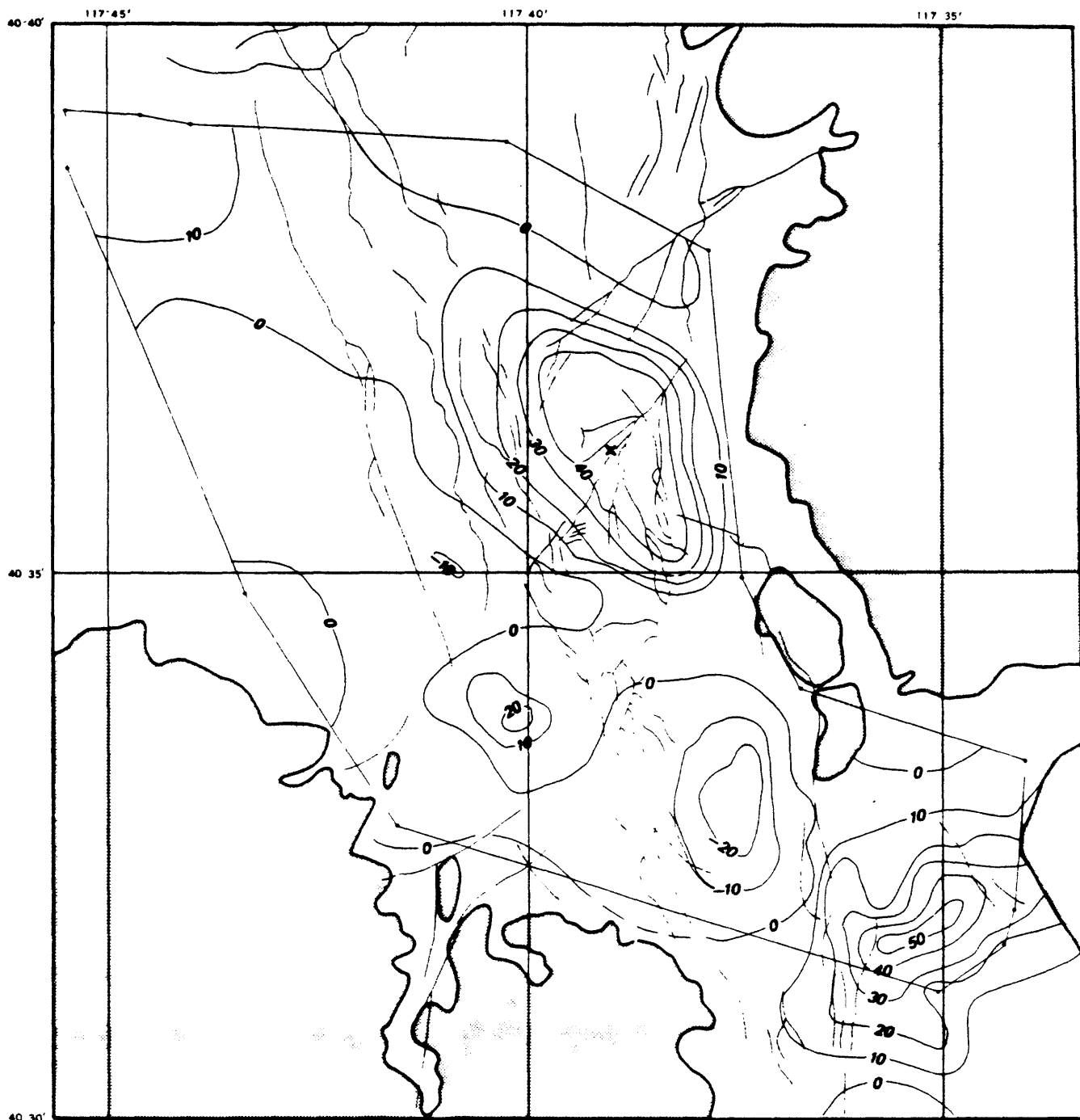
EXPLANATION
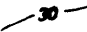
☐ Edge of pre-Tertiary bedrock outcrop

⟋30⟍ Line of equal temperature at base of valley fill.
     Interval, 10°C

⟋ᵧ⟍ Principal faults, bar and ball on downthrown side

✕ Leach Hot Springs

FIGURE 17. -- Map of southern Grass Valley showing inferred temperature at base of fill.
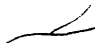
114

EXPLANATION

Edge of pre-Tertiary bedrock outcrop

Line of equal temperature anomaly at base of valley fill.
Interval, 10°C

Faults mapped by Noble (1975)

x   Leach Hot Springs

FIGURE 18. -- Map of southern Grass Valley showing temperature anamolies at base of valley fill. Anamolies calculated as the estimated or measured temperature at base of fill minus the projected temperature at base of fill using temperature gradient of 48.2°C/km corresponding to a conductive heat flow of 1.83 hfu and thermal conductivity of 3.8 tcu.

115

heat flow of 1.83 hfu outside the thermal anomalies (table 16) and an average thermal conductivity of 3.8 thermal-conductivity units (tcu), existed everywhere in the valley fill. Of course, some of the temperature differences shown in figure 18 probably result from departures of thermal conductivity from the mean of 3.8 tcu for the valley-fill deposits. However, the temperature differences are believed to be too large to be accounted for entirely, or even in large part, by this mechanism.

Because, as discussed earlier, temperature gradients within the valley fill almost everywhere indicate a conductive regime, the temperature anomalies at the base of the valley fill (top of the bedrock) are interpreted as being caused chiefly by hydrothermal convection within the bedrock. Warm anomalies probably reflect ascending water. A striking example of rising water is the warm anomaly of more than 20°C amplitude at test well QH3D, which is at or near the crest of a buried-bedrock high. The best example of the opposite case is the cool anomaly of more than 20°C amplitude between test wells Q14 and Q22 (pl.1, fig. 18), described earlier.

Vertical temperature distribution in the valley fill, as shown in sections A-A',B-B', C-C'and D-D' across the valley (figs 6,19-21), also suggest convection within the bedrock, at least in places. For example, in sections A-A' and B-B' (figs. 6 and 19), the lines of equal temperature near the base of the valley fill on much of the western side of the buried valley approximately parallel the bedrock surface. In section C-C' (fig. 20) and in the western part of section D-D' (fig. 21), the lines of equal temperature in the lower part of the valley fill are a subdued replica of the underlying buried-bedrock surface.

Additional evidence of hydrothermal convection within the bedrock is afforded by the temperature profiles in two of the deepest test wells in the area, both of which penetrated consolidated rocks for several tens of meters.
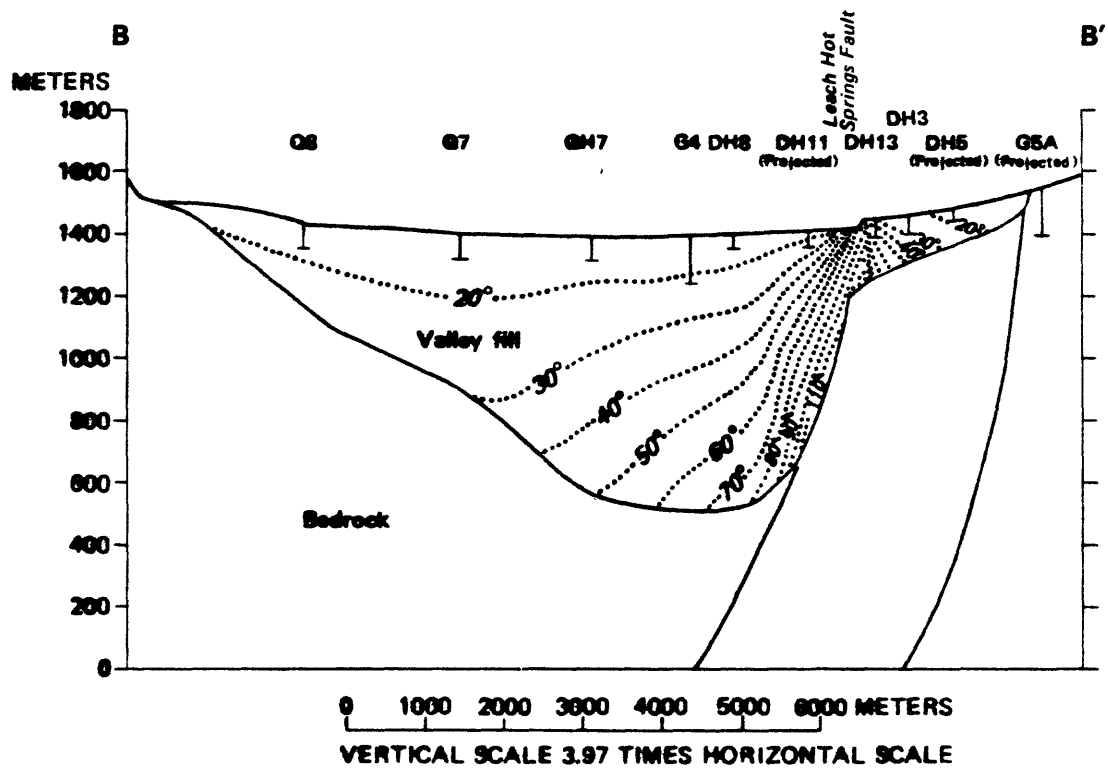
FIGURE 19. -- Generalized geologic section B-B' showing inferred distribution
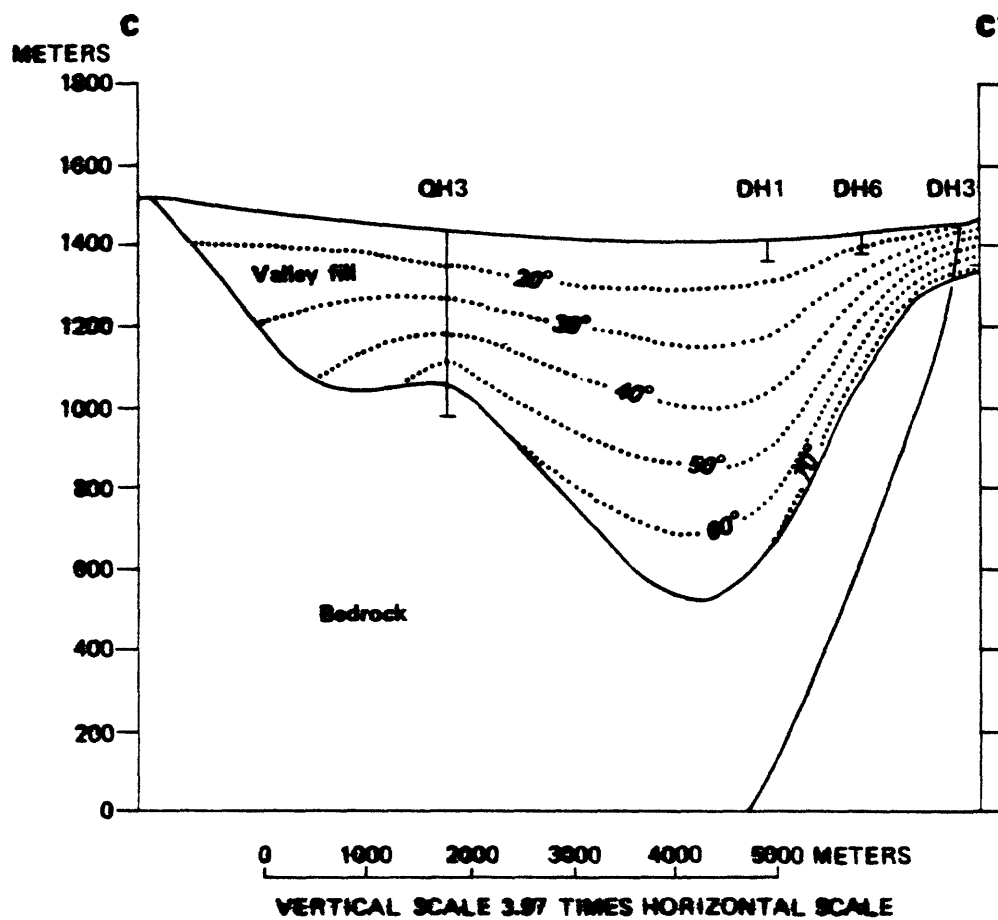of temperature in valley fill.

117

FIGURE 20. -- Generalized geologic section C-C' showing inferred distribution
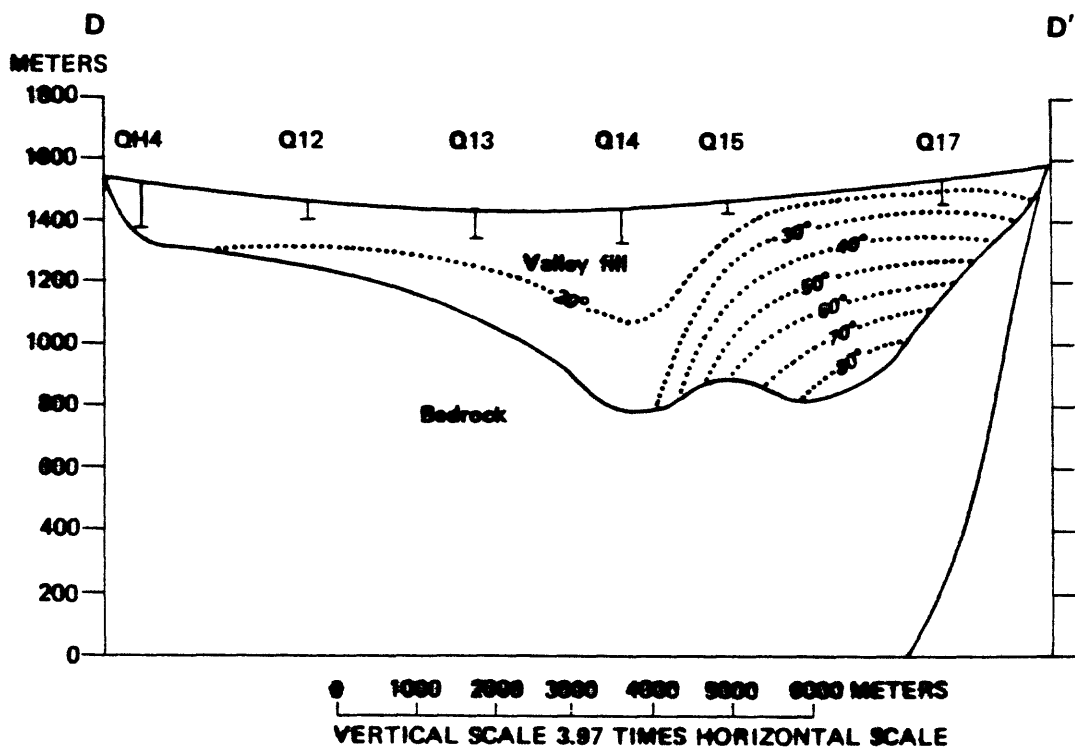of temperature in valley fill.

118

FIGURE 21. -- Generalized geologic section D-D' showing inferred distribution of temperature in valley fill.

119

Test well QH3D penetrated pre-Tertiary bedrock underlying Tertiary sedimentary rocks from a depth of 378 m to the bottom of the well at 457 m. In this well the temperature gradient changes rather abruptly from 130°C/km in the lower part of the valley fill (Tertiary sedimentary rocks and alluvium) to slightly reversed (temperature decreasing with depth) in the bedrock, which is a meta-greywacke (fig.16).

Test well G105, about 1.7 km south-southwest of Leach Hot Springs, penetrated rhyolite of probable Tertiary age from a depth of 323 m to the bottom of the hole, at 360 m. The temperature gradient in the overlying valley fill (Tertiary gravel deposits and Quaternary alluvium) averages about 250-270°C/km but decreases to zero, then reverses slightly in the rhyolite (fig. 16).

Both the rhyolite and the pre-Tertiary meta-greywacke have hydrologic properties distinctly different from the Tertiary sedimentary rocks and Quaternary alluvium in that vertical ground-water flow, probably through fractures, is much less inhibited in the former-- the consolidated rocks-- than in the latter deposits, in which almost all ground-water flow probably occurs through interconnected pores rather than through fractures. Therefore, convective heat transport probably is much less inhibited within the pre-Tertiary rocks and the Tertiary volcanic rocks than in the Tertiary sedimentary rocks and Quaternary alluvium. However, the exact causes of the slight reversals in temperature gradient within the meta-greywacke of test well QH3D and the rhyolite at test well G105 cannot be determined from present information.

Because of the evidence for rather widespread convection in the pre-Tertiary bedrock and in the Tertiary consolidated volcanic rocks the essentially conductive temperature gradient in the valley fill cannot be projected into the bedrock with any reasonable degree of assurance. Accordingly, no temperatures within the bedrock are shown in the sections (figs. 6,and 19-21). Hypothetical temperatures within the bedrock, which are based on numerical

simulations of heat and fluid flow are, however, portrayed in the section of the report "Models of Hydrothermal System", (see figs. 27, 28,31 and 34).

Components of Heat Discharge

Heat is discharged from the hydrothermal system in southern Grass Valley by convection, radiation, advection, and conduction. Radiation, which occurs from warm ground and hot-water surfaces, is believed to be small; that from warm ground is included in the estimates of conductive heat discharge, and that from hot-water surfaces is included in the estimate of convective heat discharge. Each of the three remaining components is discussed in the following sections.

Conductive Heat Discharge

Heat conduction upward through the upper part of the valley-fill deposits and, locally, through near-surface consolidated rocks is the largest item in the heat budget of southern Grass Valley. The method used in the estimate is outlined in the following paragraphs.

The area considered is the budget area described earlier in the section "Present Approach and Its Relation to Earlier Studies". The general method used is similar to that described by Sass and others (1977) and Olmsted, Glancy, Harrill, Rush, and VanDenburgh (1975), but with some modifications. As an indicator of the precision of the estimate, heat flow was calculated semi-independenty for two depth ranges: (1) The first, extending from near the top of the saturated zone to near the bottom of the well in most of the DH, QH, and Q wells, and (2) the second, at shallower depth, generally above the saturated zone , at a depth range of 14-18 m in most of the T wells and 14-20 in most of the DH, QH, and Q wells. The second range was selected so as to obtain a measure of the conductive heat flows as close to the land surface as possible but just below the approximate range of measurable seasonal temperature fluctuations, which extend to approximately 10-14 m depth in southern Grass Valley.

In both depth ranges, least-mean-squares temperature gradients measured in the test wells were used. Most of the data are from Sass and others (1977). A few measurements were made by Olmsted in DH wells near Leach Hot Springs, and Sass in G wells drilled by Geothermix Company in 1979. Departure of the gradients from linearity in the depth ranges used generally are small.

For the greater depth range, within the saturated zone, values of thermal conductivity measured by needle probe on cores or cuttings, reported

by Sass and others (1977, table Cl), were used for the QH and Q wells. However, unlike the procedure of Sass and others (1977), only those values representing saturated materials (below the measured or estimated water level in the well) were used. For DH wells in the vicinity of Leach Hot Springs, harmonic-mean thermal conductivity was calculated for the depth range in which the temperature gradient was measured. Values of thermal conductivity were assigned to several categories of materials described in the interpreted logs of the wells, as listed in table 12. The procedure used in the calculation is that described by Olmsted, Glancy, Harrill, Rush, and VanDenburgh (1975, p. 65). (Sass and others, 1977, used an assumed average value of 3.7 tcu in their estimate.)

For the shallower depth range, in unsaturated deposits, the following procedure was used to estimate thermal conductivity. For 27 of the test wells, in which temperature gradients were measured both above and below the water table, the ratio of the temperature gradient in the depth range 14-20 m (or approximately that depth range in some of the wells) to the temperature gradient below the water table was determined. These data are shown in table 13. The mean of the values of this ratio is 1.44. Because thermal conductivity is inversely related to temperature gradient (assuming uniform heat flow), the reciprocal of 1.44 --0.7-- is the average ratio of the thermal conductivity of the unsaturated materials from 14 to 20 m to that of the materials in the saturated zone. Accordingly, thermal conductivities for the 14-20 m depth zone were obtained by multiplying the measured or estimated thermal conductivities of the saturated materials in all the test wells penetrating the saturated zone by 0.7. For the T wells, all of which penetrate unsaturated materials, the average thermal conductivity in the 14-20 m depth range was obtained by interpolation or extrapolation of thermal conductivities in the 14-20 m depth range in the adjacent Q or QH wells. (Sass and

123

TABLE 12. -- Values of thermal conductivity assigned to categories
of material classified in interpreted logs.

(All materials assumed to be saturated with water.)

Category of material	Thermal conductivity (tcu)
Alluvium:	
Gravel; coarse gravel; clean gravel; gravel and sand; sandy gravel; gravelly sand; sand and gravel; "conglomerate"; cemented gravel	4.5
Sand and scattered gravel; clay and gravel; coarse sand; sand; coarse sand with clay and silt	4.0
Sand and silt; silty sand; clayey sand and silt; clay and silt with scattered gravel; fine sand	3.5
Sandy clay; silty clay; clayey silt; clay and silt	3.0
Clay (high porosity)	2.5
Tertiary sedimentary rocks:	
Sandstone; pebbly sandstone; conglomerate	5.0
Siltstone; dense mudstone; soft sandstone; dense claystone	4.0
Soft claystone; tuff; soft siltstone	3.0

TABLE 13.--Temperature gradients above and below water table.

Test well	Depth to water (m)	Depth interval (m)	Temperature gradient (°C/km)	Depth Interval (m)	Temperature gradient (°C/km)	Ratio 6:4	Remarks
DH2	>50	42-50	36	14-20	57	1.58	
DH3	26	26-38	488	14-20	621	1.27	
DH4	24	24-48	251	14-20	378	1.51	
DH5	>27	24-27	128	14-20	194	1.52	All materials unsaturated
DH13B	17	22-27	806	14-18	629	.78	
DH14A,B	32	34-42	257	14-18	377	1.47	
DH15	34	40-44	294	14-20	372	1.27	
QH1A	32	64-70	215	14-20	315	1.47	
QH3A	61	63-69	90	14-20	80	.89	
QH4A	46	125-155	42	14-20	25	.60	
QH5A	30	55-85	44	14-20	65	1.48	
QH6A	17	50-55	42	14-20	86	2.05	
QH7A	30	30-73	45.4	14-20	91	2.00	
QH8A	41	43-49	75	14-20	81	1.08	

125

TABLE 13.--Temperature gradients above and below water table (continued).

Test well	Depth to water (m)	Depth interval (m)	Temperature gradient (°C/km)	Depth Interval (m)	Temperature gradient (°C/km)	Ratio 6:4	Remarks
QH9A	66	69-75	35	14-20	83	2.66	
QH11A	38	39.6-41.1	63.1	14-20	112	1.77	
QH12A	31	47-53	92	14-20	113	1.23	
QH13A	46	49-55	95	14-20	131	1.38	
QH14A	46	68-74	31	14-20	42	1.35	
Q4	33e	53-65	32.8	15-53	57.1	1.74	Data from Sass and others (1977, table C-1)
Q6	39e	30-53	48.6	12-27	90.2	1.86	do
Q9	49e	48.8-50.3	26.0	27-55	32.6	1.25	do
Q10	38e	48.8-50.3	48.5	15-30	38.3	.79	do
Q17	43e	44-75	134.4	15-41	174.7	1.30	do
Q18	25e	38-53	71.0	14-23	98.4	1.39	do
Q19	27e	32-55	45.2	13-27	67.2	1.49	do
Q20	37e	30-69	43.0	12-30	72.2	1.68	do

Average   1.44
Standard deviation   .43
Footnote: e Estimated from figure 6.

others, 1977) used measured temperature at a depth of 15 m in the T wells and a least-mean-squares correlation between temperature a 15 m in the Q and QH wells to estimate heat flow in the T wells.)

For each depth range, heat-flow values at the sites of the DH, QH, and Q wells are calculated as the product of the thermal conductivity and the temperature gradient. At the T-well sites, only the heat flows for the 14-18 m depth interval are calculated. At most of the G-well sites, both depth intervals for which heat flows are estimated are within the saturated zone. All these data are given in table 14. In table 14, heat-flow estimates for the shallower depth intervals in the table are designated q_1; those for the greater depth interval are designated q_2. In general, the q_2 values are believed to be the more reliable, but for some of the G-wells that penetrate bedrock having poorly known thermal conductivity, the opposite is true. In most of the test wells, where q_1 and q_2 values are both available, a final estimate, designated q_3, is based on a consideration of both q_1 and q_2 values, the q_2 value generally being given considerably more weight.

All the heat-flow values listed in table 14 and shown in figure 22 are uncorrected. Corrections that must be applied to shallow temperature gradients to obtain conductive heat flow at greater depth in the crust include those related to vertical ground-water flow, drilling disturbance, climatic change, uplift, erosion, sedimentation, regions of anomalalous surface temperature such as rivers and lakes, topographic relief, and thermal refraction in dissimilar rocks (Sass and others, 1971, p. 6382). Of the factors listed above, topographic relief and thermal refraction are locally important near the margins of southern Grass Valley or near high-angle normal faults of large throw. Uplift, erosion, and sedimentation may be important, although their impact on the results of the heat-flow estimate are difficult to determine.

TABLE 14. -- Temperature gradient, thermal conductivity, and conductive heat flow in test wells.

test well	Depth to saturated zone (m)	Date	Depth interval (m)	Temperature gradient (°C/km)	Thermal conductivity (tcu)	q1 heat flow (hfu)	Date	Depth interval (m)	Temperature gradient (°C/km)	Thermal conductivity (tcu)	q2 Heat flow (hfu)	q3 Heat flow (hfu)
DH1	12.7	76 09 18	14.9-20.4	39	3.3	1.3	76 09 18	30-44	74	3.5	2.6	2.5
DH2	>50	76 09 --	14-20	68	2.4	1.6	75 06 23	42-50	36	3.6	1.3	1.4
DH3	26	76 09 19	14-20	621	2.7	17	76 09 19	26-38	488	3.9	19	18
DH4	24	76 09 --	14-20	378	2.6	9.8	76 09 --	24-48	251	4.0	10.1	10
DH5	>27	76 09 --	14-20	194	2.6	5.0	76 09 --	24-27	128	3.6	4.6	4.8
DH6	16.4	76 07 22	18-28	130	5.0	6.5	76 07 22	31-41	170	4.2	7.1	6.8
DH7	26.5	-- --	----	--	--	--	76 07 --	33-39	107	3.3	3.5	3.5
DH8	23.3	76 07 --	28-33	43	3.5	1.5	76 07 --	31-44	72	3.2	2.3	2.2
DH9	>34 7	-- --	----	--	--	--	76 07 --	37-41	641	3.3	21	21
DH10	5.8	76 09 19	10-17	2,010	3.3	66	-- --	----	--	--	--	66
DH11	29.2	-- --	----	--	--	--	76 07 --	35-44	233	3.8	8.9	8.9
DH12	25.1	-- --	----	--	--	--	76 07 --	28-42	81	4.0	3.2	3.2
DH13B	17.3	75 07 20	14-18	629	4.0	25	75 10 21	42-50	663	4.0	27	26
DH14B	32.0	75 avg	14-18	377	2.8	11	76 07 --	34-42	257	4.5	12	12
DH15	34	76 09 19	14-20	372	3.2	12	75 avg	40-44	296	4.0	12	12
QH1A	32	76 07 22	14-20	315	2.9	9.1	-- --	80-155	224	4.03	9.0	9.0
QH2A	74.9	-- --	----	--	--	--	-- --	25-130	52	2.88	1.5	1.5
QH3A	61.3	77 05 17	14-20	80	3.1	2.5	-- --	80-155	118	4.33	5.1	5.1
QH4	45.9	76 08 21	14-20	25	2.3	.6	-- --	125-155	42	3.25	1.4	1.4
QH5	30.4	76 10 29	14-20	65	3.0	1.9	-- --	55-128	37	4.26	1.6	1.7
QH6	17.0	76 09 13	14-20	86	2.9	2.5	-- --	17-50	51	4.14	2.1	2.2
QH7	30.0	76 10 30	15-30	98	2.3	2.3	-- --	30-73	45	3.69	1.7	1.8
QH8	40.7	76 09 13	14-20	81	2.4	1.9	-- --	41-49	69	3.44	2.4	2.3
QH9	65.7	76 11 03	14-20	83	2.8	2.3	-- --	67-75	40	3.96	1.6	1.8
QH11	38.1	76 09 14	14-20	-112	--	--	-- --	40-55	52	2.84	1.5	1.5
QH12	31.2	76 11 02	14-20	109	2.6	2.8	-- --	38-48	110	3.50	3.8	3.6
QH13	45.6	77 05 19	14-20	131	2.8	3.7	-- --	46-52	116	3.99	4.6	4.4
QH14	45.7	76 09 18	14-20	42	2.7	1.1	-- --	46-73	30	3.68	2.0	2.0

TABLE 14. -- Temperature gradient, thermal conductivity, and conductive heat flow in test wells (Continued).

test well	Depth to saturated zone (m)	Date	Depth interval (m)	Temperature gradient (°C/km)	Thermal conductivity (tcu)	q1 heat flow (hfu)	Date	Depth interval (m)	Temperature gradient (°C/km)	Thermal conductivity (tcu)	q2 Heat flow (hfu)	q3 Heat flow (hfu)
Q1	21.3	75 10 21	15-25	63	2.9	1.8	-- --	50-160	65.5	3.42	2.2	2.2
Q2	25e	75 10 21	15-25	32	2.6	.8	-- --	50-160	55.5	3.68	2.0	2.0
Q3	33e	76 07 25	14-20	124	2.8	3.5	-- --	50-170	120	4.06	4.9	4.8
Q4	33e	76 10 29	14-20	55	2.7	1.5	-- --	33-56	51	3.88	2.0	1.8
Q5	54e	76 10 30	14-20	65	2.8	1.8	-- --	54-107	41	4.04	1.7	1.7
Q6	31.1	76 10 31	12-27	90	3.0	2.7	-- --	39-55	45	4.15	1.9	1.9
Q7	32e	-- -- --	14-20	65	2.6	1.7	-- --	35-73	35	3.76	1.3	1.5
Q8	---	76 10 30	17-38	139	2.0	2.8	-- --	44-66	59	4.09	2.4	2.6
Q9	49e	77 05 18	14-20	47	3.1	1.5	-- --	49-57	30	4.43	1.3	1.4
Q10	38e	77 05 18	14-20	-24	2.8	1/	-- --	38-55	52	3.93	2.0	2.0
Q11	55e	76 09 14	14-20	-89	2.90	1/	-- --	46-78	37	4.21	1.6	1.6
Q12	51e	76 11 02	14-20	9	2.8	1/	-- --	51-62	45	3.93	1.8	1.8
Q13	38e	76 11 02	14-20	58	3.1	1.8	-- --	38-82	39	4.43	1.7	1.7
Q14	42e	76 11 02	14-20	45	3.2	1.4	-- --	51-116	21	4.53	.95	1.0
Q15	40e	76 11 02	26-40	95	2.45c	2.3	-- --	42-50	112	---	1/	2.3
Q16	54e	76 11 02	14-20	114	2.7	3.1	-- --	54-81	.78	3.88	3.0	3.0
Q17	43e	76 11 02	14-20	193	3.0	5.8	-- --	44-75	134	4.30	5.8	5.8
Q18	25e	76 10 31	14-23	98	2.4	2.4	-- --	38-53	71	3.48	2.5	2.5
Q19	27e	76 10 29	13-27	67	2.5	1.7	-- --	32-55	45	3.53	1.6	1.6
Q20	37e	77 05 18	12-30	72	3.2	2.3	-- --	38-69	42	4.49	1.9	2.0
Q21	49e	77 05 18	14-20	50	3.1	1.6	-- --	49-61	37	4.42	1.6	1.6
Q22	39e	76 10 29	12-24	34	2.5	.85	-- --	39-49	20	4.27	.85	.85
Q23	21.0	77 06 24	16-32	61	2.8	1.7	-- --	57-124	144	4.0	5.8	5.8
Q24	65.5	77 06 --	----	--	---	---	77 07 17	87-151	45	4.0	1.8	1.8

TABLE 14. -- Temperature gradient, thermal conductivity, and conductive heat flow in test wells (Continued).

test well	Depth to saturated zone (m)	Date	Depth interval (m)	Temperature gradient (°C/km)	Thermal conductivity (tcu)	q1 heat flow (hfu)	Date	Depth interval (m)	Temperature gradient (°C/km)	Thermal conductivity (tcu)	q2 Heat flow (hfu)	q3 Heat flow (hfu)
T1	64e	76 11 01	14.0-18.0	79	3.1	1.2						
T2	63e	76 11 01	14.0-18.3	144	3.1	4.5						
T3	65e	76 11 01	14.0-18.3	118	3.0	3.5						
T4	65e	76 10 31	14.0-18.0	131	3.0	3.9						
T5	60e	76 10 31	14.0-18.0	102	3.1	3.2						
T6	56e	76 10 31	14.0-18.0	93	3.1	2.9						
T7	54e	76 10 31	14.0-18.3	77	3.1	2.4						
T8	43e	76 11 02	14.0-18.3	59	3.0	1.8						
T9	44e	76 11 02	14.0-18.0	62	2.7	1.7						
T10	47e	76 11 02	14.0-18.4	102	2.7	2.8						
T11	40e	76 11 02	14.0-18.0	138	2.8	3.9						
T12	37e	76 11 02	14.0-17.8	207	2.9	6.0						
T13	55e	76 11 02	14.0-18.0	246	3.0	7.4						
T14	215e	76 11 02	14.0-18.0	100	2.8	2.8						
T15	51e	76 11 02	14.0-18.0	106	2.8	3.0						
T16	57e	76 11 02	14.0-15.5	115	2.7	3.1						
T17	47e	76 11 02	14.0-18.0	106	2.8	3.0						
T18	41e	76 11 02	14.0-18.0	188	2.9	5.4						
T19	48e	76 11 02	14.0-18.0	122	2.8	3.4						
T20	36e	76 11 02	14.0-18.0	171	2.7	4.6						
T21	51e	76 11 02	14.0-18.0	234	3.0	7.0						
T22	29e	76 11 02	14.0-14.9	97	2.6	2.5						
T23	28e	76 10 31	14.0-18.0	61	3.1	1.9						
T24	42e	76 10 31	14.0-18.0	68	3.0	2.0						
T25	61e	76 10 31	14.0-18.3	56	2.9	1.6						
T26	61e	76 10 31	14.0-18.3	77	3.0	2.3						
T27	33e	76 10 31	14.0-16.8	108	2.8	2.9						
T28	30e	76 10 31	14.0-18.0	126	2.5	3.2						
T29	---	76 10 31	14.0-18.0	118	2.5	3.0						

TABLE 14. -- Temperature gradient, thermal conductivity, and conductive heat flow in test wells (Continued).

test well	Depth to saturated zone (m)	Date	Depth Interval (m)	Temperature gradient (°C/km)	Thermal conductivity (tcu)	q1 Heat flow (hfu)	Date	Depth Interval (m)	Temperature gradient (°C/km)	Thermal conductivity (tcu)	q2 Heat flow (hfu)	q3 Heat flow (hfu)
G2	--	79 10 15	40-55	67	3.5	2.4	79 10 15	99-151	77	3.5	2.7	2.6
G3	--	79 10 15	40-60	50	3.4	1.7	79 10 15	80-150	56	3.4	1.9	1.8
G4	--	79 10 15	29-60	50	3.7	1.9	79 10 15	120-150	70	3.7	2.6	2.2
G5a	79	80 10	-----	--	--	--	79 10 15	75-144	109	6	6.5	6.5
G7	--	79 10 15	60-80	43	3.6	1.6	-- -- --	-----	--	--	--	1.6
G8	--	79 10 15	40-60	73	3.4	2.5	79 10 15	100-150	42	6	2.5	2.5
G9	--	-- -- --	-----	--	--	--	79 10 15	43-134	16	6	.96	.96
G10	--	79 10 14	40-80	54	3.7	2.0	79 10 14	80-152	52	6	3.1	2.6
G11	--	79 10 14	60-80	25	4.3	1.1	79 10 14	120-150	47	3.0	1.4	1.3
G12	--	79 10 14	40-60	88	3.9	3.4	79 10 14	110-152	112	3.5	3.9	3.7
G13	--	79 10 14	26-50	52	3.7	1.9	79 10 14	100-147	78	3.5	2.7	2.3
G14	--	79 10 14	30-47	21	3.7	.78	79 10 14	60-150	52	3.5	1.8	1.3
G15	--	-- -- --	-----	--	--	--	79 10 14	30-150	46	3.5	1.6	1.6
G105	20e	79 10 14	30-75	311	4.3	13	79 10 14	75-150	267	4.3	11	12
G106	--	-- -- --	-----	--	--	--	79 10 14	30-180	26	3.7	.96	.96
G108	42	79 10 14	50-120	114	4.1	4.7	79 10 14	120-150	104	4.1	4.3	4.3

Footnotes:

1/ Heat flow not estimated; gradient believed to be affected by hydrologic disturbance.

e Estimated

c Based on measurements on core.

Areal variations in shallow conductive heat flow in southern Grass Valley are shown in figure 22 and, in somewhat greater detail for the Leach Hot Springs thermal anomaly, in figure 23. The heat-flow isograms on these maps were plotted manually. Areas between adjacent isograms were measured by planimeter, then multiplied by the geometric mean of the isogram values to obtain heat-discharge increments. The increments were added to obtain the total conductive heat discharge for the budget area (fig. 22), or for the thermal anomalies at Leach Hot Springs (fig. 23), Panther Canyon, and on the Quicksilver Mine Road in the vicinity of well QH3 (fig. 22). For purposes of these last estimates the thermal anomalies are defined as the areas enclosed by the 3 hfu isograms. All the relatively small Quicksilver Mine Road thermal anomaly and virtually all the Leach Hot Springs anomaly are within the budget area, but, assuming bilateral symmetry, only about 60 percent of the Panther Canyon anomaly appears to be within the budget area for which heat discharge was estimated (fig. 22).

As would be expected, the pattern of areal variation in heat flow reflects the pattern of the temperature anomalies at the base of the valley fill-- or top of the bedrock. (Compare figs. 22 and 17.) As discussed earlier in the section, "Subsurface Temperature Distribution," available evidence indicates that temperature profiles are roughly linear throughout the valley fill, indicating predominantly conductive heat-flow regime. The gradients and heat flows are determined primarily by the temperatures at the upper and lower boundaries, that is-- the mean annual temperature at the land surface (about $11.5^{\circ}C$) and the temperature at the bedrock-valley fill interface. Thus, conductive heat-flow highs and lows in the upper valley fill are related to patterns of hydrothermal convection within the upper part of the bedrock.
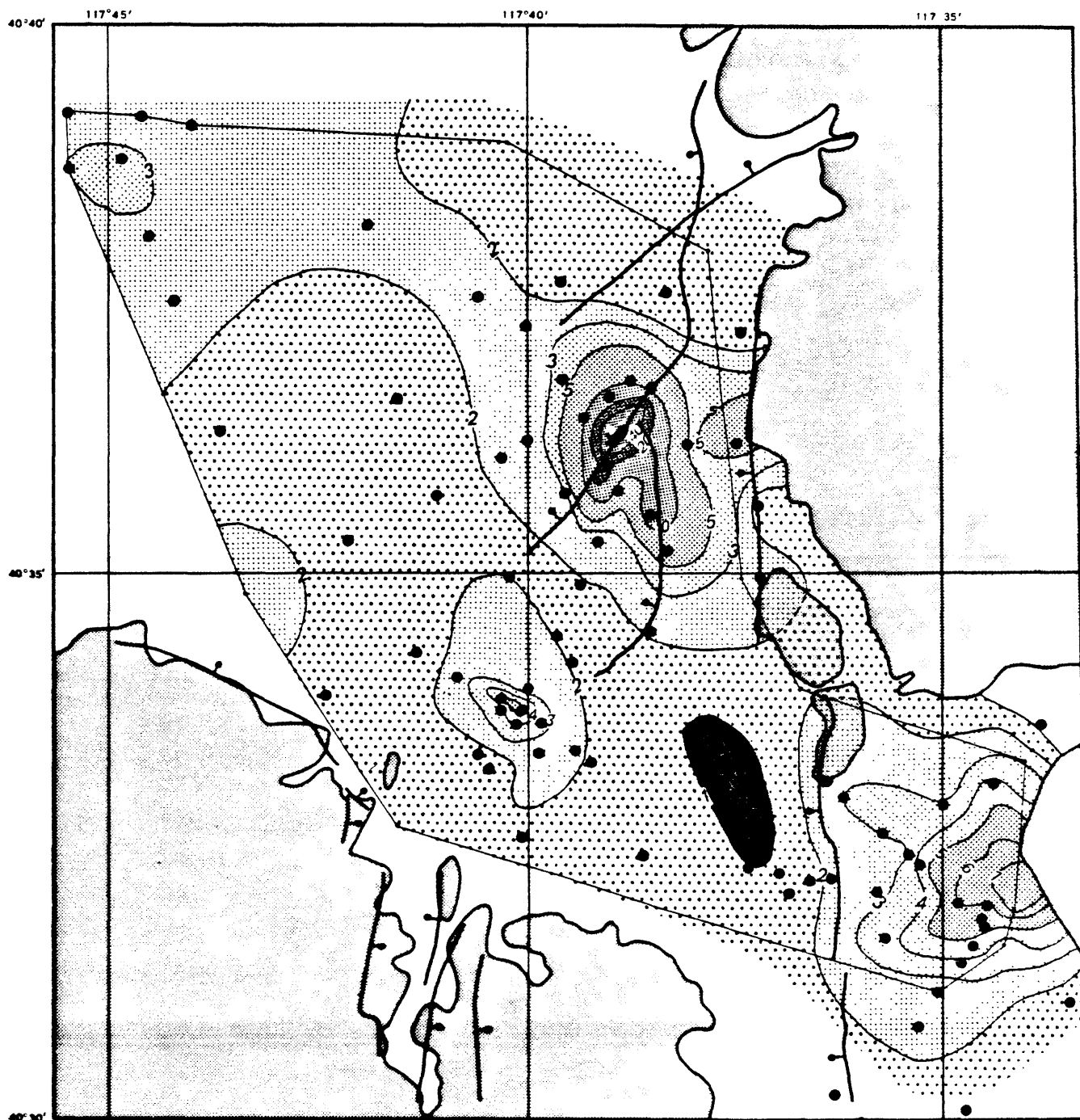
EXPLANATION

⬜ Edge of pre-Tertiary bedrock outcrop

⟋3⟋ Line of equal heat flow in heat-flow units (hfu).

⟋⟋ Principal faults, bar and ball on downthrown side

● Control points, wells

✖ Leach Hot Springs

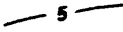FIGURE 22. — Map of southern Grass Valley showing near-surface conductive heat flow.

133
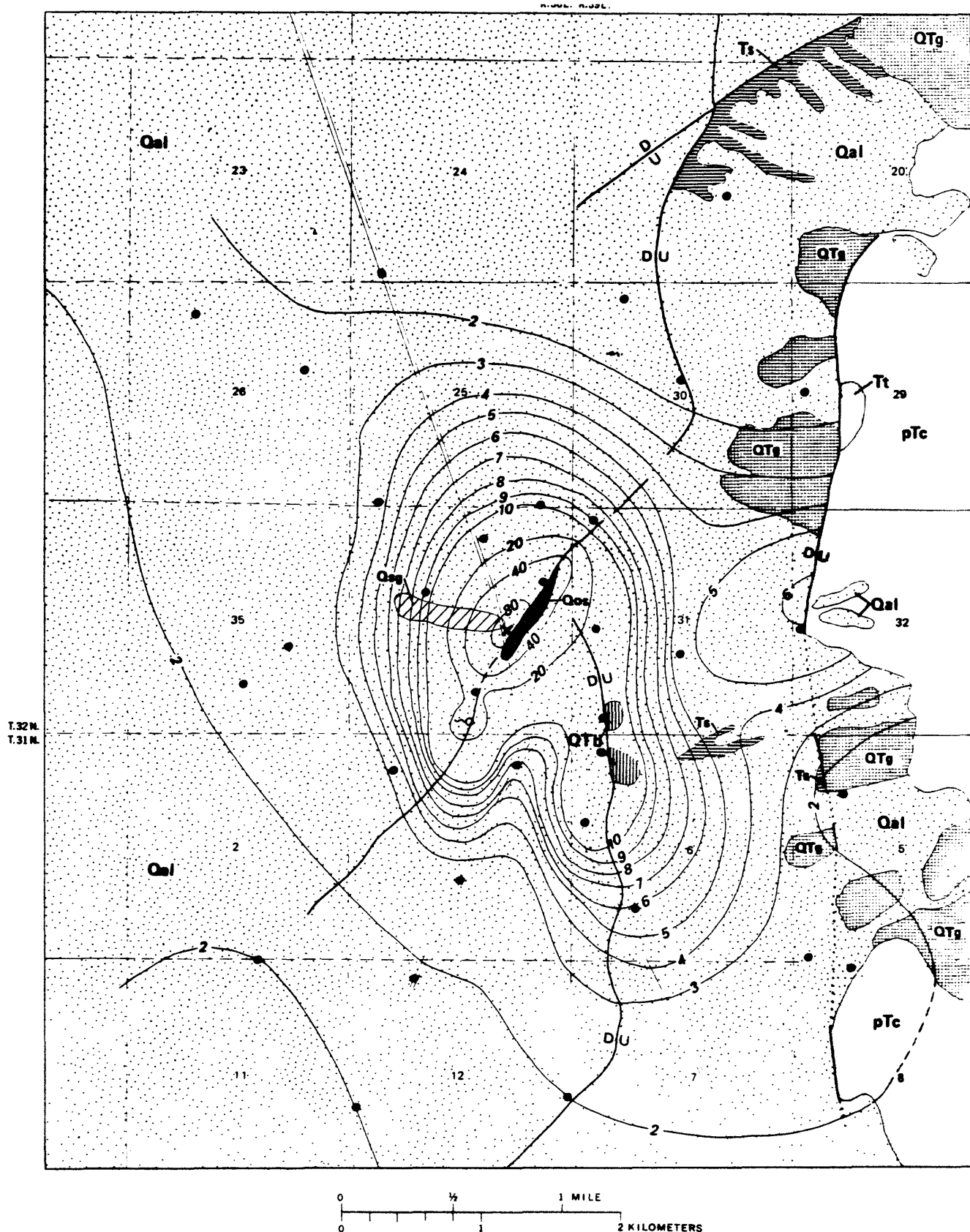
FIGURE 23. -- Geologic map of Leach Hot Springs thermal area showing near-surface conductive heat flow. Descriptions of geologic units, given on the following page are the same as in plate 1, except for unit labled pTc which includes sedimentary and volcanic rocks of Pennsylvanian to Triassic age. Heat-flow lines marked in heat-flow units (hfu) and locations of test wells provided control points shown as closed circles.

134

DESCRIPTION OF MAP UNITS

Pleistocene to Holocene

[Qal] **ALLUVIUM** — Unconsolidated fluvial deposits ranging from gravel to silt and clay. Forms thin pediment cover on flanks of mountains but thickens valleyward. Caliche fragments and coatings locally abundant.

[Qsg] **SINTER GRAVEL** — Pebbles, granules, and sand-size fragments of white to light-gray opaline sinter downgradient from Leach Hot Springs

Pleistocene

[Qos] **OLD SINTER** — Hard, dense chalcedonic sinter, in places associated with partly silicified and kaolinized alluvium; exposed on upthrown side of Leach Hot Springs fault.

Pliocene and(or) Pleistocene

[QTg] **OLD GRAVEL DEPOSITS** — Unconsolidated to semiconsolidated deposits of local provenance ranging from boulders to silt and clay. Obscurely bedded, slightly deformed (tilted). Exposures deeply dissected.

[Ts] **SEDIMENTARY ROCKS** — Predominantly fine-grained semi-consolidated deposits ranging from silicic ash and tuff and tuffaceous sand to claystone, mudstone, and marl. Slightly to moderately deformed. Characteristically pale gray, yellow, or green.

[Tt] **TUFF** — Greenish-gray to pink welded tuff of rhyolitic or rhyodacitic composition.

[QTb] **BASALT** — Dense, dark gray to brownish-gray holocrystalline rock composed of plagioclase laths, pyroxene, altered olivine (?) and opaque minerals.

[pTc] **CONSOLIDATED ROCKS, UNDIVIDED** — Includes wide variety of unmetamorphosed to slightly metamorphosed sedimentary and volcanic rocks. Chert, argillite, greenstone, and silicic to intermediate flows and pyroclastic rocks are most prominent within area of map.

QUATERNARY

TERTIARY AND(OR) QUATERNARY

TERTIARY

MIOCENE

PENNSYLVANIAN TO TRIASSIC

CONTACT — Dashed where approximately located.

FAULT — Dotted where concealed. U on upthrown side; D on downthrown side.

— 5 — Line of equal heat-flow, in heat-flow units (hfu)

● Locations of test wells providing control points

✕ Leach Hot Springs

135

In broad outline, the Leach Hot Springs anomaly is elongated in a north-northwest direction, with a smaller, perhaps slightly separated anomaly to the east, as indicated by data from test well G5a (fig. 23). The hottest part of the anomaly, however, is elongated toward the northeast, along the Leach Hot Springs fault. Maximum conductive heat flow, in the vicinity of the springs, probably exceeds 80 hfu. Another thermal high lies along the fault that extends southward from well DH3 about 0.8 km east of the springs (fig. 23). Thermal water appears to rise along this fault but does not discharge at the land surface.

As defined at the outer limit by the 3 hfu isogram, the areal extent of Leach Hot Springs anomaly is about 11 km^2. The conductive heat discharge from this area is 1.10 Mcal/s, and the average heat flow integrated over the area is 9.9 hfu (table 15). The present estimate of the extent of the anomaly is greater than that of Olmsted, Glancy, Harrill, Rush, and Van Denburgh (1975), primarily because of the additional area in the lobe of high heat flow extending southward along the fault east of the springs, which was revealed by the drilling after that study was completed. The present estimate of heat discharge from the anomaly is believed to be more accurate than that of Sass and others (1977), owing to the improved definition of the configuration of the heat-flow lines and somewhat better estimates of heat flow at some of the test-well sites.

The Panther Canyon thermal anomaly is as extensive as that at Leach Hot Springs. However, maximum heat flow is only slightly more than 7 hfu, probably because thermal water does not rise to the land surface, as it does at Leach Hot Springs. The pattern of the anomaly suggests rising thermal water along the Basin-and-Range fault at the western edge of the bedrock exposures east of the valley but also suggests high temperature in the bedrock and lower part of the

TABLE 15.--Estimates of conductive heat discharge from Leach
         Hot Springs thermal anomaly.

Estimate	Area (km^2)	Average heat flow (hfu)	Heat discharge (Mcal/s)
Olmsted and others (1975, table 24)	8.03 [1]	12.5	1.00
Sass and others (1977, p. 55-60)	12.5 [2]	13.6	1.7
This report	11.1 [3]	9.91	1.10

Footnotes:

[1] Area >2 hfu.

[2] Area within 2 km of springs.

[3] Area >3 hfu.

valley fill at depth, farther west. The extent of the anomaly within the budget area is about 7.9 km^2 (table 16), but, since only about 60 percent of the entire anomaly appears to be within the budget area, the total extent may be on the order of 13 km^2. Estimated conductive heat discharge from the budget area is about 0.36 Mcal/s (table 16); for the entire area the corresponding discharge would be about 0.6 Mcal/s-- about 55 percent of that at Leach Hot Springs.

The Quicksilver Mine Road anomaly is much less extensive than the other two anomalies, and its maximum heat flow is only slightly more than 5 hfu. As discussed earlier, the anomaly is clearly related to hydrothermal convection within the pre-Tertiary bedrock at a buried-bedrock high. Total conductive heat discharge is small-- about 10 percent of that at Panther Canyon (within the budget area) and less than 3 1/2 percent of that at Leach Hot Springs.

Outside the thermal anomalies described above, conductive heat flow ranges from less than 1 hfu near the center of the valley, south of Leach Hot Springs, to more than 3 hfu near the northwestern corner of the budget area (fig. 22). The average for the entire budget area outside the anomalies is about 1.8 hfu (table 16). Taking into account this heat flow, plus that in the three anomalies, the integrated average near-surface conductive heat flow for the budget area is about 2.7 hfu. The total near-surface conductive heat discharge for the southern Grass Valley budget area is estimated to be about 3.4 Mcal/s (table 16).

138

TABLE 16. -- Heat discharge from southern Grass Valley budget area.

	Area (km^2)	Average heat flow (hfu)	Heat discharge (Mcal/s)
Convective:			
Springflow, Leach Hot Springs	125.5	0.51	0.64
Conductive:			
Leach Hot Springs anomaly	11.1	9.91	1.10
Quicksilver Mine Road anomaly	.95	3.90	.037
Panther Canyon anomaly	7.89	4.50	.355
Area outside of anomalies	105.6	1.83	1.93
Total or average conductive	125.5	2.73	3.42
Advective:			
Outflow:			1.9
Inflow			1.2
Net advective	125.5	.6	.7
Total or average	125.5	3.8	4.8

Convective Heat Discharge

For the purpose of the present analysis, convective heat discharge from southern Grass Valley is considered as the heat discharged at the land surface by springflow and evapotranspiration of thermal water. Such discharge occurs only at Leach Hot Springs. It includes the heat transported by (1) springflow, (2) steam and heated air, (3) evaporation from spring pools and discharge channels, (4) radiation from pool surfaces and discharge channels, and (5) evapotranspiration from the vegetated area surrounding the springs. Item 1 accounts for most of the discharge. Items 2 and 4 are believed to be very small and are not estimated. Items 3 and 5 contribute small but significant amounts to the total discharge and are included in the estimate. (See table 17.)

As discussed in the section, "Deep Ground-water System", the average discharge from orifices 1-30 during the period November 1974 to July 1978 was 8.8 L/s. Evapotranspiration from the vegetated area surrounding the springs was estimated by Olmsted, Glancy, Harrill, Rush, and VanDenburgh (1975,p. 201) to be $0.012 \times 10^6 m^3/yr$ (0.38 L/s). Evaporation from spring pools and discharge channels was not estimated by Olmsted, Glancy, Harrill, Rush, and VanDenbugh (1975) but is estimated for the present study on the basis of a quasi-empirical mass-transfer equation of Harbeck(1962), using average monthly temperature, humidity, and wind velocity at the Winnemucca WBO AP weather station. Estimated annual evaporation is a function of water-surface temperature is shown in figure 24. The evaporation rate from the hot springs area is computed using data given below:

TABLE 17. -- Convective heat discharge at Leach Hot Springs

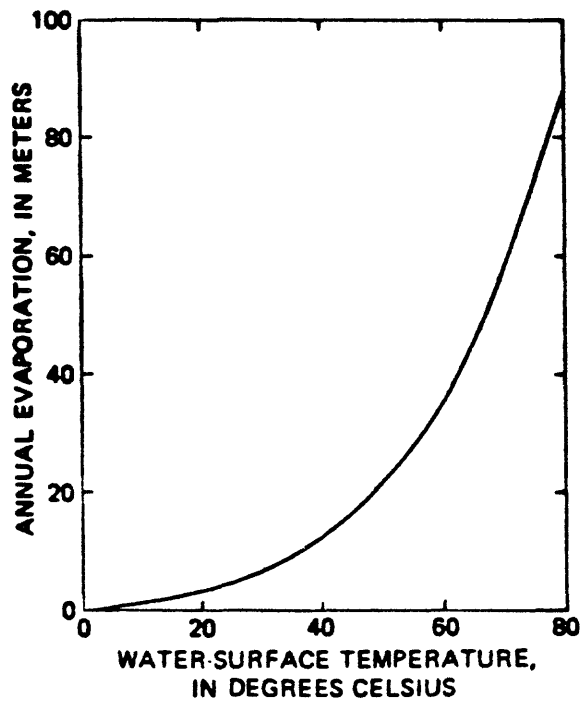| Item | Water Discharge | | Heat discharge |
	Volume rate (L/s)	Mass rate (Kg/s)	(Mcal/s)
Springflow	8.81	8.58	0.561
Evapotrans-piration from vegetated areas	.38	.37	.024
Evaporation from spring pools and discharge chan-nels	.25	.24	.016
Total	9.44	9.19	.601

FIGURE 24. -- Estimated annual evaporation from hot-water surfaces as a function of temperature. Based on a quasi-empirical mass-transfer equation of Harbeck (1962), using weather data from the Winnemuca WBO AP weather station.

	Water-surface area (m^2)	Water-surface temperature ($^\circ C$)	Evaporation (m/yr)	Evaporation ($\times 10^3 m^3$)
Runoff channels	184	60	36	6.6
Pools 1-29	16	78	81	1.3
Pool 30	10	37	10	.1
Total				8.0

The total, 8.0×10^3 m^3/yr is equivalent to a rate of 0.25 L/s, which is used in table 17.

The volume rates of discharge in table 17 are converted to mass rates, using a density of 0.974 kg/L at the weighted average-discharge temperature of $76.8^\circ C$ (table 8). The total mass rate of water discharge at the surface is estimated to be 9.2 kg/s (table 17).

The heat discharge associated with this water discharge is estimated as follows. The weighted-average temperature of the discharge is $76.8^\circ C$ (table 8). Average annual temperature at the land surface is estimated to be $11.5^\circ C$ on the basis of extrapolated temperature gradients in test wells. The net heat content of the discharge is 76.9 cal/g - 11.5 cal/g = 65.4 cal/g. total convective heat discharge at the land surface is therefore (9.2 kg/s) (65.4 cal/g) = 0.601 Mcal/s. (See table 17.)

Advective Heat Discharge

Heat transport by lateral ground-water flow is one of the items in the heat budget of southern Grass Valley. The net advective heat discharge consists of the heat advected out of the budget area by northward ground-water flow minus the heat advected into the budget area along its western, southern, and eastern sides.

Northward ground-water flow from the budget area is estimated to be 8,800 m^3/day; (see table 6) the net heat transport associated with this flow is estimated to be 1.9×10^6 cal/s.

The estimate of the heat advected into the budget area is more uncertain than that of the advective heat outflow described above. The primary reason for the uncertainty in the inflow estimate is that the proportions of ground-water inflow that occur along various parts of the western, southern, and eastern perimeter of the budget area are poorly known, owing to a lack of data to define the lateral hydraulic gradients and the permeability of the valley fill. Consequently the following simplifying assumptions are made:

(1) Total ground-water inflow along the western, southern, and eastern margins of the budget area equals ground-water outflow along the northern boundary of the area.

(2) Ground-water inflow along each of eight segments into which the western, southern and eastern margins are divided is proportional to the area of the transmitting section, adjusted for the average angle at which the ground-water flow lines intersect the segment. (See fig. 4.)

The procedure used in deriving the estimate is summarized in table 18. For each segment shown in figure 4: average saturated thickness, determined from data shown in maps showing the depth to water and the thickness of valley fill (figs. 15 and 3), is multiplied by the length of the

144

segment to obtain the area of the transmitting section. The area of the transmitting section is multiplied by the sine of the average angle of ground-water inflow to obtain an adjusted area of transmitting section. Next, the average temperature of the inflow for each segment is estimated in the same manner used for the outflowing section described in the section, "Shallow Ground-Water Systems". Finally, the weighted average temperature of the ground-water inflow is determined by multiplying the temperature for each segment by the corresponding adjusted area, summing these products, and dividing the total by the total adjusted area of inflow (table 18).

By the procedure described above, the weighted-average temperature of the ground-water inflow is estimated to be $23^{\circ}C$, as compared with the weighted average temperature of $30.1^{\circ}C$ for the outflow. Thus there is a net advective heat discharge from the area, which is represented by the difference in temperature, because ground-water inflow and outflow are assumed to be equal. The magnitude of the advective heat outflow is estimated to be 1.9 Mcal/s (table 6); the corresponding ground-water outflow is 1×10^{2} kg/s. The advective heat inflow, therefore is computed as

$$(1 \times 10^{2} kg/s)(23.1 - 11.5^{\circ}C)(1.0 \ cal/g \ ^{\circ}C) = 1.2 \ Mcal/s$$

Substracting this estimated inflow from the estimated outflow gives a net advective heat discharge of 0.7 Mcal/s.

145

TABLE 18.--Estimate of average temperature of ground-water inflow to budget area.

(See fig. 4 for location of transmitting sections and directions of ground-water flow.)

Transmitting section	Length (m)	Average saturated thickness (m)	Area of transmitting section ($\times 10^6 m^2$)	Sine of angle of inflow	Adjusted area of transmitting section ($\times 10^6 m^2$)	Average temperature of inflow ($^\circ$C)
A	8,700	350	3.04	0.64	1.95	24
B	4,600	150	.69	1.00	.69	18
C	7,200	200	1.44	.98	1.41	19
D	2,400	670	1.61	.37	.60	35
E	4,200	300	1.26	.97	1.22	27
F	2,900	100	.29	.98	.28	18
G	5,500	70	.38	1.00	.38	19
H	3,900	400	1.56	.64	1.00	22
Total or average			10.3		7.5	23

Total Heat Discharge and Average Heat Flow

The total heat discharge from the southern Grass Valley area is the sum of the convective, conductive, and advective heat discharges discussed in the previous sections. The total heat discharge, 4.8 Mcal/s, amounts to an average of 3.8 hfu for the 125.5 km^2 budget area (table 16). Of this total, nearly three-fourths is conductive; the remainder is nearly equally divided between advective and convective. All the convective component is at Leach Hot Springs. The advective component is the least well defined; the estimate could be in error by 50 percent or more. The estimated average heat flow of 3.8 hfu is in fair to good agreement with the estimate of 3.3 - 3.7 hfu of Sass and others (1977). (Their estimate did not, however, include the advective component.)

The average heat flow so determined is intended to be representative of heat-flow conditions at deeper levels in the crust, below the depths of ground-water circulation. A fundamental question is whether this value represents the average heat flow for the entire hydrologic system. In order to account for all the effects of ground-water circulation on conductive heat flow, heat-flow measurements must represent all areas of ground-water recharge, where heat flows are less than average, as well as all areas of ground-water discharge, where heat flows are above average. The boundaries of the shallow ground-water system can be reasonably assumed to be approximately coincident with drainage divides. The boundaries of the deep system, however, are unknown; in fact, it would be extremely difficult to determine them with any degree of certainty.

The budget area used in this study obviously is a biased sample of the geology and topography of the drainage basin of southern Grass Valley-- it includes most of the valley area but almost none of the tributary mountainous area. To adequately assess whether the estimated heat flow for the 125.5

km^2 budget area is representative of the 830 km^2 drainage area of which it is only a 15 percent part would require determination of the average conductive heat flow in the mountains. This was not attempted because of problems of drilling and because of large corrections required for the measured temperature gradients in the rough terrain.

It might be inferred that, because the mountains are likely to include more areas of ground-water recharge than of discharge, the average conductive heat flow would be less than the average for the drainage basin as a whole. This would imply that the heat flow estimate for the budget area is too high to represent the entire hydrologic system. However, available data from widely scattered heat-flow holes in the mountains near Grass Valley (Sass and others, 1971; 1977) yield heat-flow values as high or almost as high as those estimated in the this study or by Sass and others (1977) for southern Grass Valley.

Allowing for the various uncertainties mentioned earlier, we infer that mean heat flow in the southern Grass Valley area is between 3 and 4 hfu. Thus the hydrothermal system associated with Leach Hot Springs appears to be in approximate thermal equilibrium with crustal heat flow within the Battle Mountain High.

148

MODELS OF THE HYDROTHERMAL SYSTEM

It is apparent from the foregoing discussions that details of the circulation system supplying hot water at Leach Hot Springs are as yet unknown or speculative. There are no data on the temperature, depth, and areal extent of a possible reservoir in the southern Grass Valley area because of the lack of drilling below 450 m. In addition, the transfer of information from deep drilling in other areas in the Basin and Range to Grass Valley is of limited value without a detailed study of the similarities and differences between areas. We can, however, infer certain characteristics for the hydrothermal system on the basis of the geochemical, geophysical, and geologic data discussed previously. We can also develop useful constraints on the age, depth, and lateral extent of the Grass Valley system based on simulation of heat and fluid flow in alternative models.

Characteristics of the Hydrothermal System

The data discussed previously allow us to estimate the maximum temperature and minimum depth of circulation for the hydrothermal system. Geothermetric calculations of reservoir temperature, assuming no mixing, range from $155^{\circ}C$ to $177^{\circ}C$. The cation method is believed to give the best estimate of $163-176^{\circ}C$.

Heat-budget calculations are consistent with an average conductive heat flow of 3.5 hfu below the depth of fluid circulation in the southern Grass Valley area. Measured thermal conductivity values for the fill and bedrock suggest average values of 4×10^{-3} and 8×10^{-3} tcu, respectively. This implies that under steady-state conditions and in the absence of significant vertical ground-water flow, temperature gradients of 88 $^{\circ}C/km$ and $44^{\circ}C/km$ are required to transmit 3.5 hfu through the fill and bedrock, respectively. Thus if the hydrothermal system supplying Leach Hot Springs involves reservoir temperatures near $180^{\circ}C$, we would estimate the minimum depth of circulation to be 3 km, for a 1-km thickness of fill.

The areal extent of the deep circulation system is more difficult to delineate. Various authors have suggested that the circulation systems associated with Basin and Range hot springs are confined to a single fault zone or plane, presumably the same fault from which the springs currently discharge (Hose and Taylor, 1974; Beyers, and others, 1976; Bodvarsson, 1978). Circulation in the fault is envisioned as being driven by density differences between upflowing hot water and downflowing cold water, although the initiation of flow and setting up of hot and cold fluid columns is likely to involve some form of forced convection (e.g. recharge at higher elevations than discharge) because of the high critical Rayleigh number in a fault plane with thermally conducting side walls (Lowell, 1979). Such a model requires only the tectonism associated with active normal faulting to account for the required permeability at depths of several kilometers, and may involve no appreciable reservoir volume.

On the other hand, the widespread distribution of normal and thrust faults in southern Grass Valley, measured heat-flow anomalies at well QH3D and Panther Canyon, and evidence of convection in the bedrock near the contact with valley fill at wells QH3D and G105 suggest that a hot or warm water reservoir covering perhaps 50-100 km^2 could exist in the bedrock underlying southern Grass Valley. Attempts to use stable-isotope data from springs and wells in Grass Valley and surrounding areas to delineate recharge area(s), as done in Long Valley, California (Sorey, and others, 1978) and Iceland (Arnason, 1976), have not been successful. The isotope data do, however, suggest that circulation time in the hydrothermal system may approach 10^4 years, requiring perhaps lower velocities and longer path lengths than those corresponding to the single fault-plane model.

Constraints on the areal extent of the deep circulation system are provided by heat and mass-balance considerations. Under steady-state conditions, the rate Q_h at which heat is absorbed by the convective throughflow

150

Q_w is given by

$$Q_h = Q_w (T_r - T_s) c_w$$

where T_r is the maximum temperature attained by the flow, T_s is the temperature of recharging water, and c_w is the average specific heat of the fluid. For Leach Hot Springs we estimate Q_h as follows

$$Q_h = (9 \text{ kg/s}) (170^\circ C) (1000 \text{ cal/ } kg^\circ C)$$
$$= 1.5 \times 10^6 \text{ cal/s}$$

With heat being conducted into the circulating system from below at an average rate of 3.5 hfu, the required area (A) for heating will depend on the fraction Δq of this heat flow which is captured or absorbed in the throughflow. The measured surficial heat-flow distribution suggests that Δq might average 1.5 hfu, in which case $A = Q_h / \Delta q = 100 \text{ km}^2$. If the long-term average throughflow in Grass Valley exceeds the present-day rate, an even larger contact area is implied.

Although the age and continunity of hydrothermal activity associated with Leach Hot Springs is difficult to establish with any certainty, heat-budget calculations for the 125.5 km^2 budget area in southern Grass Valley indicate that approximate thermal equilibrium has been established within the hydrothermal system with a regional conductive heat flow between 3 and 4 hfu. For depths of circulation of several kilometers, this implies that the hydrothermal system is several hundred thousand years old. Similarly, for the thermal anomaly surrounding Leach Hot Springs, heat-budget calculations indicate that the surficial conductive regime is in approximate thermal equilibrium with an upflow of 8.3 kg/s from a deep reservoir at $180^\circ C$ to surface discharge at an average temperature of $77^\circ C$. This also tends to support the concept of a hydrothermal system with continuous flow at near present-day rates for periods of several hundred thousand years.

With these considerations as background, we present in the following

sections results of numerical modeling of heat and fluid flow in two alternative models of hydrothermal circulation applicable to Grass Valley and other Basin-and-Range systems involving a regional conductive heat source. Lack of data from deep drilling precludes the development of a detailed model for the Grass Valley hydrothermal system Consequently, our purpose is to discuss in a general sense the effects of factors such as depth, areal extent, magnitude, and duration of hydrothermal circulation on the associated thermal regime.

Fault Plane Model

The conditions under which meteoric water could descend along a single steeply-dipping fault at rates sufficient to supply the discharge at Leach Hot Springs and attain temperatures of at least $180^{\circ}C$ were analyzed numerically. Transient solutions for heat and mass flow with temperature-dependent fluid properties were obtained using the computer program SCHAFF, described by Sorey (1978). The appropriate conceptual model is illustrated in figure 25, the same general model being applicable to other hydrothermal systems in the Basin and Range.

The location of hot springs along principal basin-bounding faults, commonly at intersections with secondary fault lineaments, may be a necessary condition for maintenance of permeability in the presence of chemical desposition and sealing in the upflow portion of the circulation system. Pressure differences required for fluid circulation probably derive from a combination of elevation difference between recharge and discharge areas and the density difference between hot and cold water. In the Grass Valley area, the combined thermal-artesian pressure difference could be as much as 70 bars, equivalent to a cold-water head difference of 700 m.

For numerical analysis, a simplified vertical cross section through the region of downflow is considered as in figure 26. Although it is possible that additional heating occurs as fluid moves laterally at depth towards the discharge area, contact

152
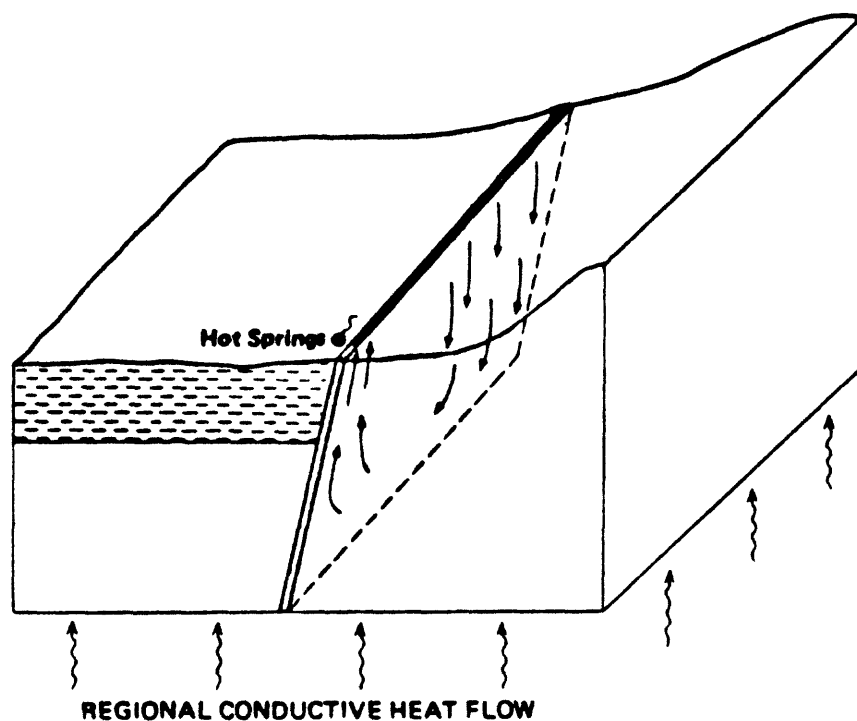
FIGURE 25. -- Fault plane conceptual model of the hydrothermal system in Grass Valley, Nevada. Directions of fluid circulation indicated by smooth arrows, regional conductive heat flow by wavy arrows. Valley fill shown by dashed pattern.

areas for heating should be small in this part of the system so that most of the increase in fluid temperature must occur in the downflow region. In effect, the fault plane acts as a heat sink by capturing a part of the regional heat flow over some distance on either side of the fault. Under transient conditions, heat is also mined from the rocks surrounding the fault and fluid temperatures at any given depth will exceed those at steady state. This makes the age of the hydrothermal system an important factor in determining fluid temperatures with this model.

Other parameters of interest in this model are the depth of fluid circulation (D), the lateral extent of the fault over which downflow occurs (L), and the rate of fluid flow Q_w. Mass inflow at the top of the fault plane is specified at a temperature of $10^\circ C$, and mass is removed from the fault at depth D at the same rate but at an unspecified temperature which varies during the course of each simulation. Values used in each simulation for the thermal conductivity of the valley fill (K_1) and bedrock (K_2), heat flow into the base of the model (q), and the depth of fill are listed below.

$$k_1 = 4 \text{ tcu}$$
$$K_2 = 8 \text{ tcu}$$
$$q = 3.5 \text{ hfu}$$
$$\text{thickness of fill} = 1.8 \text{ km}$$

The thickness of fill listed above reflects previously published values from geologic cross sections. Our current estimate based on gravity and drill hole data would be closer to 1.0 km, but the effects of using the lower value on model results for outflow temperature would not be significant. Total thickness of the model was 6 km and total width was 16.6 km. Along the vertical side boundaries both insulated and constant-temperature specifications were used for comparison. In the latter case, a vertical
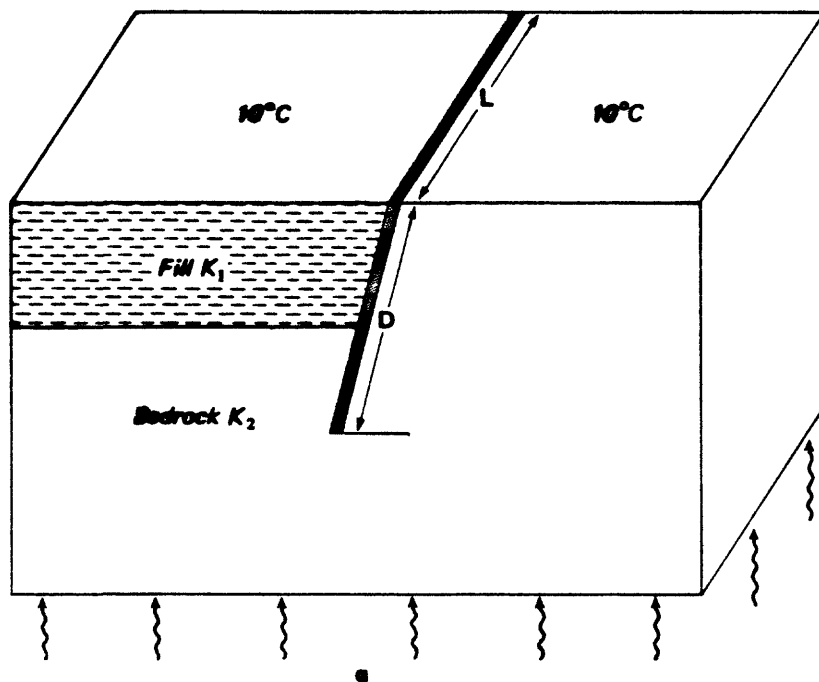
FIGURE 26. -- Fault-plane model for numerical analysis of the downflow portion of the hydrothermal system in Grass Valley, Nevada.

temperature distribution corresponding to a vertical conductive heat flow of 3.5 hfu was imposed.

The initial temperature distribution used in the model was determined by simulating steady-state heat flow without any fluid flow. The presence of the lower conductivity fill produces initial temperature conditions as shown in figure 27. The surficial heat-flow distribution associated with this no-fluid case shows an interesting anomaly, similar to previous results of Blackwell and Chapman (1977). A heat-flow high is observed on the upthrown or bedrock side of the fault, with a corresponding heat-flow low on the fill side. For the parameter values used in this model, the maximum heat flow is 5.2 hfu and the minimum is 2.8 hfu. The dip of the fault in figure 27 is 60°, a value assumed representative of the faults in Grass Valley and confirmed by test drilling in several locations. Model results were obtained for cases involving dips of both 60° and 90°, as discussed below.

The temperature pattern shown near the base of the model reflects the presence of the overlying fill and the uniform heat-flow specification at the bottom boundary. Uniform heat flow at this depth is a simplification. At midcrustal levels of 15-20 km within subprovinces of the Basin and Range like the Battle Mountain High, the analysis by Lachenbruch and Sass (1977) suggests the presence of extensive silicic partial melts. Under this condition, the isotherm pattern should reflect the surface of the melt at midcrustal depths and show a zone of transition to a pattern similar to that in figure 28 for shallower depths where ground water circulates. For steady-state conditions with magma at depths of 15-20 km, the presence of hydrothermal circulations to depths of a few kilometers could be expected to increase the regional heat flow derived from the underlying magma by about 20 percent. Our estimate of 3.5 hfu for southern Grass Valley is on the high side of values measured in conduction-dominated areas
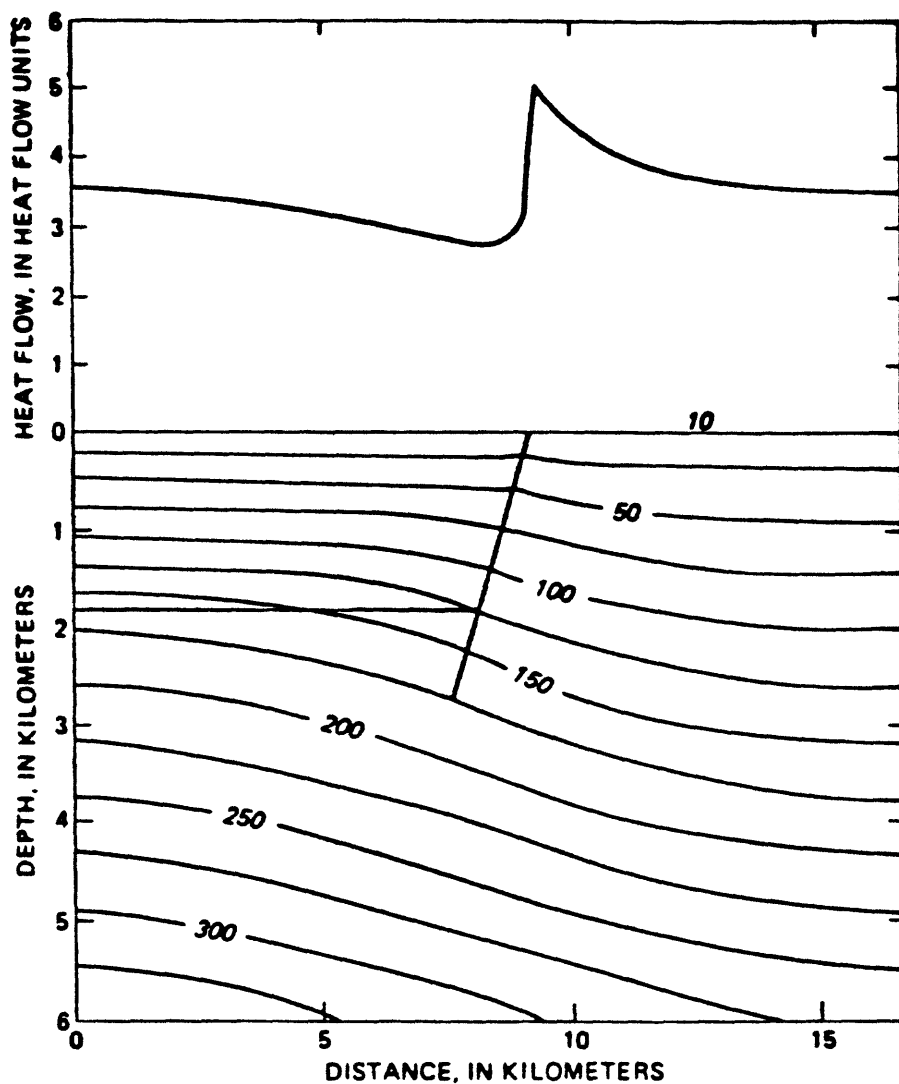
FIGURE 27. -- Steady-state temperature and surficial heat-flow distributions in fault-plane model with no fluid flow. Lines of equal temperature in degrees Celsius.

within the Battle Mountain High, perhaps reflecting the effects of hydrothermal circulation.

With fluid flow down the fault plane at 10 kg/s to a depth, D, of 2.7 km over a length, L, of 8 km, the resultant temperature distribution and surficial heat-flow values after steady state is reached are shown in figure 28. Comparison with figure 27 indicates the effects of convection by the downward bulge in the isotherms crossing the fault. Temperature of the fluid outflow is 115°C, whereas the initial temperature at 2.7 km was 173°C. At steady state almost all the heat added to the fluid as well as the conductive heat discharged at the land surface is supplied by the underlying regional heat flow. The constant-temperature side boundary conditions used in this case allow a small amount of heat to enter the model along the left side. Corresponding simulations with insulated side boundaries yielded fluid outflow temperatures only about 2 percent below values for constant temperature side-boundary conditions.

Surficial heat flows shown in figure 28 are all at or below 3.5 hfu. Beyond a distance of about 6 km on either side of the fault, heat flow is close to no fluid-flow conditions. In other words, the cooling effects of recharge down the fault do not extend beyond a distance of about twice the depth of fluid circulation. It should be noted that for the system as a whole, the area of below normal heat flow associated with recharge would be balanced under steady-state conditions by an area of above normal heat flow in the vicinity of the hot springs. This condition appears to be satisfied in the measured heat budget discussed previously.

To generalize the results from the fault plane model, we show in figure 29 curves of outflow temperature versus the throughflow per unit fault length for various depths of circulation along a fault dipping at 60°. The result
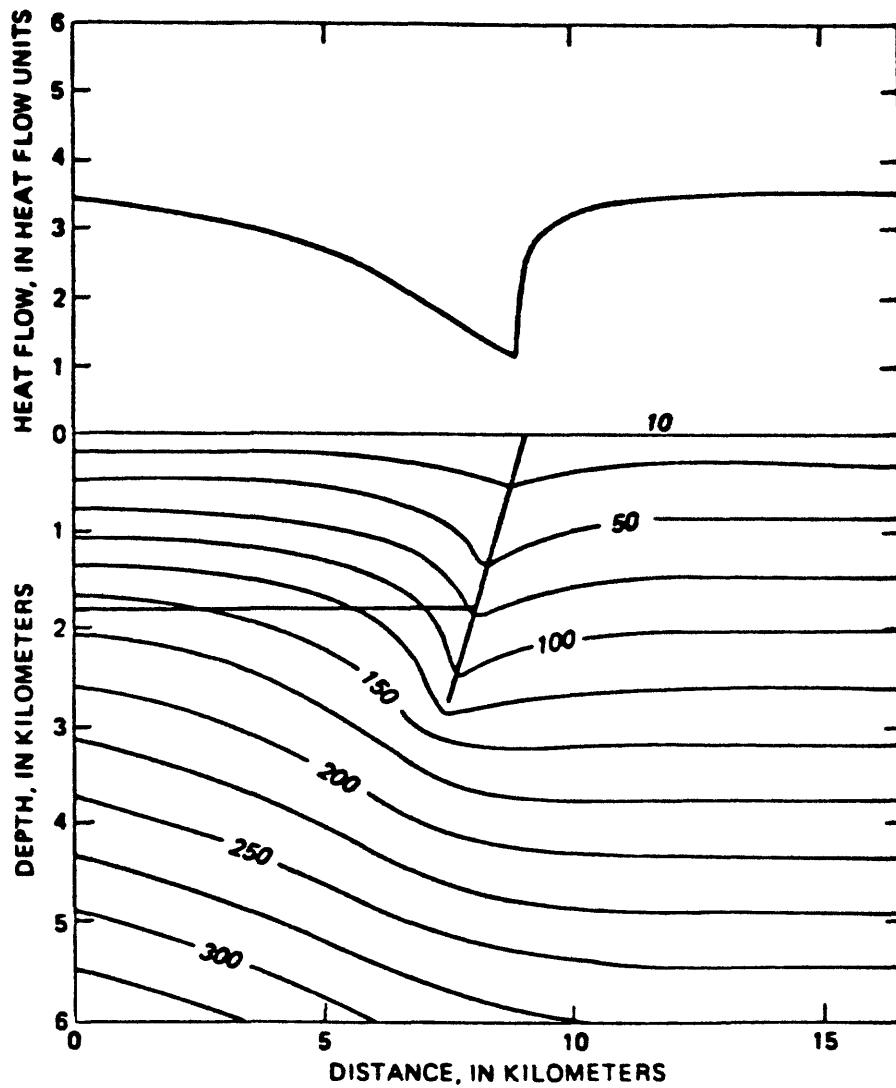
FIGURE 28. -- Steady-state temperature and surficial heat-flow distributions in fault-plane model with downward fluid flow to 2.7 km depth. Total fluid flow equals 10 kg/s over L = 8 km. Lines of equal temperature in degrees Celsius.

159

from the case in figure 28 with Q_w/L = 1.25 kg/s/km is also plotted, along with outflow temperatures at D = 2.7 for a fault plane dipping at 90°. Differences in outflow temperature between the 60° and 90° dip cases are only about 10°C for any value of Q_w/L.

These curves show that circulation depths and fault lengths must be relatively large to obtain fluid temperatures near 180°C under steady-state conditions even for the present-day throughflow estimate of 8.8 kg/s. Considering the distribution of faults passing through or near the hot springs and the drainage area boundaries shown in plate 1, a value of L=8 km would seem to be an upper limit. From figure 29 we would then infer that D must be at least 4.5 km.

Outflow temperatures of 180°C are possible for shallower depths of circulation under transient conditions when heat is being mined from storage. For example, the transient numerical solution shown in figure 30 for Q_w/L = (10 kg/s)/ 8 km and D = 3.3 km involves and outflow temperature of 180°C after about 10^4 years of circulation. Initially the outflow temperature equals the conduction-only temperature at D = 3.3 km, or 202°C, but decreases to about 150°C after 10^5 years and finally equilibirates at 138°C after 10^6 years. Little evidence exists, however, to support an age of only 10,000 years for this hydrothermal system, whereas heat-budget calculations and low-chloride concentrations in thermal waters argue for a much older system. Thus, results in figure 30 for steady-state conditions should be applicable.

Temperature distributions associated with upflow from depth D can also be simulated with the fault plane model. In figure 31 we show the steady-state temperature distribution for Q = 8.8 kg/s, L = 1.5 km, and T = 180°C at D = 2.7 km. The fault length chosen in this case corresponds with the elongation in the surficial heat-flow pattern near Leach Hot Springs shown in figure 23 and gives a realistic discharge temperature at the land surface of
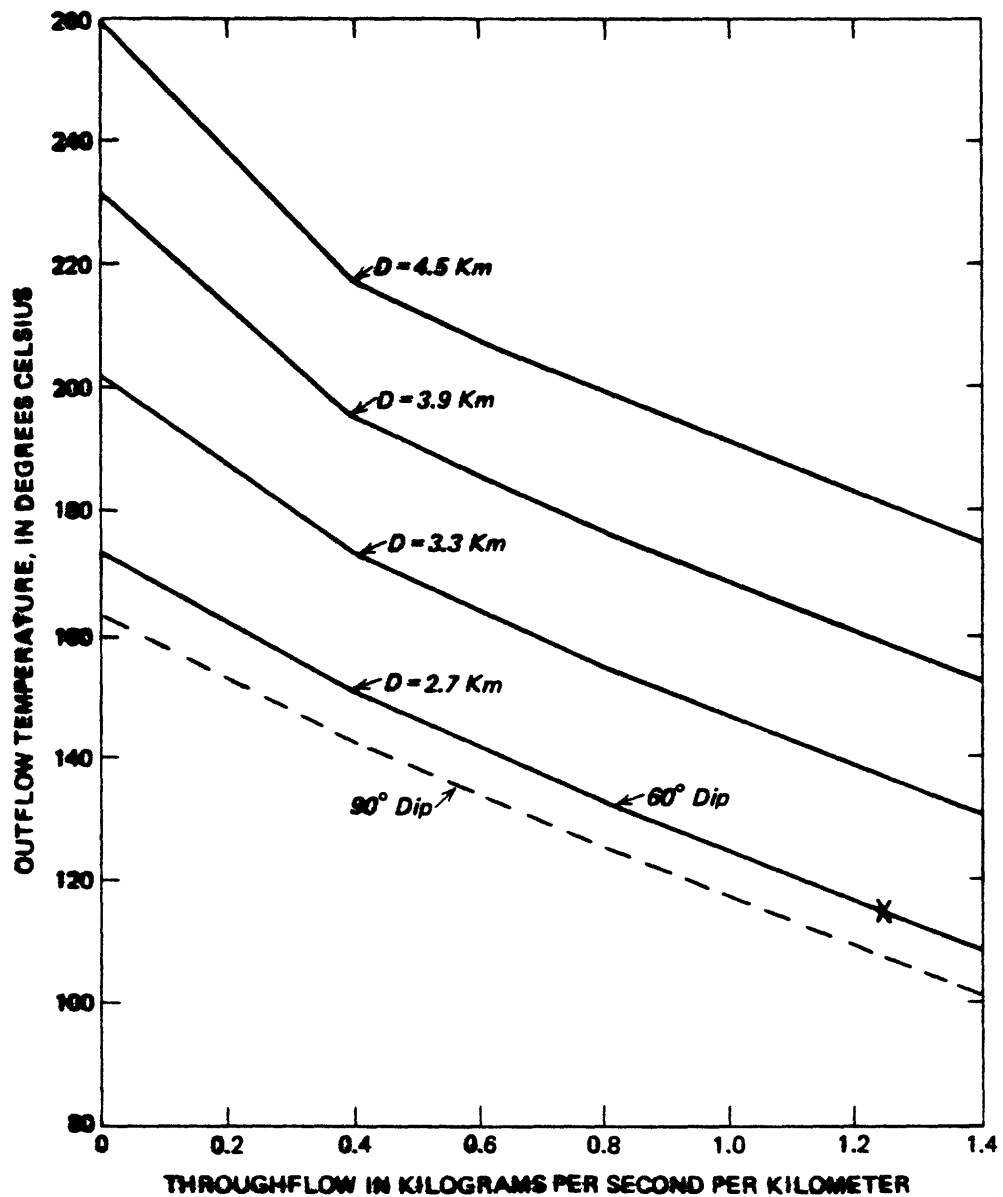
FIGURE 29. -- Fault-plane model results for outflow temperature as a function of a throughflow per kilometer of fault length, L. Each solid curve is for a fault with 60° dip and a different depth of circulation D. Results for a fault dipping at 90° with D = 2.7 km are shown as a dashed curve, and the result from figure 28 is plotted as an x.
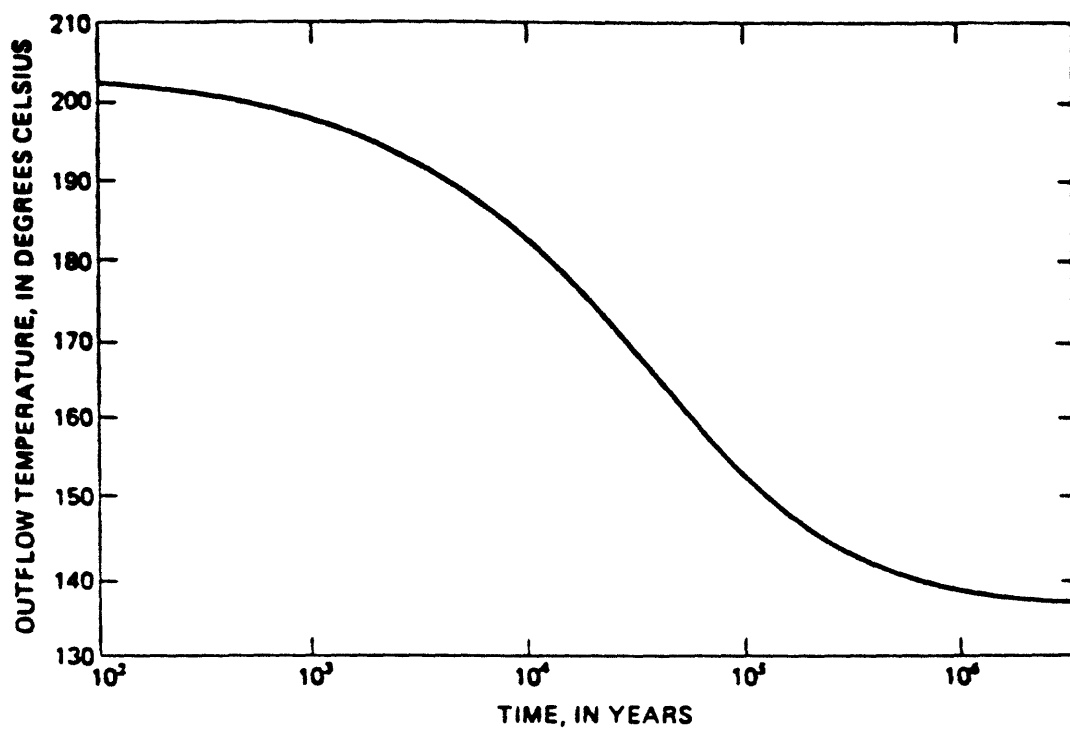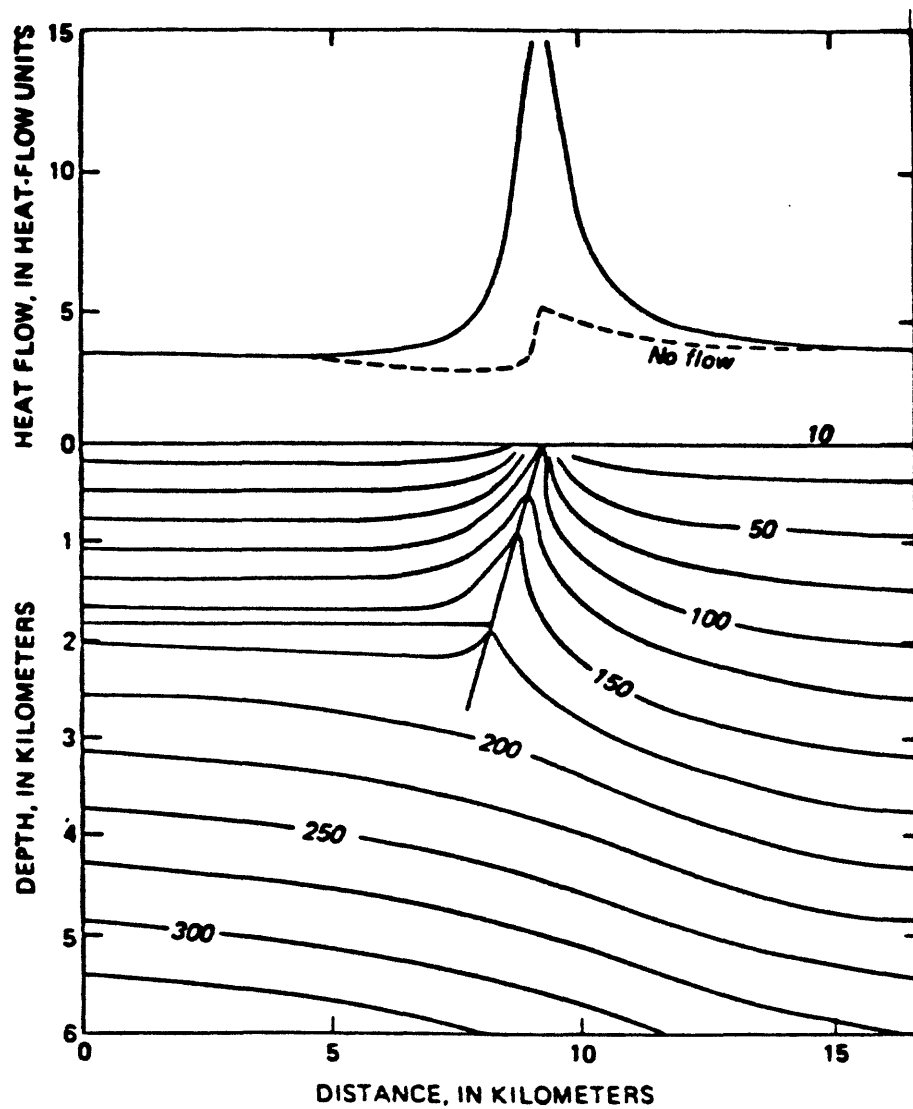
161

FIGURE 30. -- Transient response of outflow temperature at D = 3.3 km from fault-
plane model with throughflow of 10 kg/s over L = 8 km and a fault
dip of 60°.

162

FIGURE 31. -- Steady-state temperature and surficial heat-flow distribution in
fault-plane model with upward fluid flow from D = 2.7 km. Total
fluid flow = 8.8 kg/s over L = 2 km. Lines of equal temperature
in degrees Celsius.

163

100°C for this flow rate. The accompanying plot of simulated surficial heat flow shows an anomaly of considerably larger magnitude than that due solely to the thermal-conductivity contrast. The measured heat-flow pattern along a line passing through the springs and perpendicular to the lineation noted above is similar to the simulated pattern; differences may result from the effects of shallow ground-water convection and an additional zone of upflow east of the hot springs. This indicates, in agreement with the previous heat-budget calculations, that the heat-flow anomaly surrounding Leach Hot Springs is due mainly to conductive heat loss from the fault zone transmitting hot water to the springs. Alternatively, these data do not indicate that a reservoir of substantial size containing water at temperatures near 180°C exists at depths shallower than about 3 km in the vicinity of the hot springs. A more detailed analysis of heat flow associated with the upflow conduits feeding hot springs is given by Sorey (1975).

Lateral-Flow Model

An alternative conceptual model for hydrothermal circulation in Grass Valley and similar Basin-and-Range systems is referred to here as the lateral-flow model. As illustrated in figure 32, it involves recharge along a range-front fault and lateral flow through the bedrock toward the area of hot-spring discharge. Within some distance of the upflow region reservoir temperatures should reach those estimated geothermetrically, but the minimum depth of circulation is still controlled by the heat-flow-thermal conductivity constraint discussed previously. This model, in contrast with the fault-plane model, involves a reservoir of considerably greater areal extent, which tends to minimize the required depth of circulation because a larger fraction of the regional heat flow can be captured more efficiently.

Applying the lateral-flow model to Grass Valley, we note first that the direction of flow with respect to Leach Hot Springs is as yet undefined. Because heat-flow measurements indicate that additional upflow of hot water occurs toward the Sonoma
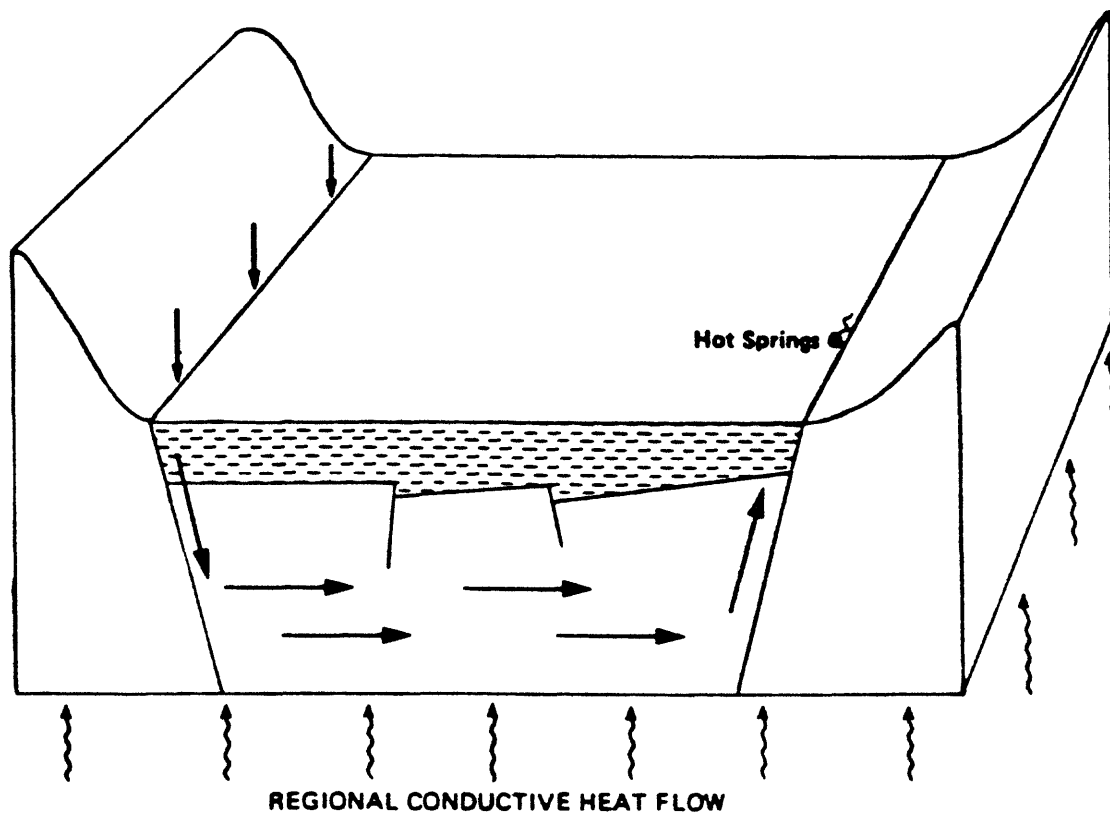
Hot Springs

REGIONAL CONDUCTIVE HEAT FLOW

FIGURE 32. -- Lateral flow conceptual model of the hydrothermal system in Grass Valley, Nevada. Diections of fluid circulation indicated by smooth arrows, regional conductive heat flow by wavy arrows. Valley fill shown by dashed pattern.

165

Range east of Leach Hot Springs.

Analysis of heat and fluid flow in the lateral-flow model is really a three-dimensional problem. We present here the results of a simplified two-dimensional simulation to assess the applicability of the basic concept. A more-detailed model, which might also simulate the flow anomalies at well QH3D and the Panther Canyon area, seems unwarranted at this time in view of the lack of deep drilling data.

The two-dimensional model is shown in figure 33. The upflow portion of the circulation system is not considered, under the assumption that reservoir temperatures at the outlet on the right side of the model will be nearly equal to temperatures under the discharge area. Land surface temperature is held at 10°C as is the temperature of the recharge water, and a uniform heat inflow of 3.5 hfu is specified at the base of the model at a depth of 6 km. Thermal conductivities of the fill and bedrock are the same as in the fault-plane model. Along the left-side boundary, heat is added over the depth of circulation D to simulate conduction from the adjacent bedrock. Lateral heat-flow specifications at the boundary were determined from the fault-plane model results; the net effect is to raise the fluid temperature at depth D on the left side by about 40°C over that for an insulated boundary condition. The right-side boundary is assumed insulated; its effect is considered below.

The initial temperature distribution (not shown) is based on the conduction-only solution for a fill thickness of 1.5 km. For a reservoir 1 km thick and centered at D = 3 km, the initial average reservoir temperature would be 200°C. For length, L, of 10 km and width, W, of 10 km, the contact area for heating is 100 km^{2}.

Steady-state temperature and surficial heat-flow distributions for this case are shown in figure 34 for a throughflow of 12 kg/s. The average reservoir temperature
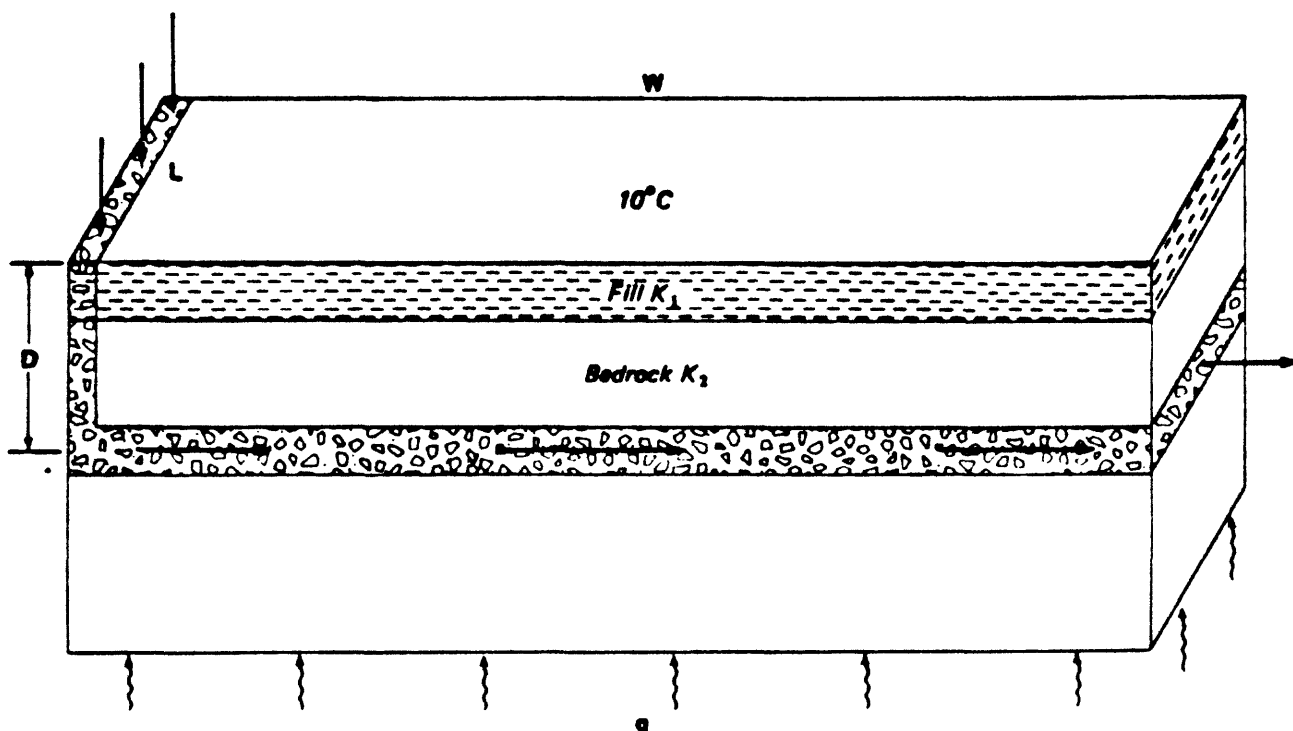
FIGURE 33. -- Lateral-flow model for numerical analysis of the hydrothermal system
in Grass Valley, Nevada.

is near 170°C at the outlet and the overlying surficial heat flow is 2.8 hfu. Additional simulations using larger values of W indicate that higher reservoir temperatures would result for this case (W = 10 km) if heat conduction across the right-side boundary were included in the model. A lateral flow distance of about 15 km is required before reservoir temperatures are in equilibrium with the vertical conductive flux of 3.5 hfu, or in order that the insulated boundary condition would be strictly appropriate. Using a smaller rate of throughflow would tend to decrease the value of W required to obtain a given reservoir temperature. It should be noted also that the age of hydrothermal circulation is not so critical in the results from this model because reservoir temperatures at the outlet do not decrease significantly over the transient period.

Vertical temperature variations shown in figure 34 within the reservoir would be reduced if a secondary convection-cell pattern were superimposed on the lateral throughflow regime. This condition can be simulated in the model when the reservoir permeability is set above about 50 μm^2 (≈50 millidarcies). However, the effects of this secondary convection pattern on temperature variations and heat flow are less significant than was found by Sorey, Lewis, and Olmsted (1978) in model simulations of the Long Valley Caldera. This difference relates to the fact that in the Long Valley model a constant temperature lower boundary condition simulating magma at 6 km was used, whereas in the Grass Valley model vertical heat transfer into the base is limited to the imposed regional heat flow.

Fluid residence time calculated for the lateral-flow model in figure 34 with a reservoir porosity of 10 percent is 25,000 years. For a reservoir less than 1 km thick (or having a porosity less than 10 percent), the corresponding residence time estimate would be proportionately smaller because the fluid velocity would be higher. Long residence times are consistent with the inference from the stable-isotope data that hot-spring water at Leach is very old. In contrast,
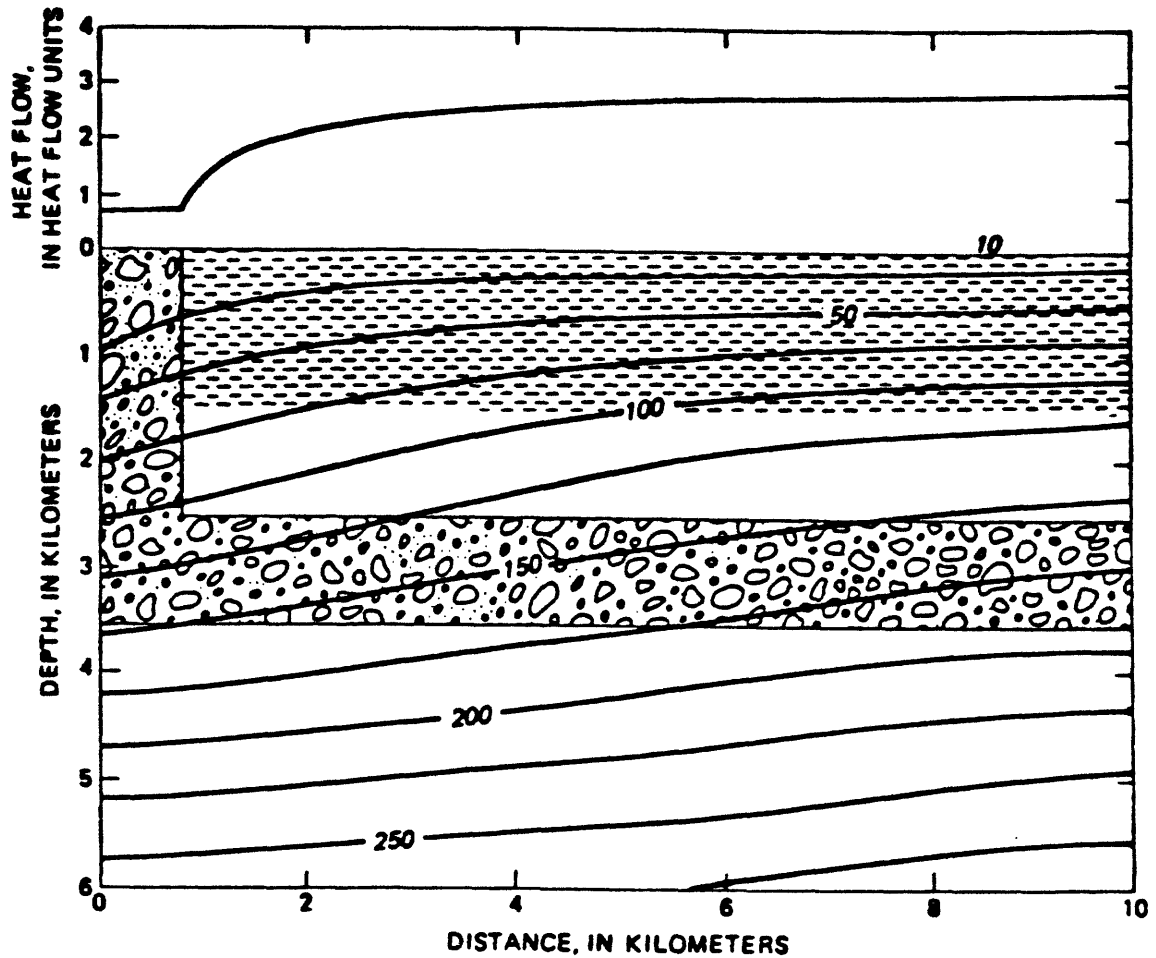
FIGURE 34. -- Steady-state temperature and surfical heat-flow distributions in lateral flow model. Total throughflow = 12 kg/s over L = 10 km. Lines of equal temperature in degrees Celsius.

169

residence time calculations for the fault-plane model yield values near 1,000 years, even for a fault zone 100 m wide.

The lateral-flow model with realistic values for the geometric parameters appears to offer a more viable explanation for the hydrothermal system in Grass Valley than does the fault-plane model. Lateral flow through fractured pre-Tertiary bedrock or perhaps through carbonate rocks at depths of about 3 km is not unreasonable, although possibly less appealing geologically than vertical flow in an active normal fault zone. Of course, if the long-term average throughflow rate for this system were several times larger than the 12 kg/s figure used here, either deeper circulation or interbasin flow over a larger area would be indicated.

ASSESSMENT OF GEOTHERMAL RESOURCES IN SOUTHERN GRASS VALLEY

In this section we consider the question of the potential for energy production from the geothermal resource in southern Grass Valley. As with our previous discussions of the characteristics of the hydrothermal system, we can draw few conclusions as yet, relying for the most part on inference, indication, and limiting cases. Nevertheless, the following outline of the possibilities which exist for energy production from this resource could serve as a guide in developing an exploitation strategy for Grass Valley and related systems.

We first make a distinction between low- and high-temperature resources, primarily on the basis of temperature and direct-heat versus electrical end use. The known and inferred characteristics of the hydrothermal system in southern Grass Valley suggest that in addition to the occurence of a high-temperature (180°C) resource at depths of several kilometers, a low-temperature resource (<90°C) may also exist nèar the bedrock-valley fill contact. Our interest here, however, is in the production of fluids with subsurface temperatures close to 180°C, which could be used for electrical generation..

We will consider three cases for which this fluid could be exploited. In the first two cases the assumption is made, on the basis of our previous results, that if the hydrothermal system feeding water to the hot springs includes a reservoir of significant size at temperatures near 180°C, it must exist at depths that are greater than about 3 km ànd hence not economically drillable within the near future. Such would be the case, for example, with the lateral-flow model considered in the previous section. However, this does not rule out the possibility of gaining access to fluid in this deeper reservoir by way of the fault conduit connecting it hydraulically to the hot springs, or the possibility examined in the third case that some of the upflowing hot water leaks out laterally to effectively charge an aquifer at shallower depths.

171

Exploitation Case A

Exploitation case A, illustrated in figure 35, represents a variation on the situation envisioned by Brook and others (1978) in their assessment of geothermal resources in high-temperature convection systems. For the Leach Hot Springs area, they estimated the volume of rock at a mean temperature of $162^{\circ}C$ as a cylinder extending from 1.3 km to 3.0 km depth with cross-sectional area of 5.8 km^2 (Mariner and others, 1978). This is approximatedly the area enclosed by the 5 hfu isogram in figure 23. The resultant volume of 10 km^3 is assumed to be heated by lateral conduction from the fault conduit feeding water to the hot springs. In exploitation case A we have refined this estimate by utilizing the results of heat-flow simulations with the fault-plane model, as shown in figure 31, to better define the subsurface temperature distribution in this situation. Interestingly, our estimate of the volume of rock above 3 km with a temperature $\geq 150^{\circ}C$ is also close to 10 km^3, even though the depth and shape of this heated volume differ from the cylinder of Brook and others (1978)

The fraction of the heat contained in this volume which could be recovered at the land surface could range from near zero to about 50 percent. The upper limit is theoretically possible in a uniformly porous and permeable reservoir with a porosity of 20 percent, assuming naturally induced recharge of surrounding colder water or injection of cold water at rates equal to the total production of hot water. Brook and others (1978) used a recovery factor of 25 percent to account for nonideal reservoir behavior, for example, non-uniform reservoir permeabilty and porosity. If, however, the thermal anomaly surrounding Leach Hot Springs is indeed due mainly to lateral heat conduction away from the Hot Springs fault, there would be little justification for assuming that the surrounding rock is sufficiently permeable to accomodate recovery of 25 percent of the stored energy over a plant life of 30 years.
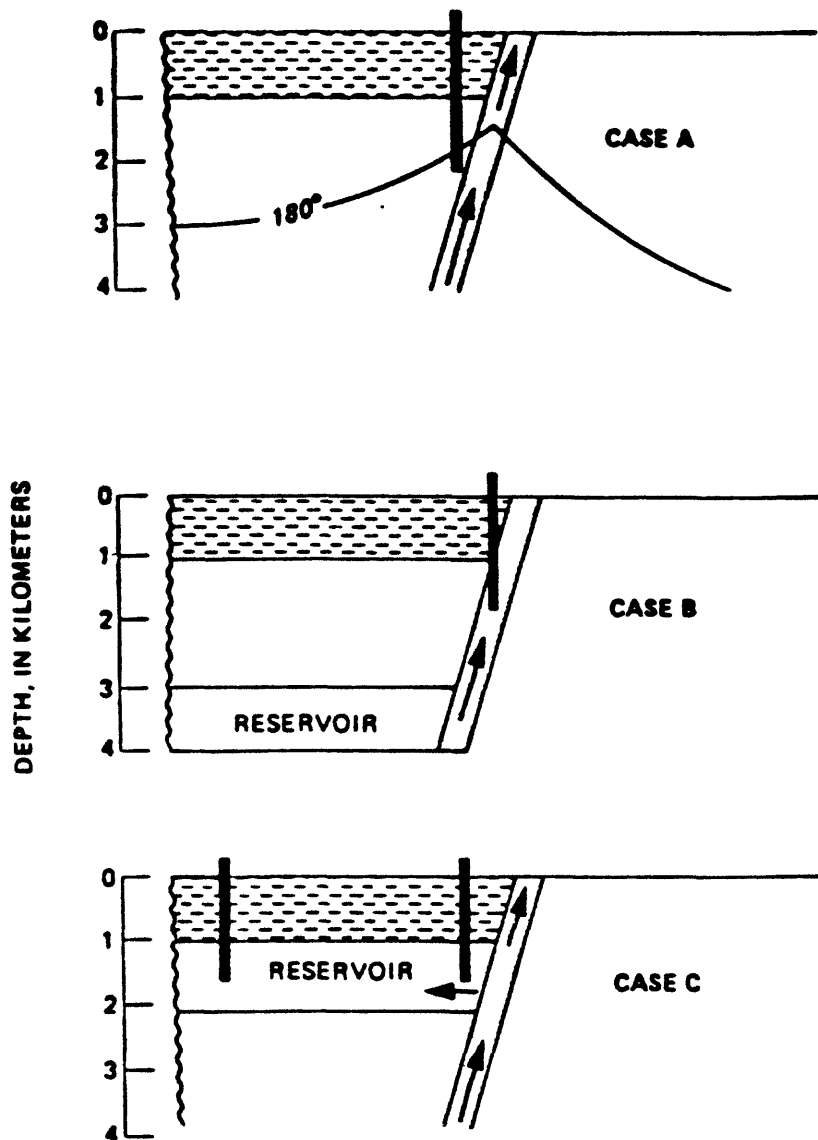
FIGURE 35. -- Three possible cases for energy recovery from high temperature portions of hydrothermal systems in the Basin and Range. Arrows indicate directions of hot-water flow. Exploitation wells shown as heavy vertical bars. Valley fill, bedrock, and fault conduits designated as in figure 26.

Exploitation Case B

Exploitation case B (figure 35) involves a permeable hot-water reservoir of significant size located at depths too deep to drill economically, connected by a permeable fault conduit to the hot springs. This corresponds with the discharge part of our lateral-flow model in figure 32. Wells drilled to intermediate depths of 1-2 km could intersect the fault conduit, capture the natural hot-water upflow, and induce additional upflow from the deep reservoir. If total mass production were limited to the natural through-flow rates at Leach Hot Springs, electrical power production would be limited to rates near 1 Mwe. Hence, the rate at which additional upflow from the deep reservoir could be induced, causing an associated mining of the heat stored in this reservoir, would be a controlling factor in making the development of this type of system economic.

From an exploitation standpoint, the hydrothermal system in southern Grass Valley appears to be most like the model in case B because heat-budget calculations for the thermal anomaly associated with Leach Hot Springs and geophysical data for the entire area show no evidence of a hot-water reservoir of significant size at depths shallower than those required for circulating fluid to reach estimated reservoir temperatures of 180°C. The most important factor in assessing the potential for energy recovery under case B conditions is the magnitude of the permeability-thickness product (kb) for the deep reservoir and the fault conduit. Assuming that the areal extent of the hydrothermal system is basin-size, the present-day throughflow rate of about 10 kg/s appears very small, indicating that portions of the circulation system effectively have a very low kb value. For example, for a total pressure drop equal to the thermal-artesian pressure difference of 70 bars and reservoir parameters L = 10 km and W = 10 km (see figure 34), a flow of 10 kg/s at an

174

average temperature of $150^{\circ}C$ implies $kb = 0.3 \times 10^{-6} cm^3$ (0.3 darcy-m). This value would apply in Grass Valley provided that values of kb for the fault conduits transmitting fluid from the surface to and from the reservoir were at least ten times greater so that the corresponding pressure drops in the fault conduits were less than 10 percent of the 70-bars figure. Interestingly, Nathenson, Urban, Diment, and Nehring (1980) obtained $kb = 2.4 \times 10^{-6} cm^3$ for a fault conduit leaking hot water upward in Cenozoic sediments in the Raft River Valley, Idaho.

Alternatively, we could have a situation in Grass Valley where most of the available pressure drop occurs in the vertical fault conduits and the reservoir is much more transmissive. Geologically, low permeability in the upflow conduit, especially where SiO_2 and $CaCO_3$ may be depositing in the fill, seems reasonable. If the average value of kb for the upflow conduit were less than $0.3 \times 10^{-6} cm^3$, the deep reservoir might have a kb of at least $3 \times 10^{-6} cm^3$. Effectively, then, we would have a permeable reservoir with a leaky seal at the discharge end controlling the rate of natural throughflow.

We can make some approximate calculations of the reservoir pressure declines accompanying production of a specified total mass flow rate for the "low" and "high" reservoir permeability cases discussed above. We will assume that production from wells drilled into the fault conduit at a depth of 1 km induces pressure drops within the deep reservoir along the fault conduit. Permeability in the conduit below 1 km is assumed large enough that pressure losses in the upflow can be neglected.

Gringarten, Ramey, and Raghavan (1975) presented an analytical solution for constant flow to a vertical fracture of finite length L in a porous reservoir of infinite lateral extent. Flow to the fracture at early times is

175

linear, or perpendicular to the fracture plane, whereas at later times radial flow dominates. To obtain solutions for the case B problem in figure 35 with the fracture forming part of one boundary of the reservoir, we must assume values for reservoir thickness b, porosity ϕ, and compressibility β in order to calculate a value for diffusivity κ. The following reasonable parameter values were selected to yield conservative estimates for the reservoir pressure drop ΔP at the fracture plane.

$$b = 1 \text{ km}$$
$$L = 2 \text{ km}$$
$$\phi = .10$$
$$\beta = 5 \times 10^{-5} \text{ bar}^{-1}$$

Then for our "low" reservoir permeability case with kb = $0.3 \times 10^{-6} \text{cm}^3$, κ would be = 40 cm^2/s and for a total flow of 100 kg/s at 180°C we obtain the following pressure history.

Time, years	0.1	1	3	10	30
ΔP, bars	35	99	150	229	300

The corresponding pressure history of our "high" reservoir permeability case with kb = $3.0 \times 10^{-6} \text{cm}^3$ and = 400 cm^2/s is shown below.

Time, years	0.1	1	3	10	30
ΔP, bars	10	23	30	41	48

Fluid production of 100 kg/s at 180°C corresponds roughly with an electrical power output of 10 MWe (Nathenson, 1975). Thus the hydrothermal system in Grsss Valley would need to be produced at about 10 times the natural throughflow rate to yield power outputs of even minimum size. We see from the results above, however, that if the value of kb for the deep reservoir is only $0.3 \times 10^{-6} \text{cm}^3$, the corresponding induced pressure drops will be very large. An estimate of the maximum allowable pressure drop for our production wells feeding at 1 km depth can be obtained from the difference between

hydrostatic pressure at that depth (90 bars) and the saturation pressure for water at 180°C (10bars). Thus, for our "low"-reservoir permeability case where any overpressure in the upflow conduit should be small, we could use 80 bars as an estimate of the allowable induced pressure drop.

On the basis of this pressure criterion, the "low" permeability reservoir could not supply 10 MWe for more than about 0.5 year. This estimate could conceivably be increased to about 3 years if the deep reservoir were permeable for a distance of several kilometers on either side of the fault conduit, rather than one side as assumed in the calculations. In spite of the many assumptions required in such an analysis, we feel justified in concluding that energy recovery from such "low" premeability reservoirs lying at depths too deep to economically drill directly is limited by low sustainable flow rates and large induced pressure drops. The principal reason for this limitation is that fluid production from the reservoir comes only from the fault conduit and cannot be more efficiently spread throughout the volume of hot water.

For our "high"-reservoir permeability case, calculated pressure drops for 10 MWe production are well within the 80 bars limit over a 30-year period. Even for a less optimum situation where the reservoir thickness is only 0.1 km yielding κ =4000 cm^2/s, the indicated pressure drop after 30 years would not be more than 80 bars. Production at even higher rates would appear possible under this exploitation scheme if $k\dot{b}$ exceeded 3×10^{-6}cm^3, although the maximum allowable pressure drop may be somewhat less than 80 bars if downhole pressure in production wells is not lowered to 10 bars.

We have assumed in these calculations that the deep reservoir extends to infinity on one side of the fault. If the lateral-flow model discussed earlier is in fact valid for areas like Grass Valley, we would expect that permeable conditions exist at considerable distance from the discharge area

177

but that reservoir temperatures would decrease with distance from the discharge area. Under these conditions, it is possible that the pressure wave induced by production from the fault conduit could diffuse out to distances of 10 km or more without encountering low-permeability barriers, and that temperature declines in production wells due to the movement of cooler water in the reservoir toward the fault conduit would be small over a 30-year time scale. Temperature declines due to induced inflow of cooler water from shallow formations adjacent to production levels in the conduit might be of more concern in some specific situations.

This sort of analysis is admittedly an over-simplification and would not be expected to yield an accurate estimate of energy recoverability in any given system. The general relationships obtained between potential electrical-power production and permeability thickness products for the reservoir do suggest, however, that under certain circumstances significant energy recovery is possible from Basin and Range hydrothermal systems even though the depths to high-temperature reservoirs may be greater than several kilometers. These circumstances include values of kb greater than about 3×10^{-6} cm^3 for the reservoir and for the hot spring fault conduit at and below depths at which production wells are drilled to intersect the conduit.

Exploitation Case C

Exploitation case C differs from case B in that a permeable volume of hot rock and water is assumed to exist at drillable depths and to be supplied with hot water by lateral leakage from the fault conduit. The source of this hot water is still the deep reservoir as in case B.

Energy recovery under case C conditions is made more efficient than under case B conditions because production and injection wells can be located throughout the area of high temperature. In this way, reservoirs with relatively

178

low permeability can still be developed without incurring unacceptably large pressure decline. Then instead of pressure drop limitations, it may be the time for breakthrough of cooler injected water near production wells which limits the rate of energy production, as shown by Morris and Campbell (1979) for the East Mesa field in California.

Although there is no geophysical or thermal evidence for such a shallow reservoir in southern Grass Valley, this model does appear valid in areas like Desert Peak, Nevada, and Humboldt House, Nevada, where permeable formations of significant lateral extent containing fluid at temperatures above $200^{o}C$ have been drilled at depths of 1 km. More commonly, however, occurrences of thermal water in shallow aquifers by lateral leakage from faults involve temperatures which are better suited to direct-heat applications than to electric-power generation.

CONCLUSIONS

Leach Hot Springs is in a seismically active region characterized by extensional tectonics. Although the background heat flow in this area is high, there does not appear to be any recent volcanic activity that might be related to a shallow magma body. The presence of the areally extensive high heat flow with active extensional tectonics has been interpreted as being due to a thin crust.

Heat-flow studies in southern Grass Valley have indicated a mean heat flow from the study area of 3-4 hfu. These values are in agreement with those typical for the Battle Mountain heat-flow high. About three-fourths the heat discharged from the southern Grass Valley area is transmitted by conduction and the remainder is conveyed by hot-spring water and shallow nonthermal ground water. The thermal data have helped define the limits of three shallow heat-flow highs and areas of cold ground-water recharge. In addition to the shallow heat-flow pattern there appears to be a non-uniform temperature distribution at the base of the sedimentary fill which is caused by fluid circulation in the consolidated bedrock. The movement of fluid near wells QH3 and G105 is particularly obvious with significant vertical and horizontal components of flow resulting in local temperature reversals. As the heat flow in the upper valley fill is primarily conductive, the shallow heat-flow anomalies are caused primarily by anamolously high temperatures at the base of the fill.

Geochemical and isotopic data combined with other information provide insight on the character of the thermal system including the reservoir temperature, fluid travel time, flow direction, and age of the system. Use of chemical and isotopic geothermometers have yielded a "best estimate" of 163-176°C for the reservoir temperature. The isotopic and chemical data also indicate that the thermal water was recharged at least 8,000 years ago under somewhat cooler and wetter conditions. The trace constituents fluoride, boron,

and lithium are all proportionately more abundant in the thermal water than in the non-thermal water and indicate that thermal water is moving upward in the sedimentary fill at QH3. Estimates of the age of the system, based on geochemical and geophysical data and several assumptions, range from 3×10^5 to 14×10^6 years, but cannot be considered as reliable. The system has been active for times sufficient to reach thermal steady state, or several hundred thousand years.

Numerical modeling of the hydrothermal system has been limited by the lack of data from deep drill holes, thereby allowing only considerations of relatively simple conceptual models. Examination of the fault-plane flow model indicates that circulation must reach depths of at least 5 km to achieve the estimated reservoir temperature under steady-state conditions. Although shallower circulation depths could exist under transient conditions, the estimated age of the system does not support this alternative. The residence time for the fluid in this model appears to be significantly shorter than that indicated by the isotope data making the fault-plane model somewhat less viable. A second model, called a lateral-flow model, was considered which consists of recharge in the mountains to the west with circulation beneath Grass Valley. The lateral-flow modeling results indicating a circulation depth of about 3 km are consistent with reasonable hydrologic properties and flow rates. The fluid residence time for the lateral flow model is consistent with the isotope data making this model more attractive.

The potential for electrical generation from the Leach Hot Springs system is obviously dependent upon the reservoir characteristics. If only that heat in the vicinity of the upflow part of the system can be extracted then there does not appear to be much potential for generation. If the lateral-flow model is a reasonably accurate representation of the system then there may be a significant potential for the utilization of the reservoir. If the

reservoir were too deep to drill directly, fluid production might still be obtained from wells drilled into the fault conduit connecting the reservoir to the land surface, provided the permeability-thickness product for the reservoir and the fault were adequately large. If the value of permeability-thickness for the reservoir were less than about $0.3 \times 10^{-6} cm^3$ exploitation even at modest rates would not be possible.

The multi-discipline approach used in this effort has proved to be valuable in evaluating alternative models despite the lack of information on the deeper part of the system. If such information does become available some revision of the current conclusions may be required.

REFERENCES

Arnason, Braggi, 1976, Ground-water systems in Iceland traced by deuterium: Societas Scientiarium Islandica, Reykjavik.

Back, William, 1961, Techniques for mapping hydrochemical facies, in Short papers in the geologic and hydrologic sciences: U.S. Geological Survey Professional Paper 424-D, p. D380-D382.

---1966, Hydrochemical facies and ground-water flow patterns in northern part of Atlantic Coastal Plain: U.S. Geological Survey Professional Paper 498-A, 42 p.

Barnes, Ivan, and McCoy, G. A., 1979, Possible role of mantle-derived CO_2 in causing two "phreatic" explosions in Alaska: Geology, v. 7, p. 434-435.

Beyer, J. H., 1977, Telluric and D. C. resistivity techniques applied to the geophysical investigation of Basin and Range geothermal systems: The analysis of data from Grass Valley, Nevada: Lawrence Berkeley Laboratory, LBL-6325 3/3, 115 p.

Beyer, J. H., Dey, Abhiji, Liaw, A. L. C, Majer, E. L, McEvelly, T. V., Morrison, H. F., and Wollenberg, H. A., 1976a, Geological and geophysical studies in Grass Valley, Nevada: Lawrence Berkeley Laboratory Preliminary Open-File Report LBL-5262, 144 p.

Beyer, J. H., Morrison, H. F., and Dey, Abhiji, 1976b, Electrical exploration of geothermal systems in the Basin and Range valleys of Nevada, in 2d U.N. Symposium on the development and use of geothermal resources, Proceedings: v. 2, p. 889-894.

Blackwell, D. D., and Chapman, D. S., 1977, Interpretation of geothermal gradient and heat-flow data for Basin and Range geothermal systems, Geothermal Resources Council, Transactions, v 1, p.19-22.

Bodvarsson, Gunnar, 1979, Convection and thermoelastic effects in narrow
    vertical fracture spaces with emphasis on analytical techniques,
    Final Report on U.S.G.S. Grant No. 14-08-0001-6-398, 111 p.

Bowman, H. R., Hebert, A. J., Wollenberg, H. A., Asaro, Frank., 1976, Trace minor,
    and major elements, in Geothermal waters and associated rock formations (north
    central Nevada): 2d U.N. symposium on the development and the general use of
    geothermal resources, Proceedings: v. 1, p. 699-702.

Brook, C. A., Mariner, R. H., Mabey, D. R., Swanson, J. R., Guffanti, M., and Muffler
    L. J. P., 1978, Hydrothermal convection systems with reservoir tempe-
    ratures $\geq 90^{\circ}C$, in Muffler, L. J. P.,(Ed.) U.S. Geological Survey Circular
    790, p. 18-85.

Cherng, Feng-ping, 1979, Geochemistry of the geothermal fields in the slate terrane:
    Geothermal Resources Council, Transactions, v. 3, p. 107-111.

Clark, S. P., Jr., 1966, Thermal conductivity, in Clark, S. P., Jr., 1966, Hand-
    book of physical properties: Geological Society of America Memoir
    97, p. 459-482.

Clayton, R. N., Muffler, L. J. P, and White, D. E., 1968, Oxygen isotope study
    of calcite and silicates of the River Ranch no. 1 well, Salton Sea Geo-
    thermal Field, California: American Journal of Science, v. 266,p. 968-979.

Cohen, Philip, 1964, A brief appraisal of the ground-water resources of the
    Grass Valley area, Humbolt and Pershing Counties, Nevada: Nevada Depart-
    ment of Conservation and Natural Resources Reconnaissance Report 29, 40 p.

Corwin, R. F., 1975, Use of the self-potential method for geothermal exploration:
    Lawrence Berkeley Laboratory Report 3225.

Craig, Harmon, 1961, Isotopic variations in meteoric waters: Science, v. 133,
    no. 3465, p. 1702-1703.

---1963, The isotopic geochemistry of water and carbon in geothermal areas, in
    Tongiorgi, E. (Ed.), Nuclear geology on geothermal areas: Conseglio Naziion-
    ale Delle Ricerche Laboratorio Di Geologia Nucleare, Pisa, p.17-53.

--- 1966, Isotopic composition and origin of the Red Sea and Salton Sea geothermal systems: American Journal of Science, p.255-267.

Craig, Harmon, Boato, G. and White, D. E., 1956, Isotopic geochemistry of thermal waters: Washington D.C., National Academy of Science and Natural Resoruces Publication 400, p.29-38.

Dansgaard, W., 1964, Stable istotopes in precipitation: Tellus, v. 16, p. 436-464.

Daly, R. A., Manger, G. E., and Clark, S. P., Jr., 1966, Density of rocks, in Clark, S. P., Jr., 1966, Handbook of physical properties: Geological Society of America Memoir 97, p.19-27.

Dey, Abhijit, and Morrison, H. F., An analysis of the dipoledipole resistivity method for geothermal exploration: Lawrence Berkeley Laboratory Report LBL-6332, 60 p.

Dreyer, R.M., 1940, Goldbanks mining district, Pershing County, Nevada: Nevada University Bulletin, Geology and Mining Series no.33, 38 p.

Epstein, S. E., and Gow, A. J., 1970, Antartic ice sheet: stable isotope analysis of Byrd Station cores and interhemispheric climatic implications: Science v. 168, p. 1570-1572.

Erwin, J. W., 1974, Bouguer gravity map of Nevada, Winnemucca sheet: Nevada Bureau of mines and Geology Map 47, Scale 1:250,000.

Fournier, R. O., and Rowe, J. J.,1966, Estimation of underground temperatures from the silica content of water from hot springs and wet-steam wells: American Journal of Science, v. 264, p.285-697.

Fournier, R. O., and Truesdell, A. H., 1973, An empirical Na-K-Ca geothermometer for natural waters: Geochimica et Cosmochimica Acta, v.27, p. 1255.

--- 1974, Geochemical indicators of subsurface temperature-part 1, Basic assumptions: U.S. Geological Survey Journal of Research, v.2, no. 3, p. 259-262.

Freeze, R. S., and Cherry, J. A., 1979, Groundwater: Englewood Cliff, N.J., Prentice-Hall, Inc., 604 p.

Friedman, Irving, and O'Neil, J. R.,1977, Compilation of stable isotope fractionation

    factors of goechemical interest: U.S. Geological Survey Professional

    Paper 440-K, 12 p.

Goldstein, N. E., and Paulsson, B., 1977, Interpretation of gravity surveys in

    Grass and Buena Vista Valleys, Nevada: Lawrence-Berkeley Laboratory

    Report LBL-7013, 43 p.

Gringarten, A. C., and Campbell, D. A., 1979, Geothermal reservoir energy recovery:

    a three dimensional simulation study of the East Mesa field, Paper SPE 8229

    presented at 54th Annual Fall Meeting of SPE of AIME, Las Vegas, Nevada.

Hansen, R. L., 1963, Surface water, in Cohen, Philip, (Ed.), An evaluation of the water

    resources of the Humbolt River valley near Winnemucca, Nevada: Nevada depart-

    ment of Conservation and Natural Resources Bulletin 24, p. 39-57.

Harbeck, G. E., Jr.,1962, A practical field technique for measuring reservoir evapor-

    ation utilizing mass-transfer theory: U.S. Geological Survey Professional Paper

    272-E, p. 1-6.

Hose, R. K., and Taylor, B. E., 1974, Geothermal systems of Northern Nevada, U.S.G.S.

    Open-file report 74-271, 20 p.

Johnson, M. G., 1977, Geology and mineral deposits of Pershing County, Nevada:

    Nevada Bureau of Mines and geology Bulletin 89, 115 p.

Jones, C. J., 1915, The pleasant Valley, Nevada earthquake of October 2, 1915:

    Seismological Society of America Bulletin, v. 5, no. 4, p.190.

Keller, G. V., 1966, Electrical properties of rocks and minerals, in Clark, S. P.,

    Jr., (Ed.), 1966, Handbook of physical properties: Geological Society of America

    Memoir 97, p. 553-578.

Kharaka, Y. K., and Barnes, Ivan, 1973, SOLMNEQ-solution mineral equilibrium com-

    putations: Menlo Park, California, U.S. Geological Survey Computer Contri-

    bution, 81 p.; available only from U.S. Department of Commerce, National

    Technical Information Service, Springfield, Va. 22151 as Report PB-215 899.

King, Clarence, 1878, Systematic geology: U.S. Geological Exploration of the 40th Parallel, v. 1, 803 p., 26 pls., 12 maps.

Kohler, M. A., Nordenson, T. J., and Baker, D. R., 1959, Evaporation maps for the United States: U.S. Department of Commerce, Weather Bureau Technical Paper 37, 13 p.

Lachenbruch, A. H., and Sass, J. H., 1977, Heat flow in the United States and the thermal regime of the crust, in Heacock, J. G. (Ed.) The Earth's Crust: American Geophysical Union Mon. 20, p. 625-675.

Lerman, J. C., 1910, Discussion, in Pearson, F. J., and Hanshaw, B. B., Sources of dissolved carbonate species in groundwater and their effects on carbon-14 dating, in Isotope Hydrology, 1970, International Atomic Energy Agency, Vienna, p. 286.

Liaw, A. L. C., 1977, Microseisms in geothermal exploration; studies in Grass Valley, Nevada: Lawrence Berkeley Laboratory Report LBL-7002, 181 p.

Liaw, A. L. C., and McEvelly, T. V., 1977, Microseisms in geothermal exploration, Studies in Grass Valley, Nevada: Lawrence Berkeley Laboratory Report 6813, 43 p.

Lowell, R. P., 1979, The onset of convection in a fault zone: effect of aniso-tropic permeability, Geothermal Resources Council, Transactions, 3, p. 377-380.

Majer, E. L., 1978, Seismological investigations in geothermal regions, Lawrence Berkeley Laboratory Report LBL 7054, 225 p.

Mariner, R. H., Rapp, J. B., Willey, L. M., and Presser, T. S., 1974, The chemical composition and estimated mimimum thermal reservoir temperature of the principal hot springs of northern and central Nevada: U.S. Geological Survey Open-file Report, 32 p.

Mariner, R. H., Presser, T. S., Rapp, J. B., and Willey, L. M., 1975, The minor and trace elements, gas, and isotope compositions of the principal hot springs of Nevada and Oregon: U.S. Geological Survey Open-file Report, 27 p.

Meidav, Tsvi, and Tonani, Franco, 1975, A critique of geothermal exploration techniques, in Proceedings of the Second United Nations Symposium of the Development and Use of Geothermal Resources, San Francisco, California, May 20-29, p. 1143-1154.

Mifflin, M. D., and Wheat, M. M., 1974, Pluvial lakes and estimated pluvial climates of Nevada: Nevada Bureau of Mines and Geology Bulletin 94, 57 p.

Moore, J. G., Bachelder, J. N., and Cunningham, C. G., 1977, CO_2-filled vesicles in mid-ocean basalt: Journal of Volcanology and Geothermal Research, v. 2, p. 309-327.

Morris, C. W., and Campbell, D. A., 1979, Geothermal reservoir energy and recovery: a three dimensional simulation study of the East Mesa field, Paper SPE 8229 presented at 54th Annual Fall Meeting of SPE of AIME, Las Vegas, Nevada.

Morrison, H. F., Lee, Ki Ha, Oppliger, Gary, and Dey, Abhijit, 1979, Magneto-telluric studies in Grass Valley, Nevada: Lawrence Berkeley Laboratory Report 8643, 160 p.

Nathenson, Manuel, 1975, Physical factors determining the fraction of stored energy recoverable from hydrothermal convection systems and conduction-dominated areas: U.S. Geological Survey Open-file report 75-525, 35 p.

Nathenson, Manuel, Urban, T. C., Diment, W. H., Nehring, N. L., 1980, Temperatures, heat flow and water chemistry from drill holes in the Raft River geothermal system, Cassia County, Idaho, Geophysics (in press)..

Nehring, N. L., and Mariner, R. H., 1979, Sulfate water isotopic equilibrium temper-atures for thermal springs and wells of the Great Basin: Geothermal Re-sources Council, Transactions, v.3, p. 485-488.

Nehring, N. L., Mariner., R. H., White, L. D., Huebner, M. A., Roberts, E. D., Harmon, Karen, Bowen, P. A., and Tanner, Lane, 1979, Sulfate geothermometry of thermal waters in the western United States: U.S. Geological Survey Open-file report 79-1135, 11 p.

Noble, D. C., Wollenberg, H. A., Silberman, M. L., and Archibald, Douglas, 1975, Late Cenozoic structural, volcanic and hydrothermal evolution of the Leach Hot Springs geothermal area, Pershing County, Nevada (abs.): Geological Society of America Abstracts with Programs, v. 7, p. 357.

O'Connell, M. F., and Kaufmann, R. F., 1976, Radioactivity associated with geothermal waters in the western United States, basic data: Las Vegas, U.S. Environmental Protection Agency, Office of Radiation Programs, Technical Note ORP/LV-75-8A , 34 p.

Ohmoto, Hiroshi and Raye, R. 0., 1979, Isotopes of sulfur and carbon, in Barnes, H. L., (Ed.), Geochemistry of hydrothermal ore deposits, 2d edition: New York, John Wiley, Chapter 10, p. 500-561.

Olmsted, F. H., Glancy, P. A., Harrill, J. R., Rush, F. E., and Van Denburgh, A. S., 1973, Sources of data for evaluation of selected geothermal areas in northern and central Nevada: U.S. Geological Survey Water-Resources Investigations 44-73, 78 p.

--- 1975, Preliminary hydrogeologic appraisal of selected hydrothermal systems in northern and central Nevada: U.S. Geological Survey Open-file report 75-56, 276 p.

Olmsted, F. H., Loeltz, O. J., and Irelan, Burdge, 1973, Geohydrology of the Yuma area, Arizona and California: U.S. Geological Survey Professional Paper 486-H, 227 p.

Page, B. M., 1935, Basin-Range faulting of 1915 in Pleasant Valley, Nevada: Journal of Geology, v. 43, no. 7, p. 690-707.

Pearson, F. J., Jr., 1975, Evaluation of natural isotopes in ground-water systems: Durham, NC, Army Research Office, Final Report, project RDRD-IP-10790-EN, 18 p.

Pineau, P., Javoy, M., and Bottinga, Y., 1976, $^{13}C/^{12}C$ ratios of rocks and inclusions in popping rocks of the Mid-Atlantic Ridge and their bearing on the

problem of isotopic composition of deep seated carbon: Earth and Planetary Science Letters, v. 29, p. 413-421.

Piper, A. M., 1944, A graphic procedure in the geochemical interpertation of water analyses: American Geophysical Union Transactions, v. 25, p. 914-923.

Presser, T. S., and Barnes, Ivan, 1974, Special techniques for determining chemical properties of geothermal water: U.S. Geological Survey Water-Resources Investigations report 22-74, 11 p.

Russell, I. C., 1895, Geologial history of Lake Lahontan, a Quaternary lake of north-western Nevada: U.S. Geological Survey Monograph XI, plate 44, p. 274.

Rightmeyer, C. T., Young, H. W., and Whitehead, R. L., 1976, Geothermal investigations in Idaho, Part 4, Isotopic and geochemical analyses of water from the Bruneau-Grand View and Weiser areas. southwest Idaho: Idaho Department Water Resources, Water Resources Information Bulletin no. 30, 28 p.

Rye, R. O., 1966, The carbon, hydrogen, and oxygen isotopic composition of the hydro-thermal fluid responsible for the lead-zinc deposits at Providencia, Zacatecas, Mexico: Economic Geology, v. 61, no. 8, p. 1399-1427.

Sass, J. H., Lachenbruch, A. H., Munroe, R. G., Greene, G. W., and Moses, T. H., Jr.,1971, Heat flow in the western United States: Journal of Geophysical Research v. 76, p. 6376-6413.

Sass, J. H., Olmsted, F. H,. Sorey M. L., Wollenberg, H. A., Lachenbruch, A. H., Monroe, R. J., and Gadanis, S. P., Jr., 1976, Geothermal data from test wells drilled in Grass Valley and Buffalo Valley, Nevada: U.S. Geological Survey Open-File Report 76-85, 41 p.

Sass, J. H., Ziagos, J. P., Wollenberg, H. A., Munroe, R. J., diSomma, D. E., and Lachenbruch, A. H., 1977, Application of heat-flow techniques to geothermal energy exploration, Leach Hot Springs area, Grass Valley, Nevada: U.S. Geological Survey Open-File Report 77-762, 126 p.

190

Scott, R. C., and Baker, F. B., 1962, Data on uranium and radium in ground water in the United States, 1954 to 1957: U.S. Geological Survey Professional Paper 426, 115 p.

Sheppard, S. M. E., Neilsen, R. L., and Taylor, H. P., Jr., 1971, Hydrogen and oxygen isotope ratios in minerals from porphyry copper deposits: Economic Geology, v. 66, p. 515-542.

Shieh, Y. N., and Taylor, H. P., 1969, Oxygen and carbon isotope studies of contact metamorphism of carbonate rocks: Journal of Petrology, v. 10, pt. 2, p. 307-331.

Sorey, M. L., 1978, Numerical modeling of liquid geothermal systems, U.S. Geological Survey Professional Paper 1044-D, 25 p.

Sorey, M. L., Lewis, R. E., and Olmsted, F. H., 1978, The hydrothermal system of Long Valley Caldera, California: U.S. Geological Survey Professional Paper 1044-A, 60 p.

Stewart, J. H., and McKee, E. H., 1977, Geology and mineral deposits of Lander County, Nevada: Nevada Bureau of Mines and Geology Bulletin 88, 106 p.

Taylor, H. P., 1974, The application of oxygen and hydrogen isotope studies to problems of hydrothermal alteration and ore deposition: Economic Geology, v. 59, p. 843-883.

Truesdell, A. H., 1975, Geochemical techniques in exploration; Second United Nations Symposium on the development and use of geothermal resources, San Francisco, Proceedings: Lawrence Berkeley Laboratory, p. liii-lxxix.

U.S. Geological Survey, 1973, Aeromagnetic map of the Leach Hot Springs and Cherry Creek quadrangles, Pershing Humboldt and Lander Counties, Nevada: U.S. Geological Survey Open-File map.

Waring, G. A., 1965, Thermal springs of the United States and other countries of the world--A summary: U.S. Geological Survey Professional Paper 492, 383 p.

White, D. E., 1970, Geochemistry applied to the discovery, evaluation, and exploitation of geothermal energy resources, in Proceedings of the United Nations symposium on the development and utilization of geothermal resources: Pisa, Geothermatics, Special Issue 2, pt. I.

White, D. E., Muffler, L. J. P., and Truesdell, A. H., 1971, Vapor dominated hydrothermal systems compared with hot-water systems: Economic Geology, v. 66, no 1, p. 75-97.

White, D. E., Barnes, Ivan, and O'Neil, J. R., 1973, Thermal and mineral waters of nonmeteoric origin, California Coast Ranges: Geological Society of America Bulletin, v. 84, p. 547-560.

Winograd, I. J., and Friedman, Irving, 1972, Deuterium as a tracer of regional ground-water flow, south Great Basin, Nevada and California: Geological Society of America Bulletin, v. 83, p.3691-3708.

Winograd, I. J., and Pearson, F. J., Jr., 1976, Major carbon 14 anomaly in a regional carbonate aquifer: possible evidence for megascale channeling, south central Great Basin: Water Resources Research, v. 12, no. 6, p. 1125-1143.

Wollenberg, H. A., 1974, Radioactivity of Nevada hot-spring system: Geophysical Research Letters, v.1, p. 359-362.

---1976, Radioactivity of geothermal systems, in Geothermal waters and associated rock formations (north-central Nevada): Second U.N. Symposium on the development and use of geothermal resources, Proceedings, v. 2, p. 1283-1292.

Wollenberg, H. A., Bowman, H. R., and Asero, Frank, 1977, Geochemical studies at four northern Nevada hot spring areas: Lawrence Berkeley Laboratory Report LBL-6808, 69 p.

Wood, W. W., 1976, Guidelines for collection and field analysis of ground-water samples for selected unstable constituents: U.S. Geological Survey Techniques of Water-Resources Investigations, Book 1, Chapter D2, 24 p.

Zietz, Isidore, Gilbert, F. P., and Kirby, J. R., 1978, Aeromagnetic map of
Nevada Color Coded intensities: U.S. Geological Survey Geophysical
Investigations Map GP-922, scale 1:1,000,000.